Smooth and Oscillating Configurations in String Theory

By

Pratik Roy

A thesis submitted in partial fulfillment of the requirements for the degree of Doctor of Philosophy

to

Chennai Mathematical Institute

H1, SIPCOT IT Park, Siruseri,
Kelambakkam, Tamil Nadu 603103,
India

December, 2019

CHENNAI MATHEMATICAL INSTITUTE

Pratik Roy

Declaration

I declare that the thesis entitled "**Smooth and Oscillating Configurations in String Theory**" submitted by me for the degree of **Doctor of Philosophy in Physics** is the record of academic work carried out by me during the period of August, 2015 to December, 2019 under the guidance of professor Amitabh Virmani, and that this work has not formed the basis for the award of any degree, diploma, associateship, fellowship, or other titles in this university or any other University or Institution of Higher Learning.

Pratik Roy
Chennai Mathematical Institute
December, 2019

CHENNAI MATHEMATICAL INSTITUTE

Amitabh Virmani

Certificate

I certify that the thesis entitled "**Smooth and Oscillating Configurations in String Theory**" submitted by Pratik Roy for the degree of **Doctor of Philosophy in Physics** is the record of research work carried out by him during the period of August, 2015 to December, 2019 under my guidance and supervision, and that this work has not formed the basis for the award of any degree, diploma, associateship, fellowship, or other titles in this university or any other University or Institution of Higher Learning. I further certify that the new results presented in this thesis represent his independent work in substantial measure.

Amitabh Virmani
Thesis Supervisor
Chennai Mathematical Institute
December, 2019

Acknowledgements

> And as no man knows the ubicity of his tumulus nor to what processes we shall thereby be ushered nor whether to Tophet or to Edenville in the like way is all hidden when we would backward see from what region of remoteness the whatness of our whoness hath fetched his whenceness.
>
> Oxen of the Sun

First and foremost, I express my gratitude for my supervisor, Amitabh Virmani, for his constant guidance, support, and patience. I am also thankful to him for the numerous discussions we had, about physics or otherwise. I am also grateful to Alok Laddha and Shamik Banerjee for sharing their time with me. A lot of what I know is a result of discussions with these three people. Collaborations with Arnab Kundu and Yogesh Srivastava are also acknowledged.

I would also like to thank my colleagues, Partha Paul, Ganesh Paul, Amit Sharma, Sujay Sil, Biswajit Das, at Bhubaneswar, and A Manu, Aneesh PB, Athira PV, Debangshu Mukherjee, Kedar Kolekar, Shanmugapriya P, Vishnu TR, at Chennai. I am grateful to the entire CMI student community for such a lively atmosphere.

Although not an active presence in my life for some time now, I cannot forego mentioning my debt to the class of 2014 of IISER Bhopal. I wish such fraternity for every individual. Special mention is due to the few people from IISER Bhopal that I am still in contact with: Aranya Lahiri, Sanjana Agarwal, and Vineet Singh for our yearly trips, Akash Jain for discussions on physics and life, and Rahul Gupta and Anurag Punia for their presence in Bangalore.

I would also like to thank my parents, specially my mother, for all their love and care.

James Joyce deserves a special mention for providing me with all the epigraphs. They are all taken from *Ulysses*.

Last, and far from the least, I would like to express my love and gratitude for Raka, for being there with me ever since I found her. I dedicate the thesis to her.

Abstract

This thesis is concerned with exploring gravitational aspects of string theory, in different contexts. The major part of the thesis deals with smooth solutions of supergravity that have black hole like charges, the so-called 'microstate geometries' or 'fuzzballs'. The other part explores gravitational solutions in AdS space that do not collapse, but instead oscillate perpetually between two radii.

For the study of smooth solutions, we employ the Riemann-Hilbert approach, which lets one associate spacetime independent monodromy matrices to solutions with sufficiently many Killing isometries. We initiate a systematic study of monodromy matrices for multi-center solutions of five-dimensional $U(1)^3$ supegravity. We obtain explicitly the monodromy matrices for a class of collinear Bena-Warner bubbling geometries, and show that they obey properties required for an inverse scattering construction to work. The theory of symmetric spaces plays an important role in this discussion. We thus include a brief overview of this subject, including relevant background material on the real forms of classical Lie algebras.

Another construction of smooth solutions of supergravity is provided by constructing a linearised left-moving perturbation on two-charge non-extremal JMaRT solutions. The perturbation is constructed by matching solutions to the perturbation equations in the inner and outer regions of the geometry to leading order, and is found to be smooth and normalisable.

In the last part of the thesis, we study timelike shells and balls in AdS space that undergo oscillatory motion. We confirm that the two-point function of the boundary CFT, calculated via the geodesic approximation in the bulk, exhibits an oscillatory behaviour following the motion of the shell. We show that similar oscillatory dynamics is possible when the perfect fluid on the shell has a polytropic equation of state. Further, we show that plausible ball like configurations in AdS also admit oscillating solutions. Such configurations are constructed by matching finite pressure Oppenheimer-Snyder like solutions in anti-de Sitter space (AdS) to Tolman–Oppenheimer–Volkoff (TOV) like stars in AdS. We also demonstrate that the weak energy condition is satisfied for all these oscillatory configurations.

Contents

1

Introduction

All these questions are purely academic...

Scylla and Charybdis

1.1 Black Holes and Entropy

In the 1960's, a number of new developments revolutionised black hole physics. Results of Hawking and Penrose showed that rather than being unphysical, singularities in spacetime are ubiquitous in general relativity. The laws of black hole mechanics, governing the 'kinematics' and 'dynamics' of black holes and their horizons, were also formulated. A good survey of the multitude of developments can be found in [1].

One crucial development during this period was Bekenstein's proposal [2] to consider a back hole's entropy as true thermodynamical entropy. He was motivated by the apparent decrease in the total entropy as an object falls into a black hole, leaving no trace because of the 'no hair' theorems. Setting out to prove Bekenstein wrong, Hawking [3] instead showed that the analogy between black hole mechanics and thermodynamics was exact. Including effects from quantum fields, he found that black holes do indeed have a temperature and emit radiation like thermal objects, with an entropy that is proportional to the area of the black hole event horizon, just as Bekenstein had conjectured.

Even though a lot has been learnt about black holes since, even more remains yet to be understood. The statistical notion of entropy implies that there is a set of possible states for a system to exist in; entropy then quantifies the ignorance on an observer's part as to exactly what the state of the system is. Taking this definition to its logical conclusion, the question arises of what exactly *are* the possible (quantum) states of a black hole.

Such a question is ill-posed within the framework of general relativity itself. The no-hair theorems tells us that there is no structure to black holes to support any finite entropy. Even Hawking's radiation is a semi-classical effect. The natural hope is that a theory of quantum gravity, when we have the knowledge of it, would answer our question.

Another related question is the fate of the stored information inside a black hole as the hole evaporates. Hawking himself suggested that unitarity is lost in the process. However, developments such as the AdS/CFT correspondence, and holography in general, have convinced most researchers that unitarity must indeed be upheld, and that some novel physics is required to explain the evaporation.

The central importance of the Bekenstein-Hawking area law lies in the fact that it can indeed also be used as a check on a quantum theory of gravity: For any such theory to be

valid, it must at least reproduce the area law. String theory is a promising candidate for a theory incorporating both quantum mechanics and gravity. In light of the discussion above, trying to understand the entropy of black holes in the context of string theory is an important problem. There has in fact been significant progress in this direction, beginning with the work of Sen [4], and Strominger and Vafa [5], who showed that the statistical entropy of BPS states matches that given by the Bekenstein-Hawking area law.

In their derivation, Strominger and Vafa had to rely on the non-renormalization theorems of supersymmetric theories, thus obscuring the nature of the states contributing to gravitational entropy. So, while providing evidence that string theory knows about the area law, their work could shed no light on what comprises the entropy of black holes. This has been a persistent question ever since, and an answer could potentially resolve the information paradox as well.

One notable attempt towards explaining black hole entropy is the "fuzzball" proposal by Mathur [6]. Fuzzballs are conjectured bound-state solutions of supergravity/string theory that carry the same charges as black holes but are instead regular everywhere, and are hoped by some to acount for the microscopic states of the black holes. Such "microstates" are solutions without event horizons that evade the no-hair theorems due to their being constructed from higher dimensional solutions [7].

The fuzzball configurations could be stringy, and not describable in supergravity; it might also happen that some configurations are in fact smooth solutions of supergravity. It is technically much more easier to investigate the second possibility, and is where most effort is invested. Reviews of early work on fuzzballs include [8–11]. In the case of two-charge D1-D5 black hole configurations, it has been shown that fuzzballs can indeed account for the full microscopic entropy obtained by counting states in string theory. The corresponding problem for three charge configurations turns out to be much more involved.

Formulating the problem in the (eleven dimensional supergravity) M-theory frame, one sees that the problem reduces to constructing source-free solutions that have bubbles threaded by non-vanishing field strengths. Such solutions are constructed by reducing M-theory on tori, and demanding that the lower dimensional theory be free of brane sources. Bubbles then refer to non-vanishing cohomology classes in the lower dimesional theory. These solutions have a rich geometrical and group-theoretical structure, and we will be interested in exploring some of it below.

1.2 Scope of the Thesis

Chapter 3, Chapter 4, and Chapter 5 are based on three published papers and contain my independent work. Chapter 3 is somewhat more technical than the rest, so we begin with providing the necessary background for Chapter 3. This is done partly in the rest of this chapter and in Chapter 2.

In Chapter 3 we are mostly concerned with the so-called Bena-Warner solutions of supergravity. These solutions provide a large class of horizonless smooth microstate geometries with three charges. In the next section we provide a brief review of these solutions. We also heavily use the coset space description of dimensionally reduced supergravity theories in Chapter 3, which was developed in [12]. With this in view, in section 1.4, we present a general framework for describing stationary solutions of (super)gravity that are obtained as consistent truncations of higher dimensional theories. The framework is largely based on using the group theoretic structure of the symmetric spaces formed by the lower dimensional scalars of the theory. Ref. [12] presented a table of all symmetric

spaces obtained by dimensional reduction, of theories with scalars and vectors, from four to three dimensions. Since the table is an important part of [12], and since an accessible exposition is not readily available, I have tried to provide mathematical background relevant to understanding how the table arises in chapter 2.

It turns out that stationary supergravity solutions have a rich underlying mathematical structure [13,14]. Ref. [15] exploited this to classify extremal solutions of the STU model, and found that non-BPS extremal solutions can also be generated using nilpotent orbits of the coset space. In Chapter 3, we explicitly recast the Bena-Warner solutions in a coset space description. Having done this, we demonstrate that the solutions satisfy most of the properties required for the inverse scattering construction of [16] to work. Although an explicit solution of the Riemann-Hilbert problem is not given, it seems that the problem can be solved.

Chapter 4 is concerned with the construction of new fuzzball solutions for three-charge solutions, although in a different context. Extending a previous contruction by [17], where they constructed a BPS perturbation on smooth BPS D1-D5 geometries, we were able to construct hair modes (BPS perturbation) over non-extremal solutions, known as JMaRT solutions for its discoverers [18].

Chapter 5 is an exploration of oscillating configurations in anti de Sitter (AdS) space. Because of the AdS/CFT correspondence, collapsing solutions in AdS correspond to states in the dual CFT that thermalise. Accordingly, states that do not collapse should correspond to states that revive themselves and never thermalise. Oscillating configurations also bear directly on questions concerning the (in)stability of AdS space, a question that has attracted much attention recently. We construct explicitly solutions with matter concentrated on a shell of varying radius that show periodic oscillations. We also demonstrate that it is plausible that Tolman-Oppenheimer-Volkoff (TOV) solutions in AdS space can be patched as an exterior solution to an oscillating interior around the centre of AdS. The existence of such simple solutions demonstrates that oscillations in AdS can be easily arranged.

1.3 Bubbling Solutions in Supergravity: A Brief Review

In this brief section we review Bena-Warner solutions. These are supergravity configurations supported by non-trivial topology. Such solutions resemble black holes far from the would-be "black hole radius", and cap off at the would-be horizon. These provide examples of microstate geometries, and are believed to contribute to the states that comprise black hole entropy. This material is based on the review [9]. We only focus on the construction of the solutions and do not discuss spacetime properties of the solutions. Many properties of these solutions have been discussed over the last fifteen years, we refer the reader to [9] for some of the earlier references.

1.3.1 Brane Configurations

We start by compactifying M-theory on a T^6, with three sets of M2-branes wrapping three mutually orthogonal T^2, along with three corresponding sets of M5-branes on the complementary T^4 to each T^2. The remaining spatial directions of the M5-branes wrap one simple, closed curve, $y^\mu(\sigma)$, in the spatial directions of the non-compact dimensions. The configuration is summarized in figure 1.1.

The metric corresponding to our configuration can be written as

$$ds_{11}^2 = ds_5^2 + ds_{T^6}^2, \tag{1.3.1}$$

Brane	0	1	2	3	4	5	6	7	8	9	10
M2	$\updownarrow$	$\star$	$\star$	$\star$	$\star$	$\updownarrow$	$\updownarrow$	$\leftrightarrow$	$\leftrightarrow$	$\leftrightarrow$	$\leftrightarrow$
M2	$\updownarrow$	$\star$	$\star$	$\star$	$\star$	$\leftrightarrow$	$\leftrightarrow$	$\updownarrow$	$\updownarrow$	$\leftrightarrow$	$\leftrightarrow$
M2	$\updownarrow$	$\star$	$\star$	$\star$	$\star$	$\leftrightarrow$	$\leftrightarrow$	$\leftrightarrow$	$\leftrightarrow$	$\updownarrow$	$\updownarrow$
M5	$\updownarrow$		$y^\mu(\sigma)$			$\leftrightarrow$	$\leftrightarrow$	$\updownarrow$	$\updownarrow$	$\updownarrow$	$\updownarrow$
M5	$\updownarrow$		$y^\mu(\sigma)$			$\updownarrow$	$\updownarrow$	$\leftrightarrow$	$\leftrightarrow$	$\updownarrow$	$\updownarrow$
M5	$\updownarrow$		$y^\mu(\sigma)$			$\updownarrow$	$\updownarrow$	$\updownarrow$	$\updownarrow$	$\leftrightarrow$	$\leftrightarrow$

Figure 1.1: Brane configuration for supertubes and black rings in an M-theory frame. $\updownarrow$ indicates directions along which the branes are extended, $\leftrightarrow$ indicates the smearing directions, $y^\mu(\sigma)$ indicates that the brane wraps a simple closed curve in $\mathbb{R}^4$ defining the tube or ring profile, and $\star$ indicates that a brane is smeared along the profile and pointlike in the other three directions.

where

$$ds_5^2 = -(Z_1Z_2Z_3)^{-2/3}(dt+k)^2 + (Z_1Z_2Z_3)^{1/3}h_{mn}dx^m dx^n, \tag{1.3.2}$$

and the metric on T^6 is

$$ds^2_{T^6} = \left(\frac{Z_2Z_3}{Z_1^2}\right)^{1/3}(d\tilde{x}_1^2+d\tilde{x}_2^2)+\left(\frac{Z_1Z_3}{Z_2^2}\right)^{1/3}(d\tilde{x}_3^2+d\tilde{x}_4^2)+\left(\frac{Z_1Z_2}{Z_3^2}\right)^{1/3}(d\tilde{x}_5^2+d\tilde{x}_6^2), \tag{1.3.3}$$

Here, k is a one-form field on the spatial section of the five-dimensional spacetime, and Z_I are 'harmonic functions' associated to the three sets of M2-branes. Note that the metric is asymptotic to $\mathbb{R}^{4,1}\times T^6$.

The eleven dimensional three-form-field looks like,

$$A_{[3]} = A^1_{[1]}\wedge d\tilde{x}_1\wedge d\tilde{x}_2 + A^2_{[1]}\wedge d\tilde{x}_3\wedge d\tilde{x}_4 + A^3_{[1]}\wedge d\tilde{x}_5\wedge d\tilde{x}_6, \tag{1.3.4}$$

where the subscript on each A indicates the degree of the form. The $A^I_{[1]}$, $I=1,2,3$, are time-independent one-form electromagnetic potentials in the 5 dimensional spacetime.

One introduces dipole field strengths as

$$\Theta^{(I)} := dA^{(I)} + d\left(Z_I^{-1}(dt+k)\right). \tag{1.3.5}$$

The most general supersymmetric configuration is then obtained by solving the following system of equations [19],

$$\Theta^{(I)} = \star_4\,\Theta^{(I)}, \tag{1.3.6}$$

$$\nabla^2 Z_I = \frac{1}{2}C_{IJK}\star_4\left(\Theta^{(J)}\wedge\Theta^{(K)}\right), \tag{1.3.7}$$

$$dk + \star_4 dk = Z_I\Theta^{(I)}, \tag{1.3.8}$$

where $\star_4$ is the Hodge dual operator taken with respect to the four-dimensional metric h_{mn}, ∇^2 is the Laplacian defined using h_{mn}, and C_{IJK} are the structure constants associated to the dimensional reduction. In the present setup, $C_{IJK} = |\epsilon_{IJK}|$. If these equations are solved sequentially, they form a linear system.

1.3.2 Gibbons-Hawking Base

We consider now the four-dimensional base space, which supersymmetry demands be hyper-Kähler. A particularly interesting family of hyper-Kähler metrics are the Gibbons-Hawking metrics. These provide for the possibility of non-trivial topology by allowing

the possibility for the signature to flip from $+4$ to -4 in certain regions. The Gibbons-Hawking metrics are U(1) fibrations over a flat $\mathbb{R}^3$ base,

$$ds_4^2 = V^{-1}(dz + A_{[1]})^2 + V(dr^2 + r^2 d\theta^2 + r^2 \sin^2\theta d\phi^2), \tag{1.3.9}$$

with

$$\star_3\, dA_{[1]} = dV, \tag{1.3.10}$$

where $\star_3$ is the Hodge-star operation in $\mathbb{R}^3$, and V is a harmonic function on $\mathbb{R}^3$.

We now let $\vec{x}^{(j)} \in \mathbb{R}^3$ be the positions of isolated sources for V, and use the notation $r_j = |\vec{x} - \vec{x}^{(j)}|$:

$$V = q_0 + \sum_{j=1}^{N} \frac{q_j}{r_j}. \tag{1.3.11}$$

Although the metric appears singular at $r_j = 0$, it is easily checked by changing coordinates to $\rho = 2\sqrt{|\vec{x} - \vec{x}^{(j)}|}$, that the metric near each center is locally of the form

$$ds_4^2 \sim d\rho^2 + \rho^2 d\Omega_3^2, \tag{1.3.12}$$

where $d\Omega_3^2$ is the standard metric on $S^3/\mathbb{Z}_{|q_j|}$.

For $q_0 \neq 0$, the base metric is asymptotically $\mathbb{R}^3 \times S^1$, so that the five-dimensional theory can be KK reduced, with non-trivial gauge-fields sourced by branes. For $q_0 = 0$, the base metric is asymptotically $\mathbb{R}^4$. One has asymptotically $V \sim q/r$, with $q = \sum_{j=1}^{N} q_j$, as a result the spatial infinity is also of the form (1.3.12), with $q_0 = q$.

The GH metrics contain topologically non-trivial two-cycles between the centers, generated by the U(1) fiber over curves between the centers. To describe the two-cycles, we let y^1, y^2, y^3 form a Cartesian coordinate system for $\mathbb{R}^3$, and define a set of frames by

$$\hat{e}^1 = V^{-1/2}(dz + A), \qquad \hat{e}^{a+1} = V^{1/2} dy^a, \quad a = 1, 2, 3, \tag{1.3.13}$$

and a set of two-forms by

$$\Omega_{\pm}^{(a)} = \hat{e}^1 \wedge \hat{e}^{a+1} \pm \frac{1}{2}\epsilon_{abc}\hat{e}^{b+1} \wedge \hat{e}^{c+1}, \quad \text{with} \quad a, b, c = 1, 2, 3. \tag{1.3.14}$$

These forms have nice properties: $\Omega_{\pm}$ are self and anti-self dual respectively, and Ω_- is harmonic.

Ω_+ are used to construct harmonic fluxes that are dual to the two-cycles in our GH base. Consider the self-dual two-form

$$\Theta = \sum_{a=1}^{3} \partial_a \left(\frac{H}{V}\right) \Omega_+^{(a)}.$$

where H is a harmonic function on $\mathbb{R}^3$, with undetermined sources. A general distrubution of such sources will correspond to having mutiple black rings and black holes in the space. To obtain a horizonless, singularity-free geometry, Θ needs to be regular, which can only happen if H/V is regular. This implies that H has sources at the same location as V,

$$H = h_0 + \sum_{j=1}^{N} \frac{h_j}{r_j}.$$

Note that Θ is invariant under a transformation of the form

$$H \to H + cV,$$

for some constant c. This implies that there are only N independent parameters in H. Also, if $q_0 = 0$, we necessarily have $h_0 = 0$, to keep Θ finite at infinity. The remaining $N-1$ parameters of H (and hence of Θ) describe the harmonic forms dual to the non-trivial two-cycles. If $q_0 \neq 0$, the extra parameter is that of a Maxwell field whose gauge potential gives the Wilson line around the S^1 at infinity.

One can write the two-form Θ as an exact form locally, $\Theta = dB$, as

$$B = \frac{H}{V}(dz + A) + \xi_a dy^a,$$

with $\star_3 d\xi = -dH$ so that

$$dB = \partial_a \left(\frac{H}{V}\right) \Omega_+^{(a)}.$$

The one-form $\xi = \xi_a dy^a$ acts as the potential for magnetic monopoles located at the singular points of H.

To find explicitly the form of the fluxes, we need to determine the solution of the equation above,

$$\star_3 d\xi = \star \partial_a \xi_b dy^a \wedge dy^b = \epsilon_{abc} \partial_a \xi_b \, dy^c = -dH = -\partial_a H \, dy^a$$

The solution is just a $3d$ vector field $\vec{v}(\equiv \vec{\xi})$ that satisfies

$$\vec{\nabla} \times \vec{v}_i = \vec{\nabla} \left(\frac{1}{r_i}\right)$$

so that

$$A_{[1]} = \sum_{j=1}^{N} q_j v_{j[1]}, \qquad \xi_{[1]} = \sum_{j=1}^{N} h_j \vec{v}_j.$$

Note that we had the conditions $\star_3 dA_{[1]} = dV$, and $\star_3 d\xi = -dH$, which are now both satisfied.

If we choose coordinates such that the sources all lie on the z-axis, $y^{(i)} = (0, 0, a)$, then a solution is given by

$$\vec{v}_i \cdot d\vec{y} = \left(\frac{z-a}{r_i} + c_i\right) d\phi. \tag{1.3.15}$$

The vector field $\vec{v}_i$ has a Dirac string singularity.

1.3.3 Solving the BPS Equations

Introduce three harmonic functions K^I of the form

$$K^I = k_0^I + \sum_{j=1}^{N} \frac{k_j^I}{r_j},$$

and use them to contruct the self-dual two-forms

$$\Theta^I = \sum_{a=1}^{3} \partial_a \left(\frac{K^I}{V}\right) \Omega_+^{(a)}.$$

Eq. (1.3.7) can then be checked to have the solution

$$Z_I = \frac{1}{2} C_{IJK} \frac{K^J K^K}{V} + L_I, \tag{1.3.16}$$

with $L_I, I = 1, 2, 3$, a set of harmonic functions.

Write the one-form, k, introduced in the ansatz for the five-dimensional metric, as

$$k = \mu(d\psi + A) + \omega, \tag{1.3.17}$$

so that (1.3.8) becomes

$$\vec{\nabla} \times \vec{\omega} = (V\vec{\nabla}\mu - \mu\vec{\nabla}V) - V\sum_{I=1}^{3} Z_I \vec{\nabla}\left(\frac{K^I}{V}\right), \tag{1.3.18}$$

which is the same as

$$\star_3\, d\omega_{[1]} = (V\, d\mu - \mu\, dV) - V\sum_{I=1}^{3} Z_I\, d\left(\frac{K^I}{V}\right). \tag{1.3.19}$$

Acting with d again gives an equation for μ which can be solved to give

$$\mu = \frac{1}{6}C_{IJK}\frac{K^I K^J K^K}{V^2} + \frac{1}{2V}K^I L_I + M, \tag{1.3.20}$$

with M a harmonic funtion on $\mathbb{R}^3$. Using this for μ into the above equation for ω then gives

$$\star_3\, d\omega_{[1]} = V\, dM - M\, dV + \frac{1}{2}(K^I\, dL_I - L_I\, dK^I). \tag{1.3.21}$$

We note that the solution is expressed in terms of *eight harmonic functions* (on $\mathbb{R}^3$), namely, $V,\ M,\ K^I,\ L_I$. The solution has two families of continuous symmetries, the so-called "gauge transformations" and "spectral flows", which act on the harmonic functions. With c^I being constants, gauge transformations here refer to changing the harmonic functions as

$$\begin{aligned} V &\to V, \\ K^I &\to K^I + c^I V, \\ L_I &\to L_I - C_{IJK}c^J K^K - \frac{1}{2}C_{IJK}c^J c^K V, \\ M &\to M - \frac{1}{2}c^I L_I + \frac{1}{12}C_{IJK}(c^I c^J c^K V + 3c^I c^J K^K), \end{aligned} \tag{1.3.22}$$

These transformations map solutions in the Bena-Warner class to solutions in the same class. Invariance under gauge transformations can be inferred from our discussion above. Bena-Warner solutions possess another symmetry, the so-called spectral flows, which refer to changing the functions as,

$$\begin{aligned} V &\to V + c_I K^I - \frac{1}{2}C^{IJK}c_I c_J L_K + \frac{1}{3}C^{IJK}c_I c_J c_K M, \\ K^I &\to K^I - C^{IJK}c_J L_K + C^{IJK}c_J c_K M, \\ L_I &\to L_I - 2c_I M, \\ M &\to M. \end{aligned} \tag{1.3.23}$$

It can be checked that this is also a symmetry. The action of this symmetry is more non-trivial as it changes the four-dimensional base space function V.

As mentioned above, the Bena-Warner class of solutions enjoy many properties. These properties have been discussed in the literature over the last fifteen years. For our purposes, the discussion presented above – construction of solutions using Harmonic functions – suffices.

1.4 Non-Linear σ-Models and Symmetric Spaces

Next we provide an overview of the non-linear σ-models with a target space Φ. These spaces are non-compact Riemannian or pseudo-Riemannian symmetric spaces of the form G/H. Our discussion is based on Appendix A of [12], with only minor changes in notation. We heavily use this material in Chapter 3. The non-compact Riemannian or pseudo-Riemannian symmetric spaces play an important role in describing scalar sectors of various supergravity theories. In three dimensions, where vectors can be dualised to scalars, such symmetric spaces play even more important role, as often it happens that the full matter dynamics is contained in the scalar sector.

1.4.1 Non-compact Riemannian symmetric spaces

Let G be a non-compact real form of some compact Lie group. Real forms of classical Lie algebras and details about involutions that define them are discussed in some detail in Chapter 2. There is an involutive transformation (cf. 2.2.1) $\tau : G \to G, \tau^2 = 1$, such that H, defined as

$$H = \{h \in G : \tau(h) = h\}, \tag{1.4.1}$$

is the maximal compact subgroup of G and the coset space G/H is a non-compact Riemannian symmetric space.

To parametrize the coset space G/H[1], we choose elements P as representatives for cosets. This amounts to introducing fields $P(x)$ transforming under gauge transformations from group H, and under the action of G on G/H,

$$P(x) \to h(x)\, P(x)\, g^{-1}, \qquad h(x) \in H,\ g \in G. \tag{1.4.2}$$

To fix the gauge symmetry H, we choose a solvable subgroup[2] which intersects each coset once. The group action is liable to lead to non-standard representatives, and must be accompanied by an induced gauge transformation to maintain the gauge choice,

$$P(x) \to h(P(x), g) P(x) g^{-1}, \qquad g \in G. \tag{1.4.3}$$

Consider the 1-form $dP(x)\, P(x)^{-1}$, taking values in the Lie algebra $\mathfrak{g}$ of G, and decompose it as

$$dP\, P^{-1} = A + B = (A_a + B_a) dx^a, \qquad \tau(A) = A,\ \tau(B) = -B, \tag{1.4.4}$$

where

$$A = \frac{1}{2}\left(dP\, P^{-1} + \tau\big(dP\, P^{-1}\big)\right), \qquad B = \frac{1}{2}\left(dP\, P^{-1} - \tau\big(dP\, P^{-1}\big)\right),$$

are the symmetric and anti-symmetric parts of $dP\, P^{-1}$ under the involution τ.

The Lie alebra-valued one form $dP\, P^{-1}$ tranforms under the group action of Eq. (1.4.2) as follows,

$$\begin{aligned} dP\, P^{-1} &\to d\big(h(x)P(x)g^{-1}\big)\big(h(x)P(x)g^{-1}\big)^{-1} \\ &= \big((dh)Pg^{-1} + h(dP)g^{-1}\big)\big(gP^{-1}h^{-1}\big) \\ &= (dh)h^{-1} + h(dP)P^{-1}h^{-1} \\ &= h(A+B)h^{-1} + (dh)h^{-1}, \end{aligned}$$

[1] For historical reasons, we consider the space of right cosets, Hg, denoting it by G/H with impunity, since the spaces $H\backslash G$ and G/H are isomorphic.

[2] *Iwasawa Decomposition*: $\mathfrak{g}$ is a direct sum $\mathfrak{g} = \mathfrak{h} \oplus \mathfrak{a} \oplus \mathfrak{n}$, with $\mathfrak{h}$ the maximal compact subalgebra of $\mathfrak{g}$, $\mathfrak{a}$ abelian, $\mathfrak{n}$ nilpotent, $\mathfrak{a} \oplus \mathfrak{n}$ a solvable Lie subalgebra of $\mathfrak{g}$, and $[\mathfrak{a} \oplus \mathfrak{n}, \mathfrak{a} \oplus \mathfrak{n}] = \mathfrak{n}$. In terms of Lie groups, this is written as $G = HAN$, where the exponentiation of the nilpotent $\mathfrak{n}$ gives the "triangular" matrices.

so that under (1.4.2),

$$A \to hAh^{-1} + (dh)h^{-1}, \qquad B \to hBh^{-1}. \tag{1.4.5}$$

This says that A can be thought of as connection for H, and that B transforms H-covariantly, with both being G-invariant.

Given any invariant scalar product $\langle \cdot, \cdot \rangle$ on the Lie algebra $\mathfrak{g}$, define an invariant (positive-definite) metric γ on G/H by

$$d\phi^i \, d\phi^j \, \gamma_{ij}(\phi) := \langle B, B \rangle, \tag{1.4.6}$$

where ϕ^i denote coordinates on G/H. For simple G, and for any faithful representation $\varrho : \mathfrak{g} \ni B \to \hat{B} := \varrho(B)$, there is a positive constant $\hat{c}$ such that

$$\langle B, B \rangle = \hat{c} \, \mathrm{Tr} \left(\hat{B} \hat{B} \right). \tag{1.4.7}$$

The involution τ canonically embeds G/H in G,

$$\begin{aligned} \tau(XY) &:= \tau \, XY \, \tau^{-1} = \tau \, X \tau^{-1} \tau \, Y \tau^{-1} = \tau(X)\tau(Y) \\ P \to M &:= \tau(P^{-1})P, \\ \tau(M) &= \tau(\tau(P^{-1})P) = \tau \, \tau \, P^{-1} \, \tau^{-1} \, P \, \tau^{-1} \\ &= \tau^2 P^{-1} \tau^{-2} \, \tau \, P \, \tau^{-1} = \tau^2(P^{-1})\tau(P) = P^{-1}\tau(P) = M^{-1} \end{aligned}$$

so that M is invariant under H, and covariant under G,

$$\tau(gP^{-1})(Pg^{-1}) = (\tau g \tau^{-1})(\tau P^{-1} \tau^{-1}) P g^{-1} = \tau(g)\tau(P^{-1})Pg^{-1} = \tau(g) M g^{-1}.$$

We note that here by, e.g., $\tau X \tau^{-1}$, we mean the natural action of τ on X by conjugation.

Thinking of M as the conserved charge, we define the corresponding current

$$J := \frac{1}{2} M^{-1} dM, \tag{1.4.8}$$

and find, with

$$d(P^{-1}) = -P^{-1}(dP)P^{-1}, \qquad e = \tau(e) = \tau(PP^{-1}) = \tau(P)\tau(P^{-1}),$$

that

$$\begin{aligned} PJP^{-1} &= \frac{1}{2} P M^{-1} (dM) P^{-1} = \frac{1}{2} (MP^{-1})^{-1} d(MP^{-1}) - \frac{1}{2} P d(P^{-1}) \\ &= \frac{1}{2} (\tau(P^{-1}))^{-1} d(\tau(P^{-1})) + \frac{1}{2} dP \, P^{-1} \\ &= \frac{1}{2} dP \, P^{-1} - \frac{1}{2} \tau(P) \, (\tau(P))^{-1} d(\tau(P)) \, (\tau(P))^{-1} \\ &= \frac{1}{2} dP \, P^{-1} - \frac{1}{2} \tau(dP \, P^{-1}) \;=\; B \\ &= (dP - A \, P) P^{-1} \\ &:= DP \, P^{-1} \end{aligned}$$

The last definition $DP = dP - A \, P$ is taken as the H-covariant derivative of P.

Using the above manipulations, the metric (1.4.6) on G/H can be reexpressed in terms of M as

$$d\phi^i \, d\phi^j \, \gamma_{ij}(\phi) = \frac{1}{4} \left\langle M^{-1} dM, M^{-1} dM \right\rangle, \tag{1.4.9}$$

and the non-linear sigma model (NLSM) field equations can be rewritten in the equivalent forms

$$D^\alpha B_\alpha = 0 \quad \text{or} \quad \nabla^\alpha J_\alpha = 0 \quad \text{or} \quad \nabla^\alpha \left(M^{-1} \partial_\alpha M \right) = 0, \tag{1.4.10}$$

where $D_\alpha B_\beta = \nabla_\alpha B_\beta - [A_\alpha, B_\beta]$. There are dim G currents J and field equations $\nabla J = 0$, but only $\dim G/H$ of them are independent: they obey the identity $\tau(J) = -MJM^{-1}$ since $\tau(M) = M^{-1}$.

1.4.2 Pseudo-Riemannian symmetric spaces

In this case, we have a non-compact Lie group G and an involutive automorphism τ which defines the subgroup H of G as above. We again choose P, decompose $dP\,P^{-1}$, and construct M, γ as before. However, due to the non-compactness of H, γ will not be a positive-definite metric.

2

Background Material: Real forms of Lie Algeras

> The leaning of sophists towards the bypaths of apocrypha is a constant quantity, John Eglinton detected. The highroads are dreary but they lead to the town.
>
> Scylla and Charybdis

This chapter discusses the classification of possible symmetric spaces. Symmetric spaces naturally arise in supergravity [20]. Specifically, Kaluza-Klein compactifications of higher dimensional supergravity theories lead to a large number of scalars, which often get organised in a symmetric space structure. Symmetric spaces that arise in toroidal compactification of ungauged supergravity were famously classified in [12] by Breitenlohner, Gibbons, and Maison. The list in [12] is obtained from the general classification of symmetric spaces by imposing further restrictions. In this chapter we focus on the general list.

The relevant background on this material can be found in [21] and [22], where the two use complementary techniques. We do not state detailed theorems and proofs for lack of space and for clarity of presentation. The material is primarily from [21] with [23] being a secondary reference. We assume familiarity with the structure theory of complex semisimple Lie algebras and their classification, including Dynkin diagrams.

2.1 Real Forms of Lie Algebras

A real Lie algebra $\mathfrak{g}_0$ is called a *real form* of a complex Lie algebra $\mathfrak{g}$ if $\mathfrak{g}$ is the complexification of $\mathfrak{g}_0$,

$$\mathfrak{g} \simeq \mathfrak{g}_0 \otimes_{\mathbb{R}} \mathbb{C}.$$

For example, the Lie algebras $\mathfrak{sl}(p+q;\mathbb{R})$, $\mathfrak{su}(p+q)$ and $\mathfrak{su}(p,q)$ all have the same complex extension, $\mathfrak{sl}(n;\mathbb{C})$. The former algebras are called real forms of $\mathfrak{sl}(n;\mathbb{C})$. Real forms differ in the reality properties imposed on the generators of the algebra, and are related to each other essentially by analytic continuation. Since the various real forms are related to a common complex extension, it is not necessary to write down the commutation relations of all of them. We only need to write the commutation relations for the common complex extension, and through appropriate analytic continuation can obtain the commutation relations for the various real forms.

From the structure theory of Lie algebras, one knows that a general complex Lie algebra generator can be written as

$$\sum_{i=1}^{\text{rank}} c^i H_i + \sum_{\boldsymbol{\alpha}\neq 0} c^{\boldsymbol{\alpha}} E_{\boldsymbol{\alpha}}, \qquad c^i, c^{\boldsymbol{\alpha}} \in \mathbb{C}. \tag{2.1.1}$$

The commutation relations between the $H_i, E_{\boldsymbol{\alpha}}$ are defined by the Dynkin diagram associated with the complex Lie algebra. The Cartan-Killing inner product in this choice of basis is of the form

$$(H_i, H_j) = \delta_{ij}, \qquad (E_{\boldsymbol{\alpha}}, E_{\boldsymbol{\beta}}) = \delta_{\boldsymbol{\alpha}+\boldsymbol{\beta},0}.$$

The *normal real form* of a complex Lie algebra is the subspace where the coefficients in (2.1.1) are restricted to be real, i.e., the space

$$\sum_{i=1}^{\text{rank}} c^i H_i + \sum_{\boldsymbol{\alpha}\neq 0} c^{\boldsymbol{\alpha}} E_{\boldsymbol{\alpha}}, \qquad c^i, c^{\boldsymbol{\alpha}} \in \mathbb{R}. \tag{2.1.2}$$

One can make a change of basis to make the inner product diagonal. We let the basis elements be

$$H_i, \quad \frac{E_{\boldsymbol{\alpha}} + E_{-\boldsymbol{\alpha}}}{\sqrt{2}}, \quad \frac{E_{\boldsymbol{\alpha}} - E_{-\boldsymbol{\alpha}}}{\sqrt{2}}.$$

The trace of the canonical diagonal metric is characteristic of the particular real form of a complex semisimple Lie algebra. This integer is called the *character*, χ, of the real form, and satisfies the relation

$$\chi = (\#\text{ of non-compact generators}) - (\#\text{ of compact generators}) \tag{2.1.3}$$

$$= \dim \mathfrak{g} - 2\dim(\text{maximal compact subalgebra}). \tag{2.1.4}$$

The character in general takes values in $\{-\dim \mathfrak{g}, \ldots, +\text{rank}\, \mathfrak{g}\}$. The character, χ, of the normal form is equal to the rank of the algebra:

$$\chi(\text{normal}) = +(\text{rank}). \tag{2.1.5}$$

A real vector space with signature (N_+, N_-) can be converted to a space with metric $(N_+ + N_-, 0)$ by choosing a new basis,

$$(\mathbf{e}_1, \ldots, \mathbf{e}_{N_+}, \mathbf{e}_{N_+ +1}, \ldots, \mathbf{e}_{N_+ +N_-}) \longrightarrow (\mathbf{e}_1, \ldots, \mathbf{e}_{N_+}, i\mathbf{e}_{N_+ +1}, \ldots, i\mathbf{e}_{N_+ +N_-}) \ .$$

This transformation between mixed and positive metrics is called the *Weyl unitary trick*.

The *compact real form* is obtained from the normal real form by an application of the Weyl unitary trick. With respect to the basis

$$iH_i, \quad \frac{i(E_{\boldsymbol{\alpha}} + E_{-\boldsymbol{\alpha}})}{\sqrt{2}}, \quad \frac{E_{\boldsymbol{\alpha}} - E_{-\boldsymbol{\alpha}}}{\sqrt{2}} \ ,$$

the metric is negative definite, i.e., all generators are compact. For this reason, the real form is called the compact real form of complex Lie algebra $\mathfrak{g}$. For this real form

$$\chi(\text{compact}) = -(\text{dimension}). \tag{2.1.6}$$

It can also be seen easily that the algebra closes, with real structure constants.

2.2 Real Forms of Classical Lie Groups

Any operator, say T, that maps a Lie algebra onto itself is called an *automorphism*, and has the property that

$$(X, Y) = (TX, TY),$$

where $(\cdot, \cdot)$ denotes the Cartan-Killing inner product of the algebra. An automorphism with the property that

$$T^2 = I,$$

is called an *involutive automorphism*. They have eigenvalues ± 1, and split the Lie algebra into corresponding eigen subspaces. Let us decompose a compact simple Lie algebra $\mathfrak{g}$ under an involutive T as

$$\mathfrak{g} = \mathfrak{k} \oplus \mathfrak{p}, \qquad T(\mathfrak{g}) = \mathfrak{k} \oplus (-\mathfrak{p}). \tag{2.2.1}$$

This is called a *Cartan decomposition* of the Lie algebra $\mathfrak{g}$. The subspaces $\mathfrak{k}$ and $\mathfrak{p}$ are orthogonal since

$$(\mathfrak{k}, \mathfrak{p}) = (T\mathfrak{k}, T\mathfrak{p}) = (\mathfrak{k}, -\mathfrak{p}) = -(\mathfrak{k}, \mathfrak{p}).$$

The subspace $\mathfrak{k}$ is also a subalgebra, since it closes under commutation. For $K, K' \in \mathfrak{k}$, $P \in \mathfrak{p}$,

$$([K, K'], P) = (T[K, K'], TP) = ([K, K'], -P) = -([K, K'], P) = 0.$$

Similarly, whenever there are an odd number of $\mathfrak{p}$ in an inner product of the form $(A, [B, C])$, the product vanishes. This gives

$$\begin{aligned} [\mathfrak{k}, \mathfrak{k}] \perp \mathfrak{p} \quad &\Rightarrow \quad [\mathfrak{k}, \mathfrak{k}] \subseteq \mathfrak{k}, \\ [\mathfrak{k}, \mathfrak{p}] \perp \mathfrak{k} \quad &\Rightarrow \quad [\mathfrak{k}, \mathfrak{p}] \subseteq \mathfrak{p}, \\ [\mathfrak{p}, \mathfrak{p}] \perp \mathfrak{p} \quad &\Rightarrow \quad [\mathfrak{p}, \mathfrak{p}] \subseteq \mathfrak{k}. \end{aligned} \tag{2.2.2}$$

So, $\mathfrak{k}$ forms a subalgebra, and $\mathfrak{p}$ is an orthogonal complementary subspace.

Performing Weyl's unitary trick on $\mathfrak{p}$, we get

$$\mathfrak{g}^* = \mathfrak{k} + i\mathfrak{p}, \tag{2.2.3}$$

which is closed under commutation with real structure constants in a basis where $\mathfrak{g}$ has real structure constants, i.e.

$$[\mathfrak{k}, \mathfrak{k}] \subset \mathfrak{k}, \quad [\mathfrak{k}, i\mathfrak{p}] = i\mathfrak{p}, \quad [i\mathfrak{p}, i\mathfrak{p}] \subset (-)\mathfrak{k}.$$

From this discussion, it is clear that the algebra $\mathfrak{g}^*$ is a real form of $\mathfrak{g}$. Also it is clear that by considering different involutions T one can obtain different real forms $\mathfrak{g}^*$. Not surprisingly, it turns out that the classification of the relevant involutions corresponds to a classification of the real forms. There are a number of ways this can be done [22]. A complete discussion of this is beyond the scope of the present chapter. Details can be found in standard references such as [24, 25].

In the next three subsections, following [23], we describe three types of mappings T of matrices into themselves with $T^2 = 1$ that can be used to construct all the real forms of the *classical Lie algebras* beginning from the respective compact real forms. We begin by introducing some notation.

The $n \times n$ *metric-preserving groups* that obey the conditions

$$\begin{gathered} (u_i{}^r)^* g_{rs} u_j{}^s = g_{ij}, \qquad g_{ij} = \epsilon(i)\delta_{ij}, \\ \epsilon(i) = +1 \text{ if } i \in \{1, \ldots, p\}, \qquad \epsilon(i) = -1 \text{ if } i \in \{p+1, \ldots, p+q = n\} \ , \end{gathered} \tag{2.2.4}$$

are $\mathrm{U}(p+q; \mathbb{F})$, where $\mathbb{F} \in \{\mathbb{R}, \mathbb{C}, \mathbb{Q}\}$. The groups are respectively denoted as $\mathrm{O}(p, q; \mathbb{R})$, $\mathrm{U}(p, q; \mathbb{C})$, $\mathrm{U}(p, q; \mathbb{Q})$. Restricting the determinant to be 1, the groups with $\mathbb{F} \in \{\mathbb{R}, \mathbb{C}\}$ become $\mathrm{SO}(p, q; \mathbb{R})$ and $\mathrm{SU}(p, q; \mathbb{C})$. The symplectic group $\mathrm{U}(p, q; \mathbb{Q})$ is generally described by $2n \times 2n$ complex matrices, using the canonical embedding of quaternions into 2×2 complex matrices:

$$a + \mathcal{I}b + \mathcal{J}c + \mathcal{K}d \to \begin{pmatrix} a + id & ib + c \\ ib - c & a - id \end{pmatrix}. \tag{2.2.5}$$

Recall that quaternions are defined as

$$\mathcal{I}^2 = \mathcal{J}^2 = \mathcal{K}^2 = \mathcal{I}\mathcal{J}\mathcal{K} = -1 \tag{2.2.6}$$

The symplectic group is then denoted as $\mathrm{USp}(2p, 2q; \mathbb{C})$.

2.2.1 Block matrix decomposition

Consider the compact classical Lie groups $U(n; \mathbb{F})$, defined via

$$(u_i{}^r)^* g_{rs} u_j{}^s = \delta_{ij} \tag{2.2.7}$$

are $\mathrm{U}(p+q; \mathbb{F})$, where $\mathbb{F} \in \{\mathbb{R}, \mathbb{C}, \mathbb{Q}\}$. Matrices M for the Lie algebras of these groups satisfy

$$M + M^\dagger = 0. \tag{2.2.8}$$

The algebras are respectively for orthogonal, unitary, and symplectic groups depending upon $\mathbb{F} \in \{\mathbb{R}, \mathbb{C}, \mathbb{Q}\}$.

All these compact Lie algebras, denoted $\mathfrak{u}(n; \mathbb{F})$, have a block submatrix decomposition $(n = p + q)$

$$\mathfrak{u}(n; \mathbb{F}) = \begin{pmatrix} A_p & \circ \\ \circ & A_q \end{pmatrix} + \begin{pmatrix} \circ & B \\ -B^\dagger & \circ \end{pmatrix}, \tag{2.2.9}$$

where $A_p^\dagger = -A_p$, $A_q^\dagger = -A_q$, and B is an arbitrary $p \times q$ matrix over $\mathbb{F}$. This is a Cartan decomposition. The procedure outlined above for the construction of real forms using a Cartan decomposition suggests that the off-diagonal block can be multiplied by i. This is equivalent to the map

$$\mathfrak{g} \to T(\mathfrak{g}) = I_{p,q}\, \mathfrak{g}\, I_{p,q}, \qquad I_{p,q} = \begin{pmatrix} I_p & \circ \\ \circ & -I_q \end{pmatrix}.$$

With this transformation, we have changed the algebra $\mathfrak{u}(n; \mathbb{F})$ to $\mathfrak{u}(p, q; \mathbb{F})$, which can be decomposed as

$$\mathfrak{u}(p, q; \mathbb{F}) = \begin{pmatrix} A_p & \circ \\ \circ & A_q \end{pmatrix} + \begin{pmatrix} \circ & B \\ B^\dagger & \circ \end{pmatrix}, \tag{2.2.10}$$

where we have absorbed the factor of i in the matrices B. The real forms obtained in this way are

$$\mathfrak{so}(n) \to \mathfrak{so}(p, q), \qquad \mathfrak{su}(n) \to \mathfrak{su}(p, q), \qquad \mathfrak{sp}(n) \to \mathfrak{sp}(p, q).$$

2.2.2 Subfield restrictions

The real numbers form a subfield of the complex numbers, which are in turn a subfield of the quaternions. Correspondingly, a complex matrix algebra can be split into real and imaginary parts, and similarly quaternionic matrix algebras can be split into a complex part and the remainder.

For example, the Lie algebra $\mathfrak{su}(n)$ of complex traceless skew-Hermitian matrices has a subalgebra of real antisymmetric matrices, $\mathfrak{so}(n)$,

$$\mathfrak{su}(n) = \mathfrak{so}(n) + [\mathfrak{su}(n) - \mathfrak{so}(n)] = A_n + iS_n, \tag{2.2.11}$$

where S_n comprises real symmetric traceless matrices. Performing Weyl's unitary trick on this Cartan decomposition, we get the subalgebra $\mathfrak{sl}(n;\mathbb{R})$,

$$\mathfrak{su}(n) \to \mathfrak{sl}(n;\mathbb{R}) = \mathfrak{so}(n) + i[\mathfrak{su}(n) - \mathfrak{so}(n)] = A_n + S_n. \tag{2.2.12}$$

The Lie group generated by this real form is $\mathrm{SL}(n;\mathbb{R})$.

Via a similar procedure, the compact real form $\mathfrak{sp}(n)$ can be transformed into the split real form, $\mathfrak{sp}(2n;\mathbb{R})$. Recall that there is an embedding of $\mathbb{Q},\mathbb{C}$ into $\mathbb{C},\mathbb{R}$, respectively, given as 2×2 matrices over the subfield. These embeddings are explicitly given as

$$a+ib \to \begin{pmatrix} a & b \\ -b & a \end{pmatrix}, \qquad a+\mathcal{I}b+\mathcal{J}c+\mathcal{K}d \to \begin{pmatrix} a+id & ib+c \\ ib-c & a-id \end{pmatrix}, \tag{2.2.13}$$

where $\mathcal{I}^2=\mathcal{J}^2=\mathcal{K}^2=-1, \mathcal{I}\mathcal{J}=\mathcal{K}$. With the replacement of complex numbers by reals, $\mathfrak{u}(n;\mathbb{C})$ becomes an algebra of $2n\times 2n$ real matrces, which we call $\mathfrak{ou}(2n)$, since this is an orthogonal representation of the unitary algebra. With the replacement of quaternions by the complex numbers, $\mathfrak{sp}(n)=\mathfrak{u}(n;\mathbb{Q})$ becomes an algebra of $2n\times 2n$ complex matrices, which we call $\mathfrak{usp}(2n)$, since this is a unitary representation of the symplectic algebra. $\mathfrak{usp}(2n)$ can be further decomposed into a real subalgebra, $\mathfrak{ou}(2n)$, and the complementary subspace. Performing the unitary trick on this Cartan decomposition gives the real form $\mathfrak{sp}(2n;\mathbb{R})$:

$$\begin{aligned} \mathfrak{sp}(n) \xrightarrow{\mathbb{Q}\to\mathbb{C}} \mathfrak{usp}(2n) &= \mathfrak{ou}(2n) + [\mathfrak{usp}(2n) - \mathfrak{ou}(2n)] \\ &\to \mathfrak{ou}(2n) + i[\mathfrak{usp}(2n) - \mathfrak{ou}(2n)] = \mathfrak{sp}(2n;\mathbb{R}). \end{aligned} \tag{2.2.14}$$

2.2.3 Field embeddings

The image of $\mathfrak{u}(n) \to \mathfrak{ou}(2n)$ consists of a set of $2n\times 2n$ antisymmetric matrices which is clearly a subset of $\mathfrak{so}(2n)$. As a result, $\mathfrak{ou}(2n)$ is a subalgebra of $\mathfrak{so}(2n)$, and one can write a Cartan decomposition with $\mathfrak{g}=\mathfrak{so}(2n), \mathfrak{k}=\mathfrak{ou}(2n)$, providing us with a new real form

$$\mathfrak{so}(2n) = \mathfrak{ou}(2n) + [\mathfrak{so}(2n) - \mathfrak{ou}(2n)] \longrightarrow \mathfrak{ou}(2n) + i[\mathfrak{so}(2n) - \mathfrak{ou}(2n)] = \mathfrak{so}^*(2n). \tag{2.2.15}$$

In a similar manner, $\mathfrak{usp}(2n)$ is a subalgebra of $\mathfrak{su}(2n)$, and provides a Cartan decomposition and a real form,

$$\mathfrak{su}(2n) = \mathfrak{usp}(2n) + [\mathfrak{su}(2n) - \mathfrak{usp}(2n)] \to \mathfrak{usp}(2n) + i[\mathfrak{su}(2n) - \mathfrak{usp}(2n)] = \mathfrak{su}^*(2n). \tag{2.2.16}$$

These operations exhaust the list of real forms. Table 2.1 summarises our results.

Table 2.1: Summary of the real forms of the classical groups

Process	non-compact Group G^*	Maximal Compact Subgroup K	Associated Compact Group G	Dimension of Coset Space G^*/K or G/K
Indefinite	$\mathrm{SO}(p,q)$	$\mathrm{SO}(p)\otimes\mathrm{SO}(q)$	$\mathrm{SO}(p+q)$	pq
metric (p,q)	$\mathrm{SU}(p,q)$	$\mathrm{S}\left[\mathrm{U}(p)\otimes\mathrm{U}(q)\right]$	$\mathrm{SU}(p+q)$	$2pq$
preserving groups	$\mathrm{USp}(2p,2q)$ $\simeq \mathrm{U}(p,q;\mathbb{Q})$	$\mathrm{USp}(2p)\otimes\mathrm{USp}(q)$ $\simeq \mathrm{U}(p;\mathbb{Q})\otimes\mathrm{U}(q;\mathbb{Q})$	$\mathrm{USp}(2p+2q)$ $\simeq \mathrm{U}(p+q;\mathbb{Q})$	$4pq$
Subfield restriction	$\mathrm{SL}(n,\mathbb{R})$	$\mathrm{SO}(n)$	$\mathrm{SU}(n,\mathbb{C})$	$\frac{n(n+1)}{2}-1$
	$\mathrm{Sp}(2n;\mathbb{R})$	$\mathrm{U}(n;\mathbb{C})$	$\mathrm{USp}(2n)$ $\simeq \mathrm{U}(n;\mathbb{Q})$	$n(n+1)$
Embedding groups	$\mathrm{SO}^*(2n)$	$\mathrm{U}(n;\mathbb{C})$	$\mathrm{SO}(2n)$	$n(n-1)$
	$\mathrm{SU}^*(2n)$	$\mathrm{USp}(2n)$ $\simeq \mathrm{U}(n;\mathbb{Q})$	$\mathrm{SU}(2n)$	$\frac{2n(2n-1)}{2}-1$

2.2.4 Cosets

Each of the non-compact groups, e.g., $\mathrm{SU}(p,q;\mathbb{C})$, $\mathrm{SO}(p,q;\mathbb{R})$, $\mathrm{USp}(2p,2q)$ has associated with it a non-compact Lie algebra $\mathfrak{g}^*$, as discussed above. One has $\mathfrak{g}^* = \mathfrak{k}\oplus\mathfrak{p}^*$, where $\mathfrak{k}$ is the subalgebra consisting of all compact generators, and $\mathfrak{p}^*$ consists of the remaining generators, all non-compact. The compact subalgebra $\mathfrak{k}$ generates the maximal compact subgroups, i.e., $\mathrm{S}\left[\mathrm{U}(p)\otimes\mathrm{U}(q)\right]$, $\mathrm{SO}(p)\otimes\mathrm{SO}(q)$, $\mathrm{USp}(2p)\otimes\mathrm{USp}(2q)$ for $\mathrm{SU}(p,q;\mathbb{C})$, $\mathrm{SO}(p,q;\mathbb{R})$, $\mathrm{USp}(2p,2q)$, respectively. The subspace $\mathfrak{p}^*$ is the orthogonal complement to $\mathfrak{k}$, and is not closed under commutation. This decomposition of the Lie algebra has a counterpart in the Lie group as the coset decomposition. If G^* is a non-compact Lie group and K the maximal subgroup, then we can write $G^* = P^*K$ or $G^* = KP^*$. A natural choice for the coset representatives is $\exp\mathfrak{p}^*$, which is non-compact.

2.3 Real Forms of the Symmetric Spaces

The spaces considered so far have been exclusively cosets of the form G/K or G^*/K, with G the compact real form of the complex extension $G^{\mathbb{C}}$, and G^* the normal real form of $G^{\mathbb{C}}$ dual to G; K is the maximal compact subgroup of the non-compact G^*. G/K has a negative definite metric induced from the Cartan-Killing form, while G^*/K has a positive definite metric on the subspace $i\mathfrak{p}\subset\mathfrak{g}$. Thus the symmetric spaces are all Riemannian spaces.

There is a rich structure of real forms between G and G^*, which is inherited by the coset spaces: a rich structure of "real forms" of the "complex extension" coset spaces $(G/K)^{\mathbb{C}} \simeq G^{\mathbb{C}}/K^{\mathbb{C}}$. The spaces G/K and G^*/K appear as the "boundary spaces", endowed with negative and positive definite metric, with all intermediate real forms of $G^{\mathbb{C}}/K^{\mathbb{C}}$ having indefinite signature.

Such pseudo-Riemannian symmetric spaces are cosets of a non-compact group by a maximal (non-compact) subgroup. Let $\mathfrak{g}$ be a simple Lie algebra with complex extension $\mathfrak{g}^{\mathbb{C}}$, and $\mathfrak{g}^*$ a real form of $\mathfrak{g}^{\mathbb{C}}$. Then, it is possible to find an involutive automorphism τ of

$\mathfrak{g}^*$ with the properties:

$$\begin{aligned} \mathfrak{g}^* &= \mathfrak{h} \oplus \mathfrak{m}, \\ \tau(\mathfrak{g}^*) &= \mathfrak{h} \oplus (-\mathfrak{m}), \end{aligned} \tag{2.3.1}$$

where, as before, we can argue that

$$(\mathfrak{h}, \mathfrak{m}) = 0.$$

Inner products of the form

$$([X, Y], Z), \qquad X, Y, Z \text{ in either } \mathfrak{h} \text{ or } \mathfrak{m},$$

vanish if an odd number of the vectors are in $\mathfrak{m}$. Since $\mathfrak{g}^*$ is simple, we have

$$\begin{aligned} ([\mathfrak{h}, \mathfrak{h}], \mathfrak{m}) = 0 \qquad &\Rightarrow [\mathfrak{h}, \mathfrak{h}] \subseteq \mathfrak{h} \\ ([\mathfrak{h}, \mathfrak{m}], \mathfrak{h}) = 0 \qquad &\Rightarrow [\mathfrak{h}, \mathfrak{m}] = \mathfrak{m} \\ ([\mathfrak{m}, \mathfrak{m}], \mathfrak{m}) = 0 \qquad &\Rightarrow [\mathfrak{m}, \mathfrak{m}] \subseteq \mathfrak{h} \end{aligned}$$

The Lie algebra $\mathfrak{g}^*$ was itself obtained from $\mathfrak{g}$ by an involutive automorphism σ:

$$\mathfrak{g} = \mathfrak{k} \oplus \mathfrak{p}, \qquad \sigma(\mathfrak{g}) = \mathfrak{k} \oplus (-\mathfrak{p}), \qquad \mathfrak{g}^* = \mathfrak{k} \oplus i\mathfrak{p}. \tag{2.3.2}$$

Similarly to the Riemannian spaces, which are obtained as coset spaces in the following manner,

$$\frac{G}{K_\sigma} = \exp \mathfrak{g} \bmod \mathfrak{k} = \exp \mathfrak{p}, \qquad \frac{G^*}{K} = \frac{G^\sigma}{K_\sigma} = \exp \mathfrak{g}^* \bmod \mathfrak{k} = \exp i\mathfrak{p}, \tag{2.3.3}$$

the pseudo-Riemannian symmetric coset spaces are obtained as

$$\frac{G^\sigma}{H_\tau} = \exp \mathfrak{g}^* \bmod \mathfrak{h} = \exp \mathfrak{m}, \qquad \left(\frac{G^\sigma}{H}\right)^\tau = \frac{G^{\sigma\tau}}{H_\tau} = \exp(\mathfrak{g}^*)^{*'} \bmod \mathfrak{h} = \exp i\mathfrak{m}. \tag{2.3.4}$$

Since σ splits $\mathfrak{g}$, any vector in $\mathfrak{k}\,(i\mathfrak{p})$ is an eigenvector of σ with eigenvalue $+1\,(-1)$. Since τ splits $\mathfrak{g}^*$, any vector in $\mathfrak{h}\,(\mathfrak{m}, i\mathfrak{m})$ is an eigenvector of τ with eigenvalue $+1\,(-1)$. The four subspaces $\mathfrak{g}_{\sigma\tau}$ exhaust $\mathfrak{g}$:

$$\mathfrak{g} = \mathfrak{g}_{++} \oplus \mathfrak{g}_{+-} \oplus \mathfrak{g}_{-+} \oplus \mathfrak{g}_{--}. \tag{2.3.5}$$

The maps σ, τ commute, and their simultaneous eigenvalues have just been used to describe $\mathfrak{g}$. Then, $\sigma, \tau, \sigma\tau$ are all involutive automorphisms and appear on an equal footing. By using the eigenvalues of σ, τ, one can see that

$$[\mathfrak{g}_{\sigma\tau}, \mathfrak{g}_{\sigma'\tau'}] \subseteq \mathfrak{g}_{\sigma\sigma', \tau\tau'}. \tag{2.3.6}$$

From this, it is possible to conclude which subspaces of $\mathfrak{g}$ are closed under commutation, e.g.,

Eigenspace with eigenvalue $+1$ of	Closed under commutation
$\mathrm{Id}, \sigma, \tau, \sigma\tau$	$\mathfrak{g}_{++}$
Id, σ	$\mathfrak{g}_{++} \oplus \mathfrak{g}_{+-}$
Id, τ	$\mathfrak{g}_{++} \oplus \mathfrak{g}_{-+}$
$\mathrm{Id}, \sigma\tau$	$\mathfrak{g}_{++} \oplus \mathfrak{g}_{--}$
Id	$\mathfrak{g}_{++} \oplus \mathfrak{g}_{+-} \oplus \mathfrak{g}_{-+} \oplus \mathfrak{g}_{--}$

2.3.1 Tables of the Real Forms

The possible involutions σ have already been listed, which also are the possible τ. The classification of all pseudo-Riemannian spaces proceeds by applying all possible mappings τ to all possible real forms already listed.

In terms of the Lie algebra decomposition, we have

$$\begin{aligned}\frac{G^\sigma}{H_\tau} &= \exp\Big\{\big(\mathfrak{g}_{++}\oplus\mathfrak{g}_{+-}\big)\oplus i\big(\mathfrak{g}_{-+}\oplus\mathfrak{g}_{--}\big)\bmod\big(\mathfrak{g}_{++}\oplus i\mathfrak{g}_{-+}\big)\Big\}\\ &= \exp\big(\mathfrak{g}_{+-}\oplus i\mathfrak{g}_{--}\big), \qquad (2.3.7)\\ \left(\frac{G^\sigma}{H}\right)^\tau &= \frac{G^{\sigma\tau}}{H_\tau} = \exp i\mathfrak{m} = \exp\big(i\mathfrak{g}_{+-}\ominus\mathfrak{g}_{--}\big). \qquad (2.3.8)\end{aligned}$$

One can draw the following diagram.

$$\begin{array}{ccccc}\mathfrak{g} & \xrightarrow{\ \tau\ } & \mathfrak{g}^\tau = \big(\mathfrak{g}_{++}\oplus\mathfrak{g}_{-+}\big)\oplus i\big(\mathfrak{g}_{+-}\oplus\mathfrak{g}_{--}\big) & & \\ & & \Big\downarrow \sigma:\mathfrak{k}_\tau\to\mathfrak{h}_\tau \qquad \Big\downarrow \sigma:\frac{G^\tau}{K_\tau}\to\frac{G^{\sigma\tau}}{H_\tau} & & \\ & & \big(\mathfrak{g}_{++}\oplus i\mathfrak{g}_{-+}\big)\oplus i\big(\mathfrak{g}_{+-}\oplus i\mathfrak{g}_{--}\big) & & \\ & & \mathfrak{h} \qquad\quad \oplus \qquad\quad i\mathfrak{m} & & \end{array} \qquad (2.3.9)$$

This discussion can be summarized as follows. The real forms of symmetric spaces are completely determined by a compact group G and by two involutions, σ,τ. One involution, say τ, singles out a compact subgroup $K_\tau=\exp(\mathfrak{g}_{++}\oplus\mathfrak{g}_{-+})$ and a symmetric space $\exp(i)(\mathfrak{g}_{+-}\oplus\mathfrak{g}_{--})$ with a definite metric. The other involution σ converts the compact subgroup to a non-compact subgroup,

$$K_\tau=\exp(\mathfrak{g}_{++}\oplus\mathfrak{g}_{-+})\xrightarrow{\sigma}\exp(\mathfrak{g}_{++}\oplus i\mathfrak{g}_{-+})=H_\tau={K_\tau}^\sigma, \qquad (2.3.10)$$

and converts the symmetric space with a definite metric to one with an indefinite metric,

$$\frac{G^{(*)}}{K_\tau}=\exp(i)(\mathfrak{g}_{+-}\oplus\mathfrak{g}_{--})\xrightarrow{\sigma}\exp(i)(\mathfrak{g}_{+-}\oplus i\mathfrak{g}_{--})=\frac{G^{(\sigma)\tau}}{{K_\tau}^\sigma}=\frac{G^{(\sigma)\tau}}{H_\tau}. \qquad (2.3.11)$$

Other real forms related to (2.3.9) are obtained by interchanging the order in which σ and τ are applied and by using $\sigma\tau$.

2.4 Example: Real Forms of D_4

Here we work out all the real forms of the root space D_4 corresponding to the complex Lie group $\mathrm{SO}(8,\mathbb{C})$. The Lie algebra comprises 8×8 complex skew-symmetric matrices. The compact real form $\mathfrak{so}(8,\mathbb{R})$ consists then of real skew-symmetric 8×8 matrices. Let us first apply the three involutions T once to the Lie algebra $\mathfrak{so}(8,\mathbb{R})$.

2.4.1 Block Matrix Decomposition

The compact Lie algebra $\mathfrak{so}(8,\mathbb{R})$ has a block submatrix decomposition, with $n=p+q$, as

$$\mathfrak{so}(8,\mathbb{R})=\begin{pmatrix}A_p & \circ\\ \circ & A_q\end{pmatrix}+\begin{pmatrix}\circ & B\\ -B^T & \circ\end{pmatrix}\quad(\equiv\mathfrak{k}\oplus\mathfrak{p}),$$

where A_p, A_q are $p \times p$ and $q \times q$ skew-symmetric matrices and B is an arbitrary $p \times q$ matrix with real entries.

Under the map $T(\mathfrak{g}) = I_{p,q}\mathfrak{g}I_{p,q}$, where

$$I_{p,q} = \begin{pmatrix} I_p & \circ \\ \circ & -I_q \end{pmatrix},$$

the subspace of block-diagonal matrices, $\mathfrak{k}$, has eigenvalue 1, and the block off-diagonal subspace, $\mathfrak{p}$, has eigenvalue -1. Performing Weyl's unitary trick, by sending $\mathfrak{p} \to i\mathfrak{p}$, we obtain the algebras $\mathfrak{g}^* = \mathfrak{k} \oplus i\mathfrak{p}$, which are the algebras for $\mathfrak{so}(p, q, \mathbb{R})$,

$$\mathfrak{so}(p, q, \mathbb{R}) = \begin{pmatrix} A_p & \circ \\ \circ & A_q \end{pmatrix} + \begin{pmatrix} \circ & B \\ B^T & \circ \end{pmatrix} \quad (\equiv \mathfrak{k} \oplus i\mathfrak{p}).$$

The compact subalgebras for the real forms are $\mathfrak{so}(p) \oplus \mathfrak{so}(q)$, so that the associated Riemannian symmetric spaces are of the form $\mathrm{SO}(p, q)/(\mathrm{SO}(p) \times \mathrm{SO}(q))$.

2.4.2 Subfield restriction

Since the compact real form $\mathfrak{so}(8, \mathbb{R})$ consists of real skew-symmetric matrices, the action of complex conjugations on the compact form is trivial. One does not obtain any new real forms by this conjugation.

2.4.3 Field embedding

The algebra $\mathfrak{u}(4)$ of 4×4 skew-Hermitian matrices can be written as an algebra of 8×8 skew-symmetric matrices using, e.g., the map that sends

$$a + ib \to \begin{pmatrix} a & b \\ -b & a \end{pmatrix}.$$

This algebra of 8×8 matrices, which we call $\mathfrak{ou}(8)$, is obviously a subalgebra of $\mathfrak{so}(8, \mathbb{R})$. Then, one can write a Cartan decomposition of $\mathfrak{so}(8, \mathbb{R})$ with $\mathfrak{k} = \mathfrak{ou}(8)$, and perform Weyl's unitary trick. This also gives the real form $\mathfrak{so}^*(8)$,

$$\mathfrak{so}(8) = \mathfrak{ou}(8) + [\mathfrak{so}(8) - \mathfrak{ou}(8)] \to \mathfrak{ou}(8) + i[\mathfrak{so}(8) - \mathfrak{ou}(8)] = \mathfrak{so}^*(8).$$

It is clear from this construction that the compact subalgebra of the real form is $\mathfrak{u}(4) = \mathfrak{su}(4) \oplus \mathfrak{u}(1)$. The associated Riemannian symmetric space is $\mathrm{SO}^*(8)/(\mathrm{SU}(4) \times \mathrm{U}(1))$.

2.4.4 Real forms of symmetric spaces

We first list all the Riemannian symmetric spaces that we have obtained. These are, with $p + q = 8$,

1. $\dfrac{\mathrm{SO}(p+q)}{\mathrm{SO}(p) \times \mathrm{SO}(q)}$
2. $\dfrac{\mathrm{SO}(p,q)}{\mathrm{SO}(p) \times \mathrm{SO}(q)}$
3. $\dfrac{\mathrm{SO}^*(8)}{\mathrm{SU}(4) \times \mathrm{U}(1)}$

To get all possible (pseudo-Riemannian) symmetric spaces from D_4, we need to apply the three involutions again on the real forms of D_4. Following the procedure outlined above, successive use of, for example, two involutions of the type $I_{p,q}$ will give rise to the coset spaces $\frac{\mathrm{SO}(p,q)}{\mathrm{SO}(h,k)\times\mathrm{SO}(p-h,q-k)}$. Using $I_{p,q}$ and field embedding, one can get the coset spaces $\frac{\mathrm{SO}(2p,2q)}{\mathrm{SU}(p,q)\times\mathrm{U}(1)}$. All other cosets can be generated similarly by the use of the involutions.

3

Geroch Group Description of Bubbling Geometries

So then the citizen begins...

Cyclops

3.1 Introduction

The Riemann-Hilbert approach [26, 27] to studying solutions to supergravity theories is remarkable in that it allows to study solutions that effectively only depend on two spacetime coordinates in terms of spacetime independent monodromy matrices. More precisely, on the one hand, to a given solution one can associate a monodromy matrix, on the other hand, given a candidate monodromy matrix one can perform its canonical factorisation with prescribed analyticity properties to obtain explicit solutions of supergravity theories.

Thus, in this approach, the problem of solving non-linear partial differential equations to obtain solutions of supergravity, is mapped into a matrix valued factorisation problem in one complex variable. This approach offers significant insight into duality symmetries of supergravity theories, and also into the organisation and classification of its solutions. It is closely related to the so-called inverse scattering approach [28–30] that has been astonishingly successful for understanding solutions of five-dimensional vacuum gravity [31–33].

In order to obtain explicit solutions in the Riemann-Hilbert approach a canonical factorisation must be performed. Over the last few years at least two different approaches have been developed. In the first approach [16, 34–36], the authors have focused on monodromy matrices with simple poles with suitable rank residues. In the the second approach [37, 38], the authors have converted the matrix valued factorisation problem into a vectorial Riemann-Hilbert problem and solved it using complex analysis. Several examples have been worked out in both these approaches. A construction of the JMaRT [18] solution was worked out in [35], and its relation to the Belinsky-Zakharov inverse scattering construction was explored in [39].

In this chapter we initiate a systematic study of monodromy matrices for multi-center solutions. The main motivation for this study is as follows. A generalisation of various known multi-center solutions to non-supersymmetric setting is a problem that has received much attention in recent years [40–44], and a variety of solutions have been obtained. Alternative approaches to such solutions, together with developments of different techniques, are much desirable to understand better the spectrum and dynamics of such solutions. In this chapter we take first steps in this direction.

We obtain monodromy matrices for a class of collinear Bena-Warner bubbling geometries [19, 45]. We consider these solutions as embedded in five-dimensional $U(1)^3$ supergravity. The five-dimensional $U(1)^3$ supergravity has SO(4,4) hidden symmetry when reduced to three-dimensions, and it has affine SO(4,4) (an infinite dimensional symmetry) as its two-dimensional duality symmetry group. This affine symmetry is called the Geroch group. The monodromy matrices are matices in this group: 8×8 matrices of one complex variable in the defining representation of SO(4,4).

We show that for collinear Bena-Warner bubbling solutions, monodromy matrices have only simple poles with residues of rank two and nilpotency degree two. These are precisely some of the conditions required for the Riemann-Hilbert factorisation developed in [16]. We have not explored the explicit factorisation of monodromy matrices in this work; we leave this investigation for future studies.

The rest of the chapter is organised as follows. In section 3.2 we present an appropriate dimensional reduction of five-dimensional $U(1)^3$ supergravity to three dimensions. This dimensional reduction is well adapted to obtain a coset description of the Bena-Warner solutions, which is worked out in detail in section 3.3. The Bena-Warner class of solutions have two well studied symmetries called "gauge transformations" and "spectral flow transformations" [46]. Under these transformations solutions are mapped to solutions within the Bena-Warner class. We show that from the three-dimensional duality symmetry point of view, the so-called "gauge transformations" are simple shifts of certain three-dimensional scalars, and the so-called "spectral flow transformations" are a class of Harrison transformations.

In section 3.4 we obtain the Geroch group (monodromy) matrices for collinear multicenter bubbling solutions. In section 3.5 we work out a few illustrative but non-trivial examples. We end with a brief summary and possible future directions in section 3.6. In the appendix to this chapter, 3.7, we work out explicit representatives for smaller nilpotent orbits of the $\mathfrak{so}(4,4)$ Lie algebra. We list matrix rank and nilpotency degree of these representatives in the defining representation of $\mathfrak{so}(4,4)$.

3.2 Dimensional reduction

We start by presenting an appropriate dimensional reduction of five-dimensional $U(1)^3$ supergravity to three dimensions. It is well known that the $U(1)^3$ supergravity when dimensionally reduced to three-dimensions has an SO(4,4) symmetry. In this section we make this manifest, and the notation introduced in the discussion will be used through the rest of the chapter. The sign conventions below are same as [47] except for the over-all sign of the Chern-Simons term in the 11d action; we refer the reader to that reference for further details and references. This sign difference results in different signs compared to that reference in some equations.

Our starting point is the Lagrangian of eleven-dimensional supergravity,

$$\mathcal{L}_{11} = R_{11} \star_{11} \mathbf{1} - \frac{1}{2} F_{[4]} \wedge \star_{11} F_{[4]} - \frac{1}{6} F_{[4]} \wedge F_{[4]} \wedge A_{[3]}. \tag{3.2.1}$$

We are interested in the five-dimensional theory obtained by dimensional reduction on T^6 with the following metric ansatz,

$$ds_{11}^2 = ds_5^2 + h^1(d\tilde{x}_1^2 + d\tilde{x}_2^2) + h^2(d\tilde{x}_3^2 + d\tilde{x}_4^2) + h^3(d\tilde{x}_5^2 + d\tilde{x}_6^2), \tag{3.2.2}$$

together with the form-field ansatz,

$$A_{[3]} = A^1_{[1]} \wedge d\tilde{x}_1 \wedge d\tilde{x}_2 + A^2_{[1]} \wedge d\tilde{x}_3 \wedge d\tilde{x}_4 + A^3_{[1]} \wedge d\tilde{x}_5 \wedge d\tilde{x}_6. \tag{3.2.3}$$

We work with the assumption that nothing depends on the six torus coordinates $\tilde{x}_i$. We also assume that the scalars h^I, with $I = 1, 2, 3$, obey the constraint[1]

$$h^1 h^2 h^3 = 1, \tag{3.2.4}$$

i.e., we assume that all complex structure moduli of the T^6 as well as the volume modulus are frozen. The constraint (3.2.4) ensures that the resulting five-dimensional metric is in the Einstein frame. The eleven dimensional Lagrangian reduces to the five-dimensional $U(1)^3$ supergravity,

$$\mathcal{L}_5 = R_5 \star_5 \mathbf{1} - \frac{1}{2} G_{IJ} \star_5 dh^I \wedge dh^J - \frac{1}{2} G_{IJ} \star_5 F^I_{[2]} \wedge F^J_{[2]} - \frac{1}{6} C_{IJK} F^I_{[2]} \wedge F^J_{[2]} \wedge A^K_{[1]}, \tag{3.2.5}$$

where $C_{IJK} = |\epsilon_{IJK}|$, and G_{IJ} is diagonal with entries $G_{II} = (h^I)^{-2}$. Note that the constraint (3.2.4) must be solved before computing variations of the action in order to obtain equations of motion for various fields. It can be solved, say, with the following choice,

$$h^1 = e^{\sqrt{\frac{2}{3}}\Psi}, \quad h^2 = e^{-\sqrt{\frac{1}{6}}\Psi - \sqrt{\frac{1}{2}}\Phi}, \quad h^3 = e^{-\sqrt{\frac{1}{6}}\Psi + \sqrt{\frac{1}{2}}\Phi}. \tag{3.2.6}$$

3.2.1 Timelike reduction: 5d to 4d

To perform Kaluza-Klein reduction from five-dimensions to four-dimensions we parameterize our 5d spacetime as

$$ds^2 = \epsilon_1 f^2 (dt + \check{A}^0_{[1]})^2 + f^{-1} ds^2_4, \tag{3.2.7}$$

and 5d vectors as

$$A^I_{[1]} = \chi^I (dt + \check{A}^0_{[1]}) + \check{A}^I_{[1]}, \tag{3.2.8}$$

where we use ϵ_1 to keep track of minus signs. The case of interest for the present discussion is $\epsilon_1 = -1$. The timelike reduction is thought of as an effective simplification of the five-dimensional dynamics in the presence of ∂_t Killing vector.

The 4d graviphoton $\check{A}^0_{[1]}$ and the 4d vectors $\check{A}^I_{[1]}$ form a symplectic vector $\check{A}^\Lambda_{[1]}$ with $\Lambda = 0, 1, 2, 3$. We define the field strength for these vectors as simply $F^\Lambda_{[2]} = d\check{A}^\Lambda_{[1]}$. Inserting ansatzes (3.2.7) and (3.2.8) in Lagrangian (3.2.5) we obtain,

$$\begin{aligned}
\mathcal{L}_4 = {} & R \star_4 \mathbf{1} - \frac{1}{2} G_{IJ} \star_4 dh^I \wedge dh^J - \frac{3}{2f^2} \star_4 df \wedge df - \epsilon_1 \frac{f^3}{2} \star_4 \check{F}^0_{[2]} \wedge \check{F}^0_{[2]} \\
& - \epsilon_1 \frac{1}{2f^2} G_{IJ} \star_4 d\chi^I \wedge d\chi^J - \frac{f}{2} G_{IJ} \star_4 (\check{F}^I_{[2]} + \chi^I \check{F}^0_{[2]}) \wedge (\check{F}^J_{[2]} + \chi^J \check{F}^0_{[2]}) \\
& - \frac{1}{2} C_{IJK} \chi^I \check{F}^J_{[2]} \wedge \check{F}^K_{[2]} - \frac{1}{2} C_{IJK} \chi^I \chi^J \check{F}^0_{[2]} \wedge \check{F}^K_{[2]} - \frac{1}{6} C_{IJK} \chi^I \chi^J \chi^K \check{F}^0_{[2]} \wedge \check{F}^0_{[2]} \,.
\end{aligned} \tag{3.2.9}$$

Note that the sign of the kinetic term for the graviphoton $\check{F}^0_{[2]}$ and that for the scalars χ^I depend on the sign ϵ_1.

The reduced Lagrangian (3.2.9) can be obtained from a cubic prepotential using split complex numbers, where the imaginary unit e squares to $+1$ instead of -1, $\bar{e} = -e$, $e^2 = +1$. Specifically, taking

$$F(X) = -\frac{X^1 X^2 X^3}{X^0}, \tag{3.2.10}$$

[1] For a discussion on the constraint (3.2.4) see e.g. [48]. We thank E. Colgáin for bringing this reference to our attention.

and using the gauge $X^0 = 1$ and $X^I = -\chi^I + efh^I$, Lagrangian (3.2.9) with $\epsilon_1 = -1$ is seen to be identical to

$$\mathcal{L}_4 = R \star_4 \mathbf{1} - 2g_{I\bar{J}} \star_4 dX^I \wedge d\bar{X}^{\bar{J}} + \frac{1}{2}\check{F}^{\Lambda}_{[2]} \wedge \check{G}_{\Lambda[2]}, \tag{3.2.11}$$

where $\check{F}^{\Lambda}_{[2]} = d\check{A}^{\Lambda}_{[1]}$. The indices I, J run from 1 to 3, and $g_{I\bar{J}} = \partial_I \partial_{\bar{J}} K$ with the potential

$$K = -\log\left[-e(\bar{X}^{\Lambda}F_{\Lambda} - \bar{F}_{\Lambda}X^{\Lambda})\right], \tag{3.2.12}$$

and where $F_\Lambda = \partial_\Lambda F$. The two form $\check{G}_{\Lambda[2]}$ is defined as

$$\check{G}_{\Lambda[2]} = -(\mathrm{Re}N)_{\Lambda\Sigma}\check{F}^{\Sigma}_{[2]} + (\mathrm{Im}N)_{\Lambda\Sigma} \star_4 \check{F}^{\Sigma}_{[2]}, \tag{3.2.13}$$

where the split complex symmetric matrix $N_{\Lambda\Sigma}$ is constructed from the prepotential as

$$N_{\Lambda\Sigma} = \bar{F}_{\Lambda\Sigma} + 2e\frac{(\mathrm{Im}F \cdot X)_\Lambda (\mathrm{Im}F \cdot X)_\Sigma}{X \cdot \mathrm{Im}F \cdot X}, \tag{3.2.14}$$

and where $F_{\Lambda\Sigma} = \partial_\Lambda \partial_\Sigma F$. Explicitly, the Re$N$ and ImN matrices are as follows

$$\mathrm{Re}N = \begin{pmatrix} 2\chi_1\chi_2\chi_3 & \chi_2\chi_3 & \chi_1\chi_3 & \chi_1\chi_2 \\ \chi_2\chi_3 & 0 & \chi_3 & \chi_2 \\ \chi_1\chi_3 & \chi_3 & 0 & \chi_1 \\ \chi_1\chi_2 & \chi_2 & \chi_1 & 0 \end{pmatrix}, \tag{3.2.15}$$

$$\mathrm{Im}N = f \begin{pmatrix} f^2 + \sum_{i=1}^{3} \frac{\chi_i^2}{(h^i)^2} & -\frac{\chi_1}{(h^1)^2} & -\frac{\chi_2}{(h^2)^2} & -\frac{\chi_3}{(h^3)^2} \\ -\frac{\chi_1}{(h^1)^2} & -\frac{1}{(h^1)^2} & 0 & 0 \\ -\frac{\chi_2}{(h^2)^2} & 0 & -\frac{1}{(h^2)^2} & 0 \\ -\frac{\chi_3}{(h^3)^2} & 0 & 0 & -\frac{1}{(h^3)^2} \end{pmatrix}. \tag{3.2.16}$$

3.2.2 Spacelike reduction: 4d to 3d

Now we perform a spacelike reduction from four to three dimensions. For this we parameterize our four-dimensional space as

$$ds_4^2 = e^{2U}(dz + \omega_3)^2 + e^{-2U}ds_3^2, \tag{3.2.17}$$

and the 4d one-forms as

$$\check{A}^{\Lambda}_{[1]} = \zeta^{\Lambda}(dz + \omega_3) + A_3^{\Lambda}, \tag{3.2.18}$$

where A_3^Λ and ω_3 are three-dimensional one-forms. We define the field strengths simply as $F_3^\Lambda := dA_3^\Lambda$ and $F_3 := d\omega_3$. Since in three dimensions, vector fields are dual to scalars, we now dualise vectors A_3^Λ and ω_3 into scalars $\tilde{\zeta}_\Lambda$ and σ. The procedure of dualisation interchanges the role of Bianchi identities and field equations. The easiest way to achieve dualisation is to treat F_3^Λ and F_3 as fundamental fields in their own right and impose Bianchi identities through Lagrange multipliers. To this end we add the following Lagrange multiplier terms to the 3d Lagrangian

$$+ \tilde{\zeta}_\Lambda F_3^\Lambda + \frac{1}{2}(\sigma + \zeta^\Lambda \tilde{\zeta}_\Lambda)F_3. \tag{3.2.19}$$

Thus the total three dimensional Lagrangian we consider is

$$\begin{aligned}\mathcal{L}_3 = R\star_3\mathbf{1} - 2\star_3 dU\wedge dU - \frac{1}{2}e^{4U}\star_3 F_3\wedge F_3 - 2g_{I\bar{J}}\star_3 dX^I\wedge d\bar{X}^{\bar{J}}\\ + \frac{1}{2}e^{2U}(\mathrm{Im}N)_{\Lambda\Sigma}\star_3(F_3^\Lambda+\zeta^\Lambda F_3)\wedge(F_3^\Sigma+\zeta^\Sigma F_3) + \frac{1}{2}e^{-2U}(\mathrm{Im}N)_{\Lambda\Sigma}\star_3 d\zeta^\Lambda\wedge d\zeta^\Sigma\\ - (\mathrm{Re}N)_{\Lambda\Sigma}\,d\zeta^\Lambda\wedge(F_3^\Sigma+\zeta^\Sigma F_3) + \tilde{\zeta}_\Lambda dF_3^\Lambda + \frac{1}{2}(\sigma+\zeta^\Lambda\tilde{\zeta}_\Lambda)dF_3.\end{aligned} \tag{3.2.20}$$

Clearly, variations of this Lagrangian with respect to σ and $\tilde{\zeta}_\Lambda$ give the required Bianchi identities. Upon integration by parts on the Lagrange multiplier terms, equations for F_3^Σ and F_3 are purely algebraic. These equations allow us to do the dualizations of the one-forms. We find

$$d\tilde{\zeta}_\Lambda = e^{2U}(\mathrm{Im}N)_{\Lambda\Sigma}\star_3(F_3^\Sigma+\zeta^\Sigma F_3) - (\mathrm{Re}N)_{\Lambda\Sigma}d\zeta^\Sigma, \tag{3.2.21}$$

and

$$d\sigma + \tilde{\zeta}_\Lambda d\zeta^\Lambda - \zeta^\Lambda d\tilde{\zeta}_\Lambda = -2e^{4U}\star_3 F_3. \tag{3.2.22}$$

Substituting these back into Lagrangian (3.2.20) we find that it takes the form

$$\mathcal{L}_3 = R\star_3\mathbf{1} - \frac{1}{2}G_{ab}d\varphi^a\wedge\star d\varphi^b. \tag{3.2.23}$$

Metric G_{ab} in our conventions is

$$\begin{aligned}G_{ab}d\varphi^a d\varphi^b = 4dU^2 + 4g_{I\bar{J}}dX^I d\bar{X}^{\bar{J}} - \frac{1}{4}e^{-4U}\left(d\sigma+\tilde{\zeta}_\Lambda d\zeta^\Lambda - \zeta^\Lambda d\tilde{\zeta}_\Lambda\right)^2\\ + e^{-2U}\left[-(\mathrm{Im}N)_{\Lambda\Sigma}d\zeta^\Lambda d\zeta^\Sigma + ((\mathrm{Im}N)^{-1})^{\Lambda\Sigma}\left(d\tilde{\zeta}_\Lambda + (\mathrm{Re}N)_{\Lambda\Xi}d\zeta^\Xi\right)\left(d\tilde{\zeta}_\Sigma + (\mathrm{Re}N)_{\Sigma\Gamma}d\zeta^\Gamma\right)\right].\end{aligned} \tag{3.2.24}$$

This metric is identical to the one obtained in [47].

The symmetric space (3.2.24) can be parameterized in the Iwasawa gauge by the coset element [14]

$$\mathcal{V} = e^{-U\,\mathbb{H}_0}\cdot\prod_{I=1,2,3}\left(e^{-\frac{1}{2}\left[\log(fh^I)\right]\mathbb{H}_I}\cdot e^{\chi^I\mathbb{E}_I}\right)\cdot e^{-\zeta^\Lambda\mathbb{E}_{q_\Lambda}-\tilde{\zeta}_\Lambda\mathbb{E}_{p^\Lambda}}\cdot e^{-\frac{1}{2}\sigma\mathbb{E}_0}, \tag{3.2.25}$$

where for an explicit parametrisation of the Lie algebra $\mathfrak{so}(4,4)\ni\mathbb{X}=\sum\underline{E}_a\mathbb{E}_a$ we use

$$\mathbb{X} = \begin{pmatrix}
\underline{H}_2+\underline{H}_3 & -\underline{E}_3 & -\underline{F}_{q_1} & \underline{F}_{q_0} & 0 & -\underline{E}_2 & \underline{E}_{p^0} & \underline{E}_{p^1}\\
-\underline{F}_3 & \underline{H}_2-\underline{H}_3 & -\underline{F}_{p^2} & \underline{F}_{q_3} & \underline{E}_2 & 0 & \underline{E}_{p^3} & -\underline{E}_{q_2}\\
-\underline{E}_{q_1} & -\underline{E}_{p^2} & \underline{H}+\underline{H}_1 & -\underline{E}_1 & -\underline{E}_{p^0} & -\underline{E}_{p^3} & 0 & -\underline{E}_0\\
\underline{E}_{q_0} & \underline{E}_{q_3} & -\underline{F}_1 & \underline{H}-\underline{H}_1 & -\underline{E}_{p^1} & \underline{E}_{q_2} & \underline{E}_0 & 0\\
0 & \underline{F}_2 & -\underline{F}_{p^0} & -\underline{F}_{p^1} & -\underline{H}_2-\underline{H}_3 & \underline{F}_3 & \underline{E}_{q_1} & -\underline{E}_{q_0}\\
-\underline{F}_2 & 0 & -\underline{F}_{p^3} & \underline{F}_{q_2} & \underline{E}_3 & \underline{H}_3-\underline{H}_2 & \underline{E}_{p^2} & -\underline{E}_{q_3}\\
\underline{F}_{p^0} & \underline{F}_{p^3} & 0 & \underline{F}_0 & \underline{F}_{q_1} & \underline{F}_{p^2} & -\underline{H}-\underline{H}_1 & \underline{F}_1\\
\underline{F}_{p^1} & -\underline{F}_{q_2} & -\underline{F}_0 & 0 & -\underline{F}_{q_0} & -\underline{F}_{q_3} & \underline{E}_1 & \underline{H}_1-\underline{H}
\end{pmatrix}.$$

In the above equation $\mathbb{E}_a$ are the 28 generators and $\underline{E}_a$ are the 28 dual coordinates. The generators $\mathbb{E}_a$ can be readily written in the basis (3.7.7)–(3.7.12)[2]. The matrix that defines the SO(4,4) group in our notation is

$$\eta = \begin{pmatrix}\mathbf{0}_4 & \mathbf{1}_4\\ \mathbf{1}_4 & \mathbf{0}_4\end{pmatrix}, \tag{3.2.26}$$

[2]Since we are doing dimensional reduction first over time and then over space, the names of the generators $\mathbb{E}_{q_\Lambda}$ and $\mathbb{E}_{p^\Lambda}$ do not have the same interpretation as they have in reference [14]. However, since in many papers this notation is used, we continue to use it for writing the coset representative.

i.e., any $X \in$ SO(4,4) satisfies

$$X^T \cdot \eta \cdot X = \eta. \tag{3.2.27}$$

The involution $\tilde{\tau}$ that defines[3] the coset

$$\frac{\mathrm{SO}(4,4)}{\mathrm{SO}(2,2) \times \mathrm{SO}(2,2)} \tag{3.2.28}$$

is:

$$\tilde{\tau}(\mathbb{H}_0) = -\mathbb{H}_0, \qquad \tilde{\tau}(\mathbb{H}_I) = -\mathbb{H}_I, \tag{3.2.29}$$

$$\tilde{\tau}(\mathbb{E}_0) = +\mathbb{F}_0, \qquad \tilde{\tau}(\mathbb{E}_I) = +\mathbb{F}_I, \tag{3.2.30}$$

$$\tilde{\tau}(\mathbb{E}_{q_0}) = +\mathbb{F}_{q_0}, \qquad \tilde{\tau}(\mathbb{E}_{q_0}) = -\mathbb{F}_{q_I}, \tag{3.2.31}$$

$$\tilde{\tau}(\mathbb{E}_{p^I}) = -\mathbb{F}_{p^0}, \qquad \tilde{\tau}(\mathbb{E}_{p^I}) = +\mathbb{F}_{p^I}. \tag{3.2.32}$$

In our basis the matrix η' that implements the involution as,

$$\tilde{\tau}(x) =: -x^\sharp = -\eta' \cdot x^T \cdot \eta', \qquad \text{for all} \quad x \in \mathfrak{so}(4,4), \tag{3.2.33}$$

is

$$\eta' = \mathtt{diagonal}\{-1,1,-1,1,-1,1,-1,1\}. \tag{3.2.34}$$

Metric (3.2.24) is obtained through the Maurer-Cartan one-form $\theta = d\mathcal{V} \cdot \mathcal{V}^{-1}$ as follows. Defining,

$$P = \frac{1}{2}\left(\theta - \tilde{\tau}(\theta)\right), \tag{3.2.35}$$

one sees that

$$G_{ab} d\varphi^a \wedge \star d\varphi^b = \mathrm{Tr}(P \wedge \star P). \tag{3.2.36}$$

3.3 Coset description of Bena-Warner solutions

The above dimensional reduction is well adapted to obtain coset description of Bena-Warner [19] solutions, since Bena-Warner solutions are naturally written in a fibre form amenable to such a reduction. In this section we work out such a coset description in our notation. Some of this discussion is implicit in the literature [15]; however, in order to work out the Geroch group description, we need those details explicitly.

To set the notation we start with a quick summary of the Bena-Warner class of solutions, following the original notation [19]. In eleven dimensions, metric takes the form,

$$ds^2_{11} = ds^2_5 + ds^2_{\mathrm{T}^6}, \tag{3.3.1}$$

where

$$ds^2_5 = -(Z_1 Z_2 Z_3)^{-2/3}(dt+k)^2 + (Z_1 Z_2 Z_3)^{1/3} h_{mn} dx^m dx^n, \tag{3.3.2}$$

and the metric on six-torus is

$$ds^2_{\mathrm{T}^6} = \left(\frac{Z_2 Z_3}{Z_1^2}\right)^{1/3}(d\tilde{x}_1^2+d\tilde{x}_2^2)+\left(\frac{Z_1 Z_3}{Z_2^2}\right)^{1/3}(d\tilde{x}_3^2+d\tilde{x}_4^2)+\left(\frac{Z_1 Z_2}{Z_3^2}\right)^{1/3}(d\tilde{x}_5^2+d\tilde{x}_6^2), \tag{3.3.3}$$

The eleven dimensional three-form-field takes the form,

$$A_{[3]} = A^1_{[1]} \wedge d\tilde{x}_1 \wedge d\tilde{x}_2 + A^2_{[1]} \wedge d\tilde{x}_3 \wedge d\tilde{x}_4 + A^3_{[1]} \wedge d\tilde{x}_5 \wedge d\tilde{x}_6. \tag{3.3.4}$$

[3] We put tilde of tau because it denotes an involution different from the standard Cartan involution.

In the above expressions k is a one-form on the four-dimensional base space $ds_4^2 = h_{mn}dx^m dx^n$ and $A^I_{[1]}$ $(I = 1, 2, 3)$ are one-forms in the five-dimensional spacetime. The BPS equations of motion determine all these fields in terms of eight harmonic functions

$$(V, M, K^I, L_I) \tag{3.3.5}$$

when the four-dimensional base metric h_{mn} is taken to be the multi-center Gibbons-Hawking space [19, 45, 49, 50]. We restrict our study to this case only. The relevant expressions are as follows. The four-dimensional base metric takes a fibre form,

$$ds_4^2 = V^{-1}(dz + A)^2 + V(dr^2 + r^2 d\theta^2 + r^2 \sin^2\theta d\phi^2), \tag{3.3.6}$$

with

$$\star_3\, dA = dV, \tag{3.3.7}$$

and where the three-dimensional hodge star operation is with respect to the three-dimensional flat base metric

$$ds_3^2 = dr^2 + r^2 d\theta^2 + r^2 \sin^2\theta d\phi^2. \tag{3.3.8}$$

The five-dimensional vector fields take the form,

$$A^I = -Z_I^{-1}(dt + k) + V^{-1}K^I(dz + A) + \xi^I, \tag{3.3.9}$$

with

$$\star_3\, d\xi^I = -dK^I, \tag{3.3.10}$$

and the functions Z_I's are given as

$$Z_I = \frac{1}{2}C_{IJK}V^{-1}K^J K^K + L_I. \tag{3.3.11}$$

The one form k on the four-dimensional Gibbons-Hawking space takes the form

$$k = \mu(dz + A) + \omega_{\rm BW}, \tag{3.3.12}$$

with

$$\mu = \frac{1}{6}C_{IJK}\frac{K^I K^J K^K}{V^2} + \frac{1}{2V}K^I L_I + M, \tag{3.3.13}$$

and

$$\star_3 d\omega_{\rm BW} = V d\mu - \mu dV - V Z_I d\left(V^{-1}K^I\right) \tag{3.3.14}$$

$$= V dM - M dV + \frac{1}{2}(K^I dL_I - L_I dK^I). \tag{3.3.15}$$

To go from (3.3.14) to (3.3.15) we have substituted the formula (3.3.13) for the function μ. We use the notation $\omega_{\rm BW}$ to denote the three-dimensional one-form that appears in (3.3.12), in order to distinguish it from the three-dimensional one-form ω_3 that we introduced in equation (3.2.17) in section 3.2.

We refer the reader to [19] and to reviews [9, 11] for further details on the solutions and the BPS equations.

3.3.1 SO(4,4) coset description

The above class of solutions can be viewed as solutions to five-dimensional $\mathrm{U}(1)^3$ supergravity upon dimensional reduction from eleven to five dimensions on the six-torus. These solutions also have ∂_t and ∂_z Killing symmetries. As a result, they can be given a three-dimensional description in the dimensionally reduced $\mathrm{U}(1)^3$ supergravity theory with three dimensional flat base space. Our first aim is to obtain that description, and in particular, how they are represented in the SO(4,4) coset variables. To this end we compute the *sixteen* three-dimensional scalars that parameterise the coset

$$\frac{\mathrm{SO}(4,4)}{\mathrm{SO}(2,2)\times\mathrm{SO}(2,2)}, \tag{3.3.16}$$

in terms of the above introduced *eight* harmonic functions (3.3.5). Note that the sixteen three-dimensional scalars are

$$\{U,\sigma,\mathrm{Re}(X^I)=-\chi^I,\mathrm{Im}(X^I)=fh^I,\zeta^\Lambda,\tilde{\zeta}_\Lambda\}. \tag{3.3.17}$$

We find in the notation of section 3.2 for the scalars $\mathrm{Im}(X^I)=fh^I$,

$$h^1=\left(\frac{Z_2Z_3}{Z_1^2}\right)^{1/3} \tag{3.3.18}$$

$$h^2=\left(\frac{Z_1Z_3}{Z_2^2}\right)^{1/3} \tag{3.3.19}$$

$$h^3=\left(\frac{Z_1Z_2}{Z_3^2}\right)^{1/3} \tag{3.3.20}$$

together with

$$f=(Z_1Z_2Z_3)^{-1/3}, \tag{3.3.21}$$

For the scalars $\mathrm{Re}(X^I)=-\chi^I$ we find

$$\chi^I=-Z_I^{-1}. \tag{3.3.22}$$

With these fields at hand we can compute the ReN and ImN matrices. We find the following simple expressions for these matrices

$$\mathrm{Re}N=\begin{pmatrix} -\frac{2}{Z_1Z_2Z_3} & \frac{1}{Z_2Z_3} & \frac{1}{Z_1Z_3} & \frac{1}{Z_1Z_2} \\ \frac{1}{Z_2Z_3} & 0 & -\frac{1}{Z_3} & -\frac{1}{Z_2} \\ \frac{1}{Z_1Z_3} & -\frac{1}{Z_3} & 0 & -\frac{1}{Z_1} \\ \frac{1}{Z_1Z_2} & -\frac{1}{Z_2} & -\frac{1}{Z_1} & 0 \end{pmatrix}, \tag{3.3.23}$$

and

$$\mathrm{Im}N=\begin{pmatrix} -\frac{2}{Z_1Z_2Z_3} & \frac{1}{Z_2Z_3} & \frac{1}{Z_1Z_3} & \frac{1}{Z_1Z_2} \\ \frac{1}{Z_2Z_3} & -\frac{Z_1}{Z_2Z_3} & 0 & 0 \\ \frac{1}{Z_1Z_3} & 0 & -\frac{Z_2}{Z_1Z_3} & 0 \\ \frac{1}{Z_1Z_2} & 0 & 0 & -\frac{Z_3}{Z_1Z_2} \end{pmatrix}. \tag{3.3.24}$$

Proceeding further we have for the scalars ζ^Λ

$$\zeta^0=\mu, \tag{3.3.25}$$

$$\zeta^I=V^{-1}K^I, \tag{3.3.26}$$

and for the scalar U,

$$e^{2U} = V^{-1}. \tag{3.3.27}$$

Out of sixteen we have listed eleven scalars so far. Now we use the dualization equations (3.2.21) and (3.2.22) to find the remaining five scalars $\tilde{\zeta}_\Lambda$ and σ. For evaluating $\tilde{\zeta}_\Lambda$ we need the combinations $\star_3(F_3^\Sigma + \zeta^\Sigma F_3)$. Interestingly, these three-dimensional hodge dualities can be performed rather straightforwardly given the equations above. To this end, we first write the relation between the five three-dimensional one-forms (ω_3, A_3^Λ) that appear in the coset description and the three-dimensional one forms that appear in Bena-Warner solutions $(A, \omega_{\rm BW}, \xi^I)$:

$$\omega_3 = A, \tag{3.3.28}$$

$$A_3^0 = \omega_{\rm BW}, \tag{3.3.29}$$

$$A_3^I = \xi^I. \tag{3.3.30}$$

For $\star_3(F_3^0 + \zeta^0 F_3)$, we have

$$\begin{aligned} \star_3(F_3^0 + \zeta^0 F_3) &= \star_3 \left(d\omega_{\rm BW} + \zeta^0 dA\right) && (3.3.31)\\ &= \star_3\, d\omega_{\rm BW} + \zeta^0 dV && (3.3.32)\\ &= V d\mu - V Z_I d\zeta^I, && (3.3.33) \end{aligned}$$

where in the first step we have used $\omega_3 = A$ and $A_3^0 = \omega_{\rm BW}$; in the second step we have used the duality relation (3.3.7); and finally in the third step we have used relations (3.3.14) and (3.3.26). Similarly,

$$\begin{aligned} \star_3(F_3^I + \zeta^I F_3) &= \star\, F_3^I + V^{-1} K^I dV && (3.3.34)\\ &= -\, dK^I + V^{-1} K^I dV, && (3.3.35) \end{aligned}$$

where we have used $\omega_3 = A$ and $A_3^I = \xi^I$ together with relations (3.3.26) and (3.3.10).

Using these expressions, an explicit calculation shows that the combination

$$e^{2U} (\mathrm{Im}N)_{\Lambda\Sigma} \star_3 (F_3^\Sigma + \zeta^\Sigma F_3) - (\mathrm{Re}N)_{\Lambda\Sigma} d\zeta^\Sigma \tag{3.3.36}$$

vanishes. Therefore, the four $\tilde{\zeta}_\Lambda$ scalars can all be chosen to be zero, which is what we will do:

$$\tilde{\zeta}_\Lambda = 0. \tag{3.3.37}$$

Doing so we have from (3.2.22)

$$d\sigma = -2V^{-2} \star_3 F_3 = -2V^{-2} dV = 2d(V^{-1}), \tag{3.3.38}$$

i.e., σ can be taken to be $2V^{-1}$:

$$\sigma = 2V^{-1}. \tag{3.3.39}$$

To summarise, the sixteen scalars of the coset model take the values

$$e^{2U} = V^{-1}, \tag{3.3.40}$$

$$\sigma = 2V^{-1}, \tag{3.3.41}$$

$$\tilde{\zeta}_\Lambda = 0, \tag{3.3.42}$$

$$\zeta^0 = \mu \;=\; \frac{1}{6}C_{IJK}\frac{K^I K^J K^K}{V^2} + \frac{1}{2V}K^I L_I + M, \tag{3.3.43}$$

$$\zeta^I = V^{-1}K^I, \tag{3.3.44}$$

$$\mathrm{Re}(X^I) = -\chi^I \;=\; Z_I^{-1} = \left(\frac{1}{2}C_{IJK}V^{-1}K^J K^K + L_I\right)^{-1}, \tag{3.3.45}$$

$$\mathrm{Im}(X^I) = fh^I \;=\; Z_I^{-1} = \left(\frac{1}{2}C_{IJK}V^{-1}K^J K^K + L_I\right)^{-1}. \tag{3.3.46}$$

Note that the right hand side of the above expressions are all written in terms of the eight Bena-Warner harmonic functions (3.3.5). These expressions provide the required embedding of the Bena-Warner class of the solutions in SO(4,4) coset model framework in our notation. The matrix of scalars

$$S(\vec{x}) = \mathcal{V}^\sharp\mathcal{V} \tag{3.3.47}$$

for the Bena Warner solutions takes the form,

$$S(\vec{x}) = \begin{pmatrix} S_{11} & L_2 & S_{13} & K^1 & -1 & L_3 & 0 & -2M \\ -L_2 & 0 & K^3 & 0 & 0 & -1 & 0 & 0 \\ S_{13} & -K^3 & S_{33} & V & 0 & -K^2 & -1 & L_1 \\ -K^1 & 0 & -V & 0 & 0 & 0 & 0 & -1 \\ -1 & 0 & 0 & 0 & 0 & 0 & 0 & 0 \\ -L_3 & -1 & K^2 & 0 & 0 & 0 & 0 & 0 \\ 0 & 0 & -1 & 0 & 0 & 0 & 0 & 0 \\ 2M & 0 & -L_1 & -1 & 0 & 0 & 0 & 0 \end{pmatrix}, \tag{3.3.48}$$

where

$$S_{11} = L_2L_3 - 2K^1M, \tag{3.3.49}$$

$$S_{13} = \frac{1}{2}\left(K^1L_1 - K^2L_2 - K^3L_3 - 2MV\right), \tag{3.3.50}$$

$$S_{33} = K^2K^3 + L_1V. \tag{3.3.51}$$

We use $\vec{x}$ to collectively denote three-dimensional base space coordinates r, θ, ϕ. Using this embedding we can now arrive at some general results.

Our first general result is that the Lie algebra valued Noether's current for the Bena-Warner solutions is nilpotent. This is seen by a simple calculation as follows. We compute

$$J = S^{-1}\cdot dS, \tag{3.3.52}$$

and find

$$J = dK^I\mathbb{F}_{p^I} - dV\mathbb{F}_0 - dL_I\mathbb{F}_I - 2dM\mathbb{E}_{q_0} + \left(MdV - VdM + \frac{1}{2}(L_I dK^I - K^I dL_I)\right)\mathbb{F}_{p^0}. \tag{3.3.53}$$

Clearly

$$d \star_3 J = 0, \tag{3.3.54}$$

since (i) functions (3.3.5) are harmonic, and (ii) from (3.3.15) we see that the term in front of $\mathbb{F}_{p^0}$ is $\star_3 d\omega_{\rm BW}$. Therefore, J is a conserved Lie algebra valued one-form. It is easily checked that as an $\mathfrak{so}(4,4)$ matrix it is nilpotent of degree three. We define the charge matrix

$$\mathcal{Q} = \frac{1}{4\pi}\int_\Sigma \star_3 J, \tag{3.3.55}$$

where Σ is a two-cycle in three-dimensional flat space. If there are no Dirac-Misner strings in the solutions, then in the charge integral there will not be a contribution from the term

$$\mathbb{F}_{p^0}\int_\Sigma d\omega_{\rm BW}, \tag{3.3.56}$$

as the integral is over a two cycle of a closed two form.

We can also connect the preceding discussion to that of reference [15]. Four-dimensional (Lorentzian) gravity embedded in the SO(4, 4) coset is parameterised by f and $\tilde{\zeta}^0$, while other scalars are to be set to zero. For this embedding, we have the gravity $\mathfrak{sl}(2)$ spanned by the generators

$$\mathbf{h} = -\frac{1}{2}\left(\mathbb{H}_0 + \sum_{I=1}^{3}\mathbb{H}_I\right), \tag{3.3.57}$$

$$\mathbf{e} = \mathbb{F}_{p^0}, \tag{3.3.58}$$

$$\mathbf{f} = \mathbb{E}_{p^0}. \tag{3.3.59}$$

The $\mathbf{h}$ gives the following grading for the generators that appear in current (3.3.53):

$$(\mathbb{F}_{p^0})^{(+2)}, \{\mathbb{F}_0, \mathbb{F}_I, \mathbb{E}_{q_0}, \mathbb{F}_{p^I}\}^{(+1)}. \tag{3.3.60}$$

For the equations of motion (3.3.54), we observe that coefficients at grade one are precisely the equations giving eight harmonic functions; moreover, coefficient of J at grade two is related to the no Dirac-Misner strings condition [15].

3.3.2 Gauge transformations and spectral flow dualities

The Bena-Warner class of solutions have two well studied symmetries called "gauge transformations" and "spectral flows". Under these transformations solutions are mapped to solutions. The first class, the so called "gauge transformations" correspond to changing the harmonic functions as [19]

$$V \quad \to \quad V, \tag{3.3.61}$$

$$K^I \quad \to \quad K^I + c^I V, \tag{3.3.62}$$

$$L_I \quad \to \quad L_I - C_{IJK}c^J K^K - \frac{1}{2}C_{IJK}c^J c^K V, \tag{3.3.63}$$

$$M \quad \to \quad M - \frac{1}{2}c^I L_I + \frac{1}{12}C_{IJK}(V c^I c^J c^K + 3c^I c^J K^K). \tag{3.3.64}$$

In the notation of coset variables, these transformations correspond to shifting the scalars ζ^I by constant c^I. Indeed, these gauge transformations are realised as simply

$$S(\vec{x}) \to g^\sharp S(\vec{x}) g, \tag{3.3.65}$$

with

$$g = \exp\left[-\sum_{I=1}^{3} c^I \mathbb{E}_{q_I}\right]. \tag{3.3.66}$$

The second class of transformations are called the spectral flow transformations [46]. They are

$$\begin{aligned}
M &\rightarrow M, && (3.3.67)\\
L_I &\rightarrow L_I - 2c_I M, && (3.3.68)\\
K^I &\rightarrow K^I - C^{IJK} c_J L_K + C_{IJK} c_J c_K M, && (3.3.69)\\
V &\rightarrow V + c^I K_I - \frac{1}{2} C^{IJK} c_I c_J L_K + \frac{1}{3} C^{IJK} c_I c_J c_K M. && (3.3.70)
\end{aligned}$$

These transformations do not correspond a simple shifting of scalars, instead these are Harrison transformations – transformations involving "negative" root vectors of the $\mathfrak{so}(4,4)$ Lie algebra,

$$S(x) \rightarrow g^\sharp S(x) g, \tag{3.3.71}$$

with

$$g = \exp\left[-\sum_{I=1}^{3} c^I \mathbb{F}_{q_I}\right]. \tag{3.3.72}$$

Harrison transformations have non-trivial action on the solutions [47,51]. One can clearly come up with a very large class of similar other transformations by exponentiating other generators.[4]

With this understanding of spectral flows as Harrison transformations, we are also able to better understand relation between references [52, 53] and [47, 51]. On the one hand, reference [53] uses the so-called TsT transformations and some generalisations to relate certain asymptotically flat black hole solutions to their subtracted geometries. It was previously understood that those TsT transformations are related to spectral flows [52]. On the other hand, references [47,51] use a class of Harrison transformations to relate the same asymptotically flat black hole solutions to their subtracted geometries. Via these inter-connections, it was expected that Harrison transformations are closely related to spectral flows. Above, we have presented a direct and simple relationship: Bena-Bobev-Warner spectral flows are a special class of Harrison transformations. To the best of our knowledge, such a direct relationship has not been elucidated before.[5]

3.4 Geroch group description of collinear bubbling solutions

Now we are in position to work out the Geroch group description of collinear bubbling solutions. We need to work with collinear centers, since only in this situation we can perform further dimensional reduction to two dimensions. We keep the initial discussion general, i.e., with finite set of isolated centers with location anywhere in flat base $\mathbb{R}^3$. Later when we discuss reduction to two dimensions, we will assume ∂_ϕ as another Killing symmetry of the full spacetime configuration.

[4] The Lie algebra generators appearing in equations (3.3.66) and (3.3.72) are all at grade zero with respect to generator $\mathbf{h}$ defined in (3.3.57), i.e., $\mathbb{E}_{q_I}$ and $\mathbb{F}_{q_I}$ also belong to the Lie algebra of the four-dimensional U-duality group.

[5] We thank Monica Guica for discussion on this point.

3.4.1 Matrix of scalars for bubbling solutions

In the Bena-Warner class of solutions, we can choose the harmonic functions to be localised anywhere on the three-dimensional base space. We take harmonic functions with finite set of isolated sources at locations $\vec{x}^{(j)}$ in the three-dimensional base space $\mathbb{R}^3$. For convenience of notation, in the equations below we put all I, J, K indices upstairs, and the indices for the centers downstairs. We have for the eight harmonic functions,

$$V = q_0 + \sum_{j=1}^{N} \frac{q_j}{r_j}, \qquad K^I = k_0^I + \sum_{j=1}^{N} \frac{k_j^I}{r_j}, \tag{3.4.1}$$

$$L^I = l_0^I + \sum_{j=1}^{N} \frac{l_j^I}{r_j}, \qquad M = m_0 + \sum_{j=1}^{N} \frac{m_j}{r_j}, \tag{3.4.2}$$

where $r_j = |\vec{x} - \vec{x}^{(j)}|$. We can easily read off the various matrix elements of the matrix (3.3.48). There are only three matrix elements that are slightly non-trivial. We calculate them here,

$$S_{11} = L_2 L_3 - 2K^1 M \tag{3.4.3}$$

$$= \left(l_0^2 + \sum_{s=1}^{N} \frac{l_s^2}{r_s}\right)\left(l_0^3 + \sum_{t=1}^{N} \frac{l_t^3}{r_t}\right) - 2\left(k_0^1 + \sum_{s=1}^{N} \frac{k_s^1}{r_s}\right)\left(m_0 + \sum_{t=1}^{N} \frac{m_t}{r_t}\right) \tag{3.4.4}$$

Expanding it out we get,

$$S_{11} = \left(l_0^2 l_0^3 - 2k_0^1 m_0\right) + \sum_{s=1}^{N} \frac{1}{r_s}\left(l_s^2 l_0^3 + l_0^2 l_s^3 - 2k_s^1 m_0 - 2k_0^1 m_s\right) + \sum_{s,t=1}^{N} \frac{1}{r_s r_t}\left(l_s^2 l_t^3 - 2k_s^1 m_t\right). \tag{3.4.5}$$

In this expansion there *are* double pole terms.

For bubbling solutions, i.e., solutions without brane sources, all harmonic functions must have singularities only at the Gibbons-Hawking centres. Such solutions have [19]:

$$l_j^I = -\frac{1}{2} C_{IJK} \frac{k_j^J k_j^K}{q_j}, \qquad m_j = \frac{1}{2} \frac{k_j^1 k_j^2 k_j^3}{q_j^2}. \tag{3.4.6}$$

Since q_j appears in the denominator in these equations, in order for these equations to make sense, we must have Gibbons-Hawking center at location $\vec{x}^{(j)}$, i.e., $q_j \neq 0$. For this sub-class of solutions double pole terms in (3.4.5) all cancel out:

$$l_s^2 l_s^3 - 2k_s^1 m_s = \left(-\frac{k_3^s k_3^s}{q_s}\right)\left(-\frac{k_1^s k_2^s}{q_s}\right) - (2k_s^1)\left(\frac{1}{2}\frac{k_s^1 k_s^2 k_s^3}{q_s^2}\right) = 0. \tag{3.4.7}$$

Similarly, double pole terms all cancel out for S_{13} and S_{33}. The expansion of S_{13} is as follows,

$$\begin{aligned} S_{13} &= \frac{1}{2}\left(K^1 L_1 - K^2 L_2 - K^3 L_3 - 2MV\right) \\ &= \frac{1}{2}\left(k_0^1 l_0^1 - k_0^2 l_0^2 - k_0^3 l_0^3 - 2m_0 q_0\right) \\ &\quad + \sum_{s=1}^{N} \frac{1}{2r_s}\left(k_s^1 l_0^1 - k_s^2 l_0^2 - k_s^3 l_0^3 - 2m_s q_0 + k_0^1 l_s^1 - k_0^2 l_s^2 - k_0^3 l_s^3 - 2m_0 q_s\right) \\ &\quad + \sum_{\substack{s,t=1,\\ s\neq t}}^{N} \frac{1}{2r_s r_t}\left(k_s^1 l_t^1 - k_s^2 l_t^2 - k_s^3 l_t^3 - 2m_s q_t\right), \end{aligned} \tag{3.4.8}$$

and expansion of S_{33} is as follows,

$$\begin{aligned} S_{33} &= K^2K^3 + L_1V \\ &= \left(k_0^2k_0^3 + l_0^1q_0\right) + \sum_{s=1}^{N}\frac{1}{r_s}\left(k_s^2k_0^3 + k_0^2k_s^3 + l_s^1q_0 + l_0^1q_s\right) + \sum_{\substack{s,t=1,\\ s\neq t}}^{N}\frac{1}{r_sr_t}\left(k_s^2k_t^3 + l_s^1q_t\right). \end{aligned} \tag{3.4.9}$$

With these expansions at hand we can write the expanded $S(\vec{x})$ matrix schematically as,

$$S(\vec{x}) = S_\infty + \sum_{s=1}^{N}\frac{1}{r_s}S_s(\vec{x}) + \sum_{\substack{s,t=1,\\ s\neq t}}^{N}\frac{1}{r_sr_t}S_{st}. \tag{3.4.10}$$

Properties of S_s and S_{st} matrices are of interest to us. Remarkably, these matrices satisfy a number of simple properties. The key properties are,

1. The matrices $S_\infty^{-1}S_s$ are nilpotent of degree three. When conditions (3.4.6) for the bubbling solutions are imposed in addition, $S_\infty^{-1}S_s$ are nilpotent of degree two. Unless otherwise stated we will implicitly assume conditions (3.4.6). We define

$$B_s := S_\infty^{-1}S_s, \qquad\qquad B_s\cdot B_s = 0. \tag{3.4.11}$$

2. Nilpotent matrices B_s are in the 8×8 vector representation of the Lie algebra $\mathfrak{so}(4,4)$. These matrices are of rank 2. In fact, these matrices as Lie algebra generators belong to the unique minimal nilpotent orbit of $\mathfrak{so}(4,4)$. In the notation of the appendix 3.7, the orbit is $\mathcal{O}_1$ with α and β labels (0,1,0,0) and (1,1,1,1) respectively.

3. When we multiply any three such matrices we get zero,

$$B_r\cdot B_s\cdot B_t = 0. \tag{3.4.12}$$

4. The matrices S_{st} are,

$$S_{st} = \frac{1}{2}S_\infty\cdot(B_s\cdot B_t + B_t\cdot B_s). \tag{3.4.13}$$

5. The full matrix $S(\vec{x})$ is therefore simply

$$S(\vec{x}) = S_\infty\cdot\exp\left[\sum_{s=1}^{N}\frac{B_s}{r_s}\right]. \tag{3.4.14}$$

Some of these comments admit appropriate generalisation when the bubbling conditions (3.4.6) are not imposed. However, since for such solutions matrices B_s are not of rank 2, we do not expect them to fit into the inverse scattering approach of [16]. For this reason we have not explored that case in detail. We leave a more detailed study of those solutions for the future.

3.4.2 Charge matrices at each center

One can write expressions for B_s matrices for any given set of harmonic functions of the form of (3.4.1)–(3.4.2) by reading off the coefficients of r_s^{-1} in $S(\vec{x})$. We find

$$B_s = -q_s \mathbb{F}_0 - l_s^I \mathbb{F}_I - \beta_s \mathbb{F}_{p^0} + k_s^I \mathbb{F}_{p^I} - 2m_s \mathbb{E}_{q_0}, \tag{3.4.15}$$

where

$$\beta_s = q_0 m_j - m_0 q_j + \frac{1}{2}(l_j^I k_0^I - k_j^I l_0^I). \tag{3.4.16}$$

To calculate the charge matrix at each center, we evaluate $J = S^{-1}dS$, and integrate on a small sphere around the s^{th} center to find

$$\mathcal{Q}_{(s)} = \frac{1}{4\pi}\int_{\Sigma_s} \star_3 J = -B_s - \frac{1}{2}\sum_{\substack{t=1\\ t\neq s}}^{N} \frac{[B_s, B_t]}{|r_s - r_t|}. \tag{3.4.17}$$

The commutator involved can be written in a nice way as well. One finds,

$$[B_s, B_t] = q_s q_t \left(\frac{k_t^1}{q_t} - \frac{k_s^1}{q_s}\right)\left(\frac{k_t^2}{q_t} - \frac{k_s^2}{q_s}\right)\left(\frac{k_t^3}{q_t} - \frac{k_s^3}{q_s}\right) \mathbb{F}_{p^0}. \tag{3.4.18}$$

We have not used all regularity conditions up to now. The bubble equations require that [19]

$$\frac{1}{2}\sum_{\substack{t=1\\ t\neq s}}^{N} q_s q_t \left(\frac{k_t^1}{q_t} - \frac{k_s^1}{q_s}\right)\left(\frac{k_t^2}{q_t} - \frac{k_s^2}{q_s}\right)\left(\frac{k_t^3}{q_t} - \frac{k_s^3}{q_s}\right)\frac{1}{|r_s - t_t|} = \beta_s, \tag{3.4.19}$$

which, using (3.4.18) becomes

$$\frac{1}{2}\sum_{\substack{t=1\\ t\neq s}}^{N} \frac{[B_s, B_t]}{|r_s - r_t|} = \beta_s \mathbb{F}_{p^0}. \tag{3.4.20}$$

As a result, the charge matrix at each center of the bubbling solutions is then given by

$$\mathcal{Q}_{(s)} = q_s \mathbb{F}_0 + l_s^I \mathbb{F}_I - k_s^I \mathbb{F}_{p^I} + 2m_s \mathbb{E}_{q_0}. \tag{3.4.21}$$

It only depends on the charges at the location $\vec{x}^{(s)}$ and the Dirac-Misner strings have all cancelled upon using the bubble equations, as expected. Note that $\mathcal{Q}_{(s)}$ is a linear combination of grade $+1$ terms alone, cf. (3.3.60).

3.4.3 Monodromy matrix for bubbling solutions

Let us now understand the above class of solutions from the Geroch group perspective. In order to reduce the solution to two dimensions, we need to take collinear centers; the matrix $S(\vec{x})$ then only depends on two coordinates (r, θ). A recipe for obtaining the Geroch group matrix $\mathcal{M}(w)$ for a solution with known $S(\vec{x})$ was given in [26, 36]; see also [37]. To use this recipe we first need to change coordinates of the base space from (r, θ, ϕ) to the Weyl canonical coordinates (ρ, z, ϕ). The canonical coordinates have the property that the three-dimensional base space has the cylindrical metric

$$ds_3^2 = d\rho^2 + dz^2 + \rho^2 d\phi^2. \tag{3.4.22}$$

The change of coordinates that takes from flat base space in polar coordinates $ds_3^2 = dr^2 + r^2 d\theta^2 + r^2 \sin^2\theta d\phi^2$ to canonical coordinates is:

$$\rho = r\sin\theta, \qquad\qquad z = r\cos\theta. \tag{3.4.23}$$

In canonical coordinates recipe to obtain Geroch group matrix is:

$$\mathcal{M}(w) = S(\rho = 0,\ z = w \quad \text{with} \quad z < -R), \tag{3.4.24}$$

where R is the radius of a sufficiently large semicircle in the (ρ, z) half-plane, such that all "corners" that feature in the "rod-structure" of a given solution are inside this semicircle. We refer the reader to [36] for a more precise discussion of these phrases. For practical calculations we simply take the limit $\rho = 0$, z near $-\infty$. The "rod-structure" of the Bena-Warner solutions has been recently studied in detail by Breunhölder and Lucietti [54].

To use the recipe, we need to understand how various functions of (r, θ) appearing in $S(\vec{x})$ change into functions of w. Let the centres be located along the third axis

$$\vec{x}^{(j)} = \vec{R}_j = (0, 0, w_j). \tag{3.4.25}$$

With this convention the functions r_j become,

$$r_j = |\vec{x} - \vec{x}^{(j)}| = \sqrt{r^2 - 2rw_j\cos\theta + w_j^2}. \tag{3.4.26}$$

In the Weyl canonical coordinates

$$r_j = \sqrt{\rho^2 + (z - w_j)^2}. \tag{3.4.27}$$

As a result, the harmonic functions $\frac{1}{r_j}$ upon taking the limit $\rho = 0$, z near $-\infty$ takes the form

$$\frac{1}{r_j} \longrightarrow -\frac{1}{w - w_j}. \tag{3.4.28}$$

Using replacement (3.4.28) we get the matrix $\mathcal{M}(w)$ from matrix (3.4.10),

$$\mathcal{M}(w) = S_\infty - \sum_{s=1}^{N} \frac{S_s(\vec{x})}{w - w_s} + \sum_{\substack{s,t=1 \\ s\neq t}}^{N} \frac{S_{st}}{(w - w_s)(w - w_t)}. \tag{3.4.29}$$

A more useful expression can be obtained using (3.4.14), and expanding the exponential.

$$\mathcal{M}(w) = S_\infty \cdot \left(\mathbb{I} - \sum_{s=1}^{N} \frac{B_s}{w - w_s} + \frac{1}{2} \sum_{\substack{s,t=1 \\ s\neq t}}^{N} \frac{\{B_s, B_t\}}{(w - w_s)(w - w_t)} \right), \tag{3.4.30}$$

We have a final expression

$$S_\infty^{-1} \cdot \mathcal{M}(w) = \mathbb{I} + \sum_{s=1}^{N} \frac{A_s}{w - w_s}, \tag{3.4.31}$$

where

$$A_s = -B_s + \frac{1}{2} \sum_{\substack{t=1 \\ t\neq s}}^{N} \frac{1}{w_s - w_t} \{B_s, B_t\}. \tag{3.4.32}$$

This is one of our main results. We have shown that the Geroch group matrices (3.4.31) for bubbling solutions only have simple poles. In the next subsection we explore further properties of the residue matrices.

3.4.4 Properties of the monodromy matrix for bubbling solutions

We start by recalling an elementary result from linear algebra that rank of an $n \times n$ matrices A is equal to

$$\text{rank}(A) = n - \text{dim of null space of } A. \tag{3.4.33}$$

Using this we argue that rank of A_s is same as rank of B_s. Consider an arbitrary vector v in the null space of B_s: $B_s v = 0$. It follows that

$$w = \left(\mathbb{I} + \frac{1}{2} \sum_{\substack{t=1 \\ t \neq s}}^{N} \frac{1}{w_s - w_t} B_t \right) \cdot v, \tag{3.4.34}$$

is in the null space of A_s. To see this simply consider,

$$A_s w = A_s v + \frac{1}{2} \sum_{\substack{t=1 \\ t \neq s}}^{N} \frac{1}{w_s - w_t} A_s B_t v \tag{3.4.35}$$

$$= \frac{1}{2} \sum_{\substack{t=1 \\ t \neq s}}^{N} \frac{1}{w_s - w_t} B_s B_t v + \frac{1}{2} \sum_{\substack{t=1 \\ t \neq s}}^{N} \frac{1}{w_s - w_t} A_s B_t v \tag{3.4.36}$$

$$= \frac{1}{2} \sum_{\substack{t=1 \\ t \neq s}}^{N} \frac{1}{w_s - w_t} B_s B_t v - \frac{1}{2} \sum_{\substack{t=1 \\ t \neq s}}^{N} \frac{1}{w_s - w_t} B_s B_t v \tag{3.4.37}$$

$$= 0 \tag{3.4.38}$$

where we have used $B_s \cdot B_t \cdot B_p = 0$. The map (3.4.34) is maximal rank (invertible):

$$\left(\mathbb{I} + \frac{1}{2} \sum_{\substack{t=1 \\ t \neq s}}^{N} \frac{B_t}{w_s - w_t} \right)^{-1} = \left(\mathbb{I} - \frac{1}{2} \sum_{\substack{t=1 \\ t \neq s}}^{N} \frac{B_t}{w_s - w_t} + \frac{1}{8} \sum_{\substack{t,r=1 \\ t,r \neq s}}^{N} \frac{\{B_t, B_r\}}{(w_s - w_t)(w_s - w_r)} \right), \tag{3.4.39}$$

so for every v there is a w.

For the converse, consider a vector w in the null space of A_s. Then it follows that we can find a vector v, using (3.4.39), that belongs to the null space of B_s. Consider:

$$0 = A_s w = -B_s w + \frac{1}{2} \sum_{t \neq s}^{N} \frac{\{B_s, B_t\}}{w_s - w_t} w. \tag{3.4.40}$$

This is the same as

$$B_s w = \frac{1}{2} B_s \sum_{t \neq s}^{N} \frac{B_t}{w_s - w_t} w + \frac{1}{2} \sum_{t \neq s}^{N} \frac{B_t}{w_s - w_t} B_s w. \tag{3.4.41}$$

Multiplying both sides by B_p for any p makes the RHS vanish. So we get that

$$B_p B_s w = 0 \qquad \forall\, w \qquad \text{s.t.} \qquad A_s w = 0, \tag{3.4.42}$$

which in turn implies

$$0 = A_s w = -B_s \cdot \left(\mathbb{I} - \frac{1}{2} \sum_{\substack{t=1 \\ t \neq s}}^{N} \frac{B_t}{w_s - w_t} \right) w \tag{3.4.43}$$

$$= -B_s \cdot \left(\mathbb{I} - \frac{1}{2} \sum_{\substack{t=1 \\ t \neq s}}^{N} \frac{B_t}{w_s - w_t} + \frac{1}{8} \sum_{\substack{t,r=1 \\ t,r \neq s}}^{N} \frac{\{B_t, B_r\}}{(w_s - w_t)(w_s - w_r)} \right) w. \tag{3.4.44}$$

It follows that generically A_s is also a rank-2 matrix. This is our second main result. We have shown that the Geroch group matrices (3.4.31) for bubbling solutions only have simple poles with residues of rank-2. It is precisely for this setup that the Riemann-Hilbert factorisation was developed in reference [16]. We leave the explicit factorisation of these matrices for future work. Due to the property that $B_s \cdot B_p \cdot B_q = 0$, it follows that A_s matrices are also nilpotent of degree 2. Generically, the A_s matrices do not belong to the Lie algebra $\mathfrak{so}(4,4)$, due to the presence of the anti-commutator terms in (3.4.32).

3.5 Some explicit examples

We now discuss some simple examples of Bena-Warner solutions and obtain their Geroch group matrices.

3.5.1 Supertube in Taub-NUT and the related bubbling geometry

Supertube in Taub-NUT

Our first example is one supertube in Taub-NUT [55]. The eight harmonic functions take the form in the notation of [46]

$$K^1 = 0, \qquad K^2 = 0, \qquad K^3 = -\frac{q_3}{2\Sigma} \qquad L_1 = 1 + \frac{Q_1}{4\Sigma}, \tag{3.5.1}$$

$$L_2 = 1 + \frac{Q_2}{4\Sigma}, \qquad L_3 = 1 \qquad V = \epsilon_0 + \frac{1}{r}, \qquad M = \frac{J_T}{16R} - \frac{J_T}{16}\frac{1}{\Sigma} \tag{3.5.2}$$

where $\vec{R} = (0,0,R)$ is the position of the round supertube in Taub-NUT along the Taub-NUT fibre, and

$$\Sigma = |\vec{r} - \vec{R}| = \sqrt{r^2 - 2rR\cos\theta + R^2}. \tag{3.5.3}$$

The requirement of the smoothness of the solution results in [46, 55]

$$q_3 J_T = Q_1 Q_2, \tag{3.5.4}$$

$$J_T \left(\epsilon_0 + \frac{1}{R} \right) = 4q_3. \tag{3.5.5}$$

This last condition is to be thought of as a condition on the separation R in terms of charges.

Charges for the configuration at the centre $\vec{r} = 0$ and the centre $\vec{r} = \vec{R}$ are

$$\{q_1, l_1^I, k_1^I, m_1\} = \{1,0,0,0,0,0,0,0\}, \tag{3.5.6}$$

$$\{q_2, l_2^I, k_2^I, m_2\} = \{0, \frac{1}{4}Q_1, \frac{1}{4}Q_2, 0, 0, 0, -\frac{1}{2}q_3, -\frac{1}{16}J_T\}. \tag{3.5.7}$$

We note that the Gibbons-Hawking charge at the second centre is zero ($q_2 = 0$), though M2 charges l_1, l_2 are non-zero. Thus, there are "brane sources" in this solution, it is not a bubbling solution. As a consequence, the general analysis of bubbling solutions given in section 3.4.3 does not apply. Nevertheless, the solution admits a very similar Geroch group description which we elucidate.

The charge matrices at the two centres can be calculated using the analysis of section 3.3.1, cf. (3.3.55). The general form of the charge matrix (3.3.55) when the two-cycle is taken to be a two-sphere enclosing only jth center is:

$$\mathcal{Q}_{(j)} = -q_j \mathbb{F}_0 - l_j^I \mathbb{F}_I + k_j^I \mathbb{F}_{p^I} - 2m_j \mathbb{E}_{q_0}, \tag{3.5.8}$$

where we have used the smoothness condition; cf. discussion around equation (3.3.56). Therefore for the above example we have

$$\mathcal{Q}_{(1)} = -\mathbb{F}_0, \tag{3.5.9}$$

$$\mathcal{Q}_{(2)} = -\frac{1}{4}Q_1 \mathbb{F}_1 - \frac{1}{4}Q_2 \mathbb{F}_2 - \frac{q_3}{2}\mathbb{F}_{p_3} + \frac{J_T}{8}\mathbb{E}_{q_0}, \tag{3.5.10}$$

To obtain the Geroch group matrix for the above solution, we need to first find the matrix of scalars $S(\vec{x})$ and then relate $S(\vec{x})$ with $\mathcal{M}(w)$ via (3.4.24). Writing as above

$$S(\vec{x}) = S_\infty \cdot \exp\left[\frac{B_1}{r} + \frac{B_2}{|\vec{r} - \vec{R}|}\right], \tag{3.5.11}$$

and using (3.4.15), we have

$$B_1 = -\mathbb{F}_0 + \frac{J_T}{16R}\mathbb{F}_{p^0}, \tag{3.5.12}$$

$$B_2 = -\frac{Q_1}{4}\mathbb{F}_1 - \frac{Q_2}{4}\mathbb{F}_2 - \frac{q_3}{2}\mathbb{F}_{p^3} + \frac{J_T}{8}\mathbb{F}_{q_0} - \frac{J_T}{16R}\mathbb{F}_{p^0}, \tag{3.5.13}$$

and

$$S_\infty = \begin{pmatrix} 1 & 1 & -\frac{J_T\epsilon_0}{16R} & 0 & -1 & 1 & 0 & -\frac{J_T}{8R} \\ -1 & 0 & 0 & 0 & 0 & -1 & 0 & 0 \\ -\frac{J_T\epsilon_0}{16R} & 0 & \epsilon_0 & \epsilon_0 & 0 & 0 & -1 & 1 \\ 0 & 0 & -\epsilon_0 & 0 & 0 & 0 & 0 & -1 \\ -1 & 0 & 0 & 0 & 0 & 0 & 0 & 0 \\ -1 & -1 & 0 & 0 & 0 & 0 & 0 & 0 \\ 0 & 0 & -1 & 0 & 0 & 0 & 0 & 0 \\ \frac{J_T}{8R} & 0 & -1 & -1 & 0 & 0 & 0 & 0 \end{pmatrix}. \tag{3.5.14}$$

From these expressions it is easy to verify equation (3.4.17)

$$\mathcal{Q}_{(1)} = -B_1 - \frac{1}{2R}[B_1, B_2], \qquad \mathcal{Q}_{(2)} = -B_2 + \frac{1}{2R}[B_1, B_2]. \tag{3.5.15}$$

Now, from relations (3.4.32) one can now readily calculate matrices A_1, A_2:

$$A_{(1)} = -B_1 - \frac{1}{2R}\{B_1, B_2\}, \qquad A_{(2)} = -B_2 + \frac{1}{2R}\{B_1, B_2\}, \tag{3.5.16}$$

and the monodromy matrix is

$$\mathcal{M}(w) = S_\infty \cdot \left(\mathbb{I} + \frac{A_1}{w} + \frac{A_2}{w - R}\right). \tag{3.5.17}$$

The A_1, A_2 matrices satisfy several properties required for inverse scattering construction [16] to work, e.g.,

$$A_k^\sharp = S_\infty \cdot A_k \cdot S_\infty^{-1}, \qquad A_k \cdot \eta \cdot A_k^T = 0. \tag{3.5.18}$$

Spectral flowed bubbling geometries

A bubbling solution associated to the above configuration is obtained by applying a combination of gauge and spectral flow transformations [46]. The harmonic functions are given as

$$K_1 = -\gamma - \frac{\gamma Q_2}{4\Sigma}, \qquad K_2 = -\gamma - \frac{\gamma Q_1}{4\Sigma}, \tag{3.5.19}$$

$$K_3 = \left(\epsilon_0 + \frac{1}{r}\right)\frac{q_3}{2} - \frac{q_3}{2\Sigma}, \qquad L_1 = 1 + \frac{Q_1}{4\Sigma}, \tag{3.5.20}$$

$$L_2 = 1 + \frac{Q_2}{4\Sigma}, \qquad L_3 = 1 + \frac{\gamma q_3}{2} - \frac{\gamma J_T}{8R} + \frac{\gamma J_T}{8\Sigma}, \tag{3.5.21}$$

$$V = \left(\epsilon_0 + \frac{1}{r}\right)\left(1 + \frac{\gamma q_3}{2}\right) - \frac{\gamma q_3}{2\Sigma}, \qquad M = \frac{J_T}{16R} - \frac{q_3}{4} - \frac{J_T}{16\Sigma}. \tag{3.5.22}$$

The charges at the centers are

$$\{q_1, l_1^I, k_1^I, m_1\} = \left\{1 + \frac{\gamma q_3}{2}, 0, 0, 0, 0, 0, \frac{q_3}{2}, 0\right\}, \tag{3.5.23}$$

$$\{q_2, l_2^I, k_2^I, m_2\} = \left\{-\frac{\gamma q_3}{2}, \frac{Q_1}{4}, \frac{Q_2}{4}, \frac{\gamma J_T}{8}, -\frac{\gamma Q_2}{4}, -\frac{\gamma Q_1}{4}, -\frac{q_3}{2}, -\frac{J_T}{16}\right\}, \tag{3.5.24}$$

and we still have the smoothness conditions (resulting from the bubble equations now) (3.5.4) and (3.5.5). Again, we write the matrix of scalars as an exponential of matrices B_1, B_2 as before, finding

$$B_1 = -\left(1 + \frac{\gamma q_3}{2}\right)\mathbb{F}_0 + \frac{J_T}{16R}\mathbb{F}_{p^0} + \frac{q_3}{2}\mathbb{F}_{p^3}, \tag{3.5.25}$$

$$\begin{aligned} B_2 = {} & \frac{\gamma q_3}{2}\mathbb{F}_0 - \frac{Q_1}{4}\mathbb{F}_1 - \frac{Q_2}{4}\mathbb{F}_2 - \frac{\gamma J_T}{8}\mathbb{F}_3 - \frac{J_T}{16R}\mathbb{F}_{p^0} - \frac{\gamma Q_2}{4}\mathbb{F}_{p^1} \\ & - \frac{\gamma Q_1}{4}\mathbb{F}_{p^2} - \frac{q_3}{2}\mathbb{F}_{p^3} + \frac{J_T}{8}\mathbb{E}_{q_0}. \end{aligned} \tag{3.5.26}$$

Matrices $\mathcal{Q}_{(1)}, \mathcal{Q}_{(2)}$ and A_1, A_2 and can now be readily computed. Once again matrices A_1 and A_2 matrices satisfy properties required for inverse scattering construction of [16] to work.

3.5.2 Many supertubes in Taub-NUT and the related bubbling geometries

The above example is easily generalised to N two-charge supertubes in Taub-NUT. Such a configuration is specified by the following eight harmonic functions [55]

$$V = \epsilon_0 + \frac{1}{r}, \qquad K^1 = 0, \qquad K^2 = 0, \qquad K^3 = k_0^3 - \sum_{i=1}^{N}\frac{q_3^i}{2r_i} \tag{3.5.27}$$

$$M = m_0 - \sum_{i=1}^{N}\frac{J_i}{16r_i}, \quad L_1 = l_0^1 + \sum_{i=1}^{N}\frac{Q_1^i}{4r_i}, \quad L_2 = l_0^2 + \sum_{i=1}^{N}\frac{Q_2^i}{4r_i}, \quad L_3 = l_0^3, \tag{3.5.28}$$

where $r_i = |\vec{r} - \vec{R}_i|$, with $\vec{R}_i = (0, 0, R_i)$ the positions of the supertubes. Smoothness conditions give N relations [55],

$$Q_1^i Q_2^i = q_3^i J_i, \tag{3.5.29}$$

and the condition that the solution be free of Dirac-Misner strings at each center gives the following $N+1$ conditions, for $i = 1, \ldots, N$,

$$\left(\epsilon_0 + \frac{1}{R_i}\right) J_i = 4 l_0^3 q_3^i, \qquad m_0 = \frac{1}{16} \sum_{i=1}^{N} \frac{J_i}{R_i}. \tag{3.5.30}$$

For this configuration, matrices B_j for $j = 1, \ldots, N$, are

$$B_j = -\frac{Q_1^j}{4}\mathbb{F}_1 - \frac{Q_2^j}{4}\mathbb{F}_2 - \frac{q_3^j}{2}\mathbb{F}_{p^3} + \frac{J_j}{8}\mathbb{E}_{q^0} - \frac{J_j}{16 R_j}\mathbb{F}_{p^0}, \tag{3.5.31}$$

and the matrix B_0 for the Taub-NUT center is

$$B_0 = -\mathbb{F}_0 + \frac{1}{16}\sum_{i=1}^{N} \frac{J_i}{R_i}\mathbb{F}_{p^0}. \tag{3.5.32}$$

The B_j matrices anti-commute with each other, $\{B_j, B_k\} = 0$. It then follows that the residue matrices A_j are

$$A_j = -B_j + \frac{1}{2R_j}\{B_j, B_0\} \tag{3.5.33}$$

$$= -B_j - \frac{J_j}{16 R_j}(\mathbf{e}_{53} + \mathbf{e}_{71}) - \frac{Q_1^j}{4R_j}\mathbf{e}_{73}, \tag{3.5.34}$$

and A_0 is

$$A_0 = -B_0 - \frac{1}{2R_i}\sum_{i=1}^{N}\{B_0, B_i\}, \tag{3.5.35}$$

$$= -B_0 + \sum_{i=1}^{N}\frac{J_j}{16 R_j}(\mathbf{e}_{53} + \mathbf{e}_{71}) + \sum_{i=1}^{N}\frac{Q_1^j}{4R_j}\mathbf{e}_{73}, \tag{3.5.36}$$

where symbol $\mathbf{e}_{ij}$ denote a 8×8 matrix with 1 in the i-th row and j-th column and 0 elsewhere.

Spectral flowed geometries with multiple supertubes

An $N+1$-center bubbling solution associated to the above configuration can be obtained by applying a combination of gauge and spectral flow transformations [46]. The final set of harmonic functions are,

$$V = \epsilon_0(1+\gamma c) + \gamma k_0^3 + \frac{1+\gamma\, c}{r} - \sum_{i=1}^{N}\frac{\gamma\, q_3^i}{2r_i}, \qquad K^1 = -\gamma\, l_0^2 - \sum_{i=1}^{N}\frac{\gamma\, Q_2^i}{4r_i},$$

$$K^2 = -\gamma\, l_0^1 - \sum_{i=1}^{N}\frac{\gamma\, Q_1^i}{4r_i}, \qquad K^3 = k_0^3 + c\,\epsilon_0 + \frac{c}{r} - \sum_{i=1}^{N}\frac{q_3^i}{2r_i},$$

$$M = m_0 - \frac{c\, l_0^3}{2} - \sum_{i=1}^{N}\frac{J_i}{16 r_i}, \qquad L_1 = l_0^1 + \sum_{i=1}^{N}\frac{Q_1^i}{4r_i},$$

$$L_2 = l_0^2 + \sum_{i=1}^{N}\frac{Q_2^i}{4r_i}, \qquad L_3 = l_0^3 - 2\gamma\, m_0 + \gamma\, c\, l_0^3 + \sum_{i=1}^{N}\frac{\gamma\, J_i}{8r_i},$$

where $c = \frac{1}{2}\sum_{i=1}^{N} q_3^i$ so that the net Gibbons-Hawking charge is +1. Smoothness conditions (3.5.29) and (3.5.30) remain the same. The B_j and B_0 matrices are

$$\begin{aligned} B_j = & \frac{\gamma\, q_3^j}{2}\mathbb{F}_0 - \frac{Q_1^j}{4}\mathbb{F}_1 - \frac{Q_2^j}{4}\mathbb{F}_2 - \frac{\gamma J_j}{8}\mathbb{F}_3 - \frac{\gamma\, Q_2^j}{4}\mathbb{F}_{p^1} \\ & - \frac{\gamma\, Q_1^j}{4}\mathbb{F}_{p^2} - \frac{q_3^j}{2}\mathbb{F}_{p^3} + \frac{J_j}{8}\mathbb{E}_{q^0} - \frac{J_j}{16R_j}\mathbb{F}_{p^0}, \end{aligned} \tag{3.5.37}$$

$$B_0 = -(1+\gamma\, c)\mathbb{F}_0 + m_0\mathbb{F}_{p^0} + c\mathbb{F}_{p^3}. \tag{3.5.38}$$

The B_j matrices anti-commute with each other, $\{B_j, B_k\} = 0$. It then follows that the residue matrices A_j are

$$A_j = -B_j + \frac{1}{2R_j}\{B_j, B_0\} \tag{3.5.39}$$

$$= -B_j - \frac{J_j}{16R_j}(\mathbf{e}_{53} + \mathbf{e}_{71}) - \frac{Q_1^j}{4R_j}\mathbf{e}_{73}, \tag{3.5.40}$$

and A_0 is

$$A_0 = -B_0 - \frac{1}{2R_i}\sum_{i=1}^{N}\{B_0, B_i\}, \tag{3.5.41}$$

$$= -B_0 + \sum_{i=1}^{N}\frac{J_j}{16R_j}(\mathbf{e}_{53} + \mathbf{e}_{71}) + \sum_{i=1}^{N}\frac{Q_1^j}{4R_j}\mathbf{e}_{73}. \tag{3.5.42}$$

3.6 Discussion and future directions

In vacuum five-dimensional gravity, many of the known interesting solutions can be constructed via the inverse scattering approach. The approach developed in [16, 34–36] for five-dimensional STU supergravity is akin to the inverse scattering approach of vacuum gravity. It has been shown in those references that certain non-extermal black holes and certain non-supersymmetric bubbling solutions of STU supergravity are captured in that formalism.

One of the main motivation of the present work is to extend that discussion to collinear BPS solutions. In this chapter, we have made significant progress on this problem, though some important questions remain unexplored. We obtained the Geroch group matrices for collinear bubbling solution, and exhibited that for these solutions the SO(4,4) monodromy matrices have only simple poles in the spectral parameter w with residues of rank two. These are precisely the conditions under which the formalism developed in [16] is applicable. In this work, we have not attempted explicit factorisation of these matrices, though we have checked that various consistency conditions of [16] are satisfied.

The Geroch group description obtained in this chapter is valuable for future developments. As mentioned in the introduction, to find explicit (novel) solutions in the Riemann-Hilbert approach one needs to perform a canonical factorisation of a monodromy matrix. Which monodromy matrix should one pick to start with? One strategy to obtain novel solutions can be to modify monodromy matrices of the known solutions in some controlled systematic way. This is the strategy we hope to adopt in the future. We would like to modify the monodromy matrices of bubbling solutions with N centers so as to make $2k$ of its centers akin to that of the JMaRT solution. Then, naively it appears that upon

factorisation one would be able to construct a solution with $N-2k$ BPS centers with k JMaRT type bolts.

It will be interesting to explore the Geroch group description of the full class of BPS, non-BPS, and almost BPS solutions and better understand the double (or higher) pole structure of monodromy matrices. We expect the techniques of [37, 38] to be applicable for their explicit factorisation. It will also be interesting to relate monodromy matrices to rod-structure [54] in some precise way.

We hope to return to some of these problems in our future work.

3.7 Appendix: Explicit representatives for smaller nilpotent orbits of $\mathfrak{so}(4,4)$ Lie algebra

Let us recall that a linear transformation X on a finite dimensional vector space is called nilpotent if for some r, $X^r = 0$. Let $\mathfrak{g}_{\mathbb{C}}$ be an arbitrary complex Lie algebra. Let $\mathfrak{h}_{\mathbb{C}}$ denote its Cartan subalgebra. We say an element X of the complex Lie algebra $\mathfrak{g}_{\mathbb{C}}$ is nilpotent if ad_X is nilpotent. A classification of nilpotent elements of the Lie algebra is obtained through the study of conjugacy classes of such elements using the natural action of Lie group attached to the Lie algebra. These conjugacy classes are called nilpotent orbits. For applications to black holes in a theory with three-dimensional symmetry G/K, we need to know the K orbits of nilpotent elements of the Lie algebra of G. Classifying all such orbits is a detailed exercise, see e.g., [56–58]. In this appendix we are interested in listing representatives of some of the smaller orbits of the real Lie algebra $\mathfrak{so}(4,4)$. We exhibit these representatives in the vector representation. We are interested in knowing ranks and nilpotency degree of these representatives in the vector representation. This data is of interest in the main text of our paper.

$\mathfrak{so}(8,\mathbb{C})$ basis

In order to list the representatives we define a basis. We do this in steps. Let us define four vectors in a four dimensional vector space,

$$v_1 = \{1,0,0,0\}, \qquad v_2 = \{0,1,0,0\}, \tag{3.7.1}$$
$$v_3 = \{0,0,1,0\}, \qquad v_4 = \{0,0,0,1\}, \tag{3.7.2}$$

then the twelve positive roots for the $\mathfrak{so}(8,\mathbb{C})$ Lie algebra can be taken to be

$$e_1 = v_1 - v_2, \qquad e_2 = v_1 - v_3, \qquad e_3 = v_1 - v_4, \tag{3.7.3}$$
$$e_4 = v_2 - v_3, \qquad e_5 = v_2 - v_4, \qquad e_6 = v_3 - v_4, \tag{3.7.4}$$
$$e_7 = v_1 + v_2, \qquad e_8 = v_1 + v_3, \qquad e_9 = v_1 + v_4, \tag{3.7.5}$$
$$e_{10} = v_2 + v_3, \qquad e_{11} = v_2 + v_4, \qquad e_{12} = v_3 + v_4. \tag{3.7.6}$$

The 8×8 dimensional Cartan-Weyl basis that realises the above root vectors is as follows. Let the symbol $\mathbf{e}_{ij}$ denote a 8×8 matrix with 1 in the i-th row and j-th column and 0 elsewhere. We have the Cartan subalgebra generators

$$\mathbb{H}_1 = \mathbf{e}_{11} - \mathbf{e}_{55}, \qquad \mathbb{H}_2 = \mathbf{e}_{22} - \mathbf{e}_{66},$$
$$\mathbb{H}_3 = \mathbf{e}_{33} - \mathbf{e}_{77}, \qquad \mathbb{H}_4 = \mathbf{e}_{44} - \mathbf{e}_{88}, \tag{3.7.7}$$

and the positive root generators

$$\mathbb{E}_1 = \mathbf{e}_{12} - \mathbf{e}_{65}, \qquad \mathbb{E}_2 = \mathbf{e}_{13} - \mathbf{e}_{75}, \qquad \mathbb{E}_3 = \mathbf{e}_{14} - \mathbf{e}_{85}, \tag{3.7.8}$$

$$\mathbb{E}_4 = \mathbf{e}_{23} - \mathbf{e}_{76}, \qquad \mathbb{E}_5 = \mathbf{e}_{24} - \mathbf{e}_{86}, \qquad \mathbb{E}_6 = \mathbf{e}_{34} - \mathbf{e}_{87}, \tag{3.7.9}$$

$$\mathbb{E}_7 = \mathbf{e}_{16} - \mathbf{e}_{25}, \qquad \mathbb{E}_8 = \mathbf{e}_{17} - \mathbf{e}_{35}, \qquad \mathbb{E}_9 = \mathbf{e}_{18} - \mathbf{e}_{45}, \tag{3.7.10}$$

$$\mathbb{E}_{10} = \mathbf{e}_{27} - \mathbf{e}_{36}, \qquad \mathbb{E}_{11} = \mathbf{e}_{28} - \mathbf{e}_{46}, \qquad \mathbb{E}_{12} = \mathbf{e}_{38} - \mathbf{e}_{47}, \tag{3.7.11}$$

together with the negative root generators,

$$\mathbb{F}_i = \mathbb{E}_i^T. \tag{3.7.12}$$

The simple step generators are $\mathbb{E}_1, \mathbb{E}_2, \mathbb{E}_3$, and $\mathbb{E}_{12}$.

α- and β-labels

For each nilpotent orbit of the complex Lie algebra $\mathfrak{g}_{\mathbb{C}}$ there is a triple (e, f, h) of elements where e is a nilpotent element of the orbit, such that [56]

$$[h, e] = 2e, \qquad [h, f] = -2f, \qquad [e, f] = h. \tag{3.7.13}$$

Such a triple is called a standard triple. We can take h to be in the Cartan subalgebra $\mathfrak{h}_{\mathbb{C}}$, and furthermore conjugate $\{h, e, f\}$ such that h lies in the "fundamental domain" [56]. Then the element h is characterized by its eigenvalues under the adjoint action on simple root generators e_i's

$$[h, e_i] = \alpha_i(h) e_i, \qquad i = 1, 2, \ldots, \text{rank } \mathfrak{g}. \tag{3.7.14}$$

Moreover, we can always find a standard triple such that the eigenvalues $\alpha_i(h) \in \{0, 1, 2\}$. If we label every node of the Dynkin diagrams with the eigenvalue $\alpha_i(h)$ of h on the corresponding simple root, we get the weighted Dynkin diagrams for the orbits. These are called α-labels of the nilpotent orbit. There are twelve such orbits[6] for $\mathrm{SO}(8, \mathbb{C})$. We are only interested in the smaller orbits with weighted Dynkin diagrams:

$\mathcal{O}_1$ 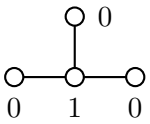

$\mathcal{O}_2$ 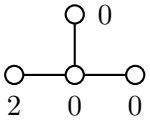

$\mathcal{O}_3$ 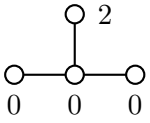

$\mathcal{O}_4$ 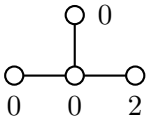

[6] In the table on page 84 of [56] there is a typo. Our $\mathcal{O}_6$ orbit in their notation corresponds to the partition $[3^2, 1^2]$ and is not listed in the table.

$\mathcal{O}_5$ 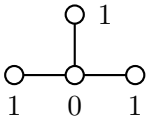

$\mathcal{O}_6$ 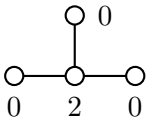

where we use the standard ordering convention

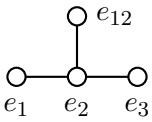

with $\{e_1, e_2, e_3, e_{12}\}$ as simple root generators.

The α-labels uniquely specify the nilpotent orbits of the complex Lie algebra $\mathfrak{so}(8,\mathbb{C})$. It may happen that two nilpotent elements X, Y in $\mathfrak{so}(4,4)$ are in the same $\mathfrak{so}(8,\mathbb{C})$ orbit but different $\mathfrak{so}(4,4)$ orbits, i.e.,

$$gXg^{-1} = Y, \tag{3.7.15}$$

for some g in SO$(8,\mathbb{C})$ but not for any g in SO(4,4). That is, for a given α-label there can be several real orbits. The real orbits are classified by the β-labels. The β-labels are defined as follows. For an SO(8,$\mathbb{C}$) orbit consider a standard triple (h, e, f) such that under Chevalley involution θ,

$$\theta(h) = -h, \quad \theta(e) = -f, \quad \theta(f) = -e. \tag{3.7.16}$$

Such standard triples are called Cayley triples. All the triples listed below for SO(8,$\mathbb{C}$) orbits are of this type. The Cayley transform of a Cayley triple (e, f, h) is now defined as the standard triple (e', f', h') where

$$e' = \frac{1}{2}(e + f + ih), \tag{3.7.17}$$

$$f' = \frac{1}{2}(e + f - ih), \tag{3.7.18}$$

$$h' = i(e - f). \tag{3.7.19}$$

It follows that $h' \in \mathfrak{k}_{\mathbb{C}}$ and $e', f' \in \mathfrak{p}_{\mathbb{C}}$, where $\mathfrak{k}_{\mathbb{C}}$ is the subalgebra of $\mathfrak{g}_{\mathbb{C}}$ fixed under the Chevalley involution. The algebra $\mathfrak{k}_{\mathbb{C}}$ in our case is

$$[\mathfrak{sl}(2,\mathbb{C})]^4\,. \tag{3.7.20}$$

One can take the h' in the Cartan subalgebra of $\mathfrak{k}_{\mathbb{C}}$. We label each node of the Dynkin diagram of $\mathfrak{k}_{\mathbb{C}}$ by the eigenvalue of the corresponding simple root on h'. The weighted Dynkin diagram thus obtained is called the β-label of the orbit, and is an invariant of the real orbits of SO(4,4). α- and β- labels are classified for the case of our interest in [57].

$[\mathfrak{sl}(2,\mathbb{C})]^4$ generators

There are many ways to make manifest the four commuting $\mathfrak{sl}(2,\mathbb{C})$. We find a set that will be useful for the smaller orbits, in the sense that h' will be in Cartan subalgebra of $\mathfrak{k}_{\mathbb{C}}$.

Recall that we have 12 positive roots e_i's and 12 negative roots f_i's. The set of generators fixed under the Chevalley involution are of the type

$$k_i = e_i - f_i. \tag{3.7.21}$$

We start with observation that k_1, k_6, k_7 and k_{12} commute with each other. These are a maximal set of commuting generators, so they can be taken to span the Cartan subalgebra of $\mathfrak{k}_{\mathbb{C}}$. Consider the general element in the Cartan subalgebra

$$X = a_1 k_1 + a_6 k_6 + a_7 k_7 + a_{12} k_{12}, \tag{3.7.22}$$

and consider $\mathrm{ad}_X k_i$, $i = 1, 2, \ldots, 12$, i.e.,

$$[X, k_i] = \sum_{j=1}^{12} c_i^j k_j. \tag{3.7.23}$$

We observe that by tuning (a_1, a_6, a_7, a_{12}) we can make 10 out of 12 eigenvalues of the matrix c_i^j zeros. The combinations that diagonalise the matrix c_i^j make the four commuting $\mathfrak{sl}(2,\mathbb{C})$ manifest. Such a set of generators are

$$H_1 = \frac{i}{2}\left(k_1 + k_6 + k_7 + k_{12}\right), \tag{3.7.24}$$

$$H_2 = \frac{i}{2}\left(k_1 - k_6 + k_7 - k_{12}\right), \tag{3.7.25}$$

$$H_3 = \frac{i}{2}\left(k_1 + k_6 - k_7 - k_{12}\right), \tag{3.7.26}$$

$$H_4 = \frac{i}{2}\left(k_1 - k_6 - k_7 + k_{12}\right), \tag{3.7.27}$$

$$E_1 = \frac{i}{4}\left(-k_2 + ik_3 + ik_4 + k_5 - k_8 + ik_9 + ik_{10} + k_{11}\right), \tag{3.7.28}$$

$$E_2 = \frac{i}{4}\left(+k_2 + ik_3 - ik_4 + k_5 + k_8 + ik_9 - ik_{10} + k_{11}\right), \tag{3.7.29}$$

$$E_3 = \frac{i}{4}\left(+k_2 - ik_3 - ik_4 - k_5 - k_8 + ik_9 + ik_{10} + k_{11}\right), \tag{3.7.30}$$

$$E_4 = \frac{i}{4}\left(-k_2 - ik_3 + ik_4 - k_5 + k_8 + ik_9 - ik_{10} + k_{11}\right), \tag{3.7.31}$$

$$F_1 = \frac{i}{4}\left(-k_2 - ik_3 - ik_4 + k_5 - k_8 - ik_9 - ik_{10} + k_{11}\right), \tag{3.7.32}$$

$$F_2 = \frac{i}{4}\left(+k_2 - ik_3 + ik_4 + k_5 + k_8 - ik_9 + ik_{10} + k_{11}\right), \tag{3.7.33}$$

$$F_3 = \frac{i}{4}\left(+k_2 + ik_3 + ik_4 - k_5 - k_8 - ik_9 - ik_{10} + k_{11}\right), \tag{3.7.34}$$

$$F_4 = \frac{i}{4}\left(-k_2 + ik_3 - ik_4 - k_5 + k_8 - ik_9 + ik_{10} + k_{11}\right). \tag{3.7.35}$$

$\mathcal{O}_1$ orbit

As an example consider the $\mathcal{O}_1$ orbit. A standard triple for this orbit is[7]

$$h = h_1 - h_2, \tag{3.7.36}$$
$$e = {}_1, \tag{3.7.37}$$
$$f = f_1. \tag{3.7.38}$$

In the vector representation, matrices in this orbit have nilpotency $X^2 = 0$ and have `rank` $X = 2$. The α label for this orbit is

$$(0, 1, 0, 0), \tag{3.7.39}$$

Now using Cayley transform

$$h' = i(e_1 - f_1) = ik_1 = \frac{1}{2}(H_1 + H_2 + H_3 + H_4). \tag{3.7.40}$$

Therefore the β-label is $(1, 1, 1, 1)$. The $\mathcal{O}_1$ orbit is of main interest in the main text of our paper. It is the unique orbit with nilpotency degree two in the vector representation, and matrix rank of representatives in this orbit is 2. In the adjoint this orbit has degree 3, i.e.,

$$(\mathrm{ad}_X)^3 = 0. \tag{3.7.41}$$

With a bit more work, one can similarly find other representatives. On the next page we present a list.

[7] To avoid any confusion, let us remark that the h is in the Cartan subalgebra, but is not in the fundamental domain. Hence, its eigenvalues on the simple root generators do not give the α-label. The same comment applies to the standard triples listed in table 3.1.

Orbit	**α-label**	**Neutral**	**β-label**	**Nilpositive**	**Nilp.**	**Rank(X)**
$[2^2,1^4]$	$(0,1,0,0)$	h_1-h_2	$(1,1,1,1)$	e_1	2	2
$[3,1^5]$	$(2,0,0,0)$	$2h_1$	$(2,2,0,0)$ $(0,0,2,2)$	e_1+e_7 e_1-e_7	3	2
$[2^4]^I$	$(0,0,2,0)$	$h_1-h_2+h_3-h_4$	$(2,0,2,0)$ $(0,2,0,2)$	e_1+e_6 e_1-e_6	2	4
$[2^4]^{II}$	$(0,0,0,2)$	$h_1-h_2+h_3+h_4$	$(2,0,0,2)$ $(0,2,2,0)$	e_1+e_{12} e_1-e_{12}	2	4
$[3,2^2,1]$	$(1,0,1,1)$	$2h_1+h_3-h_4$ $2h_1+h_3+h_4$ $h_1-h_2+2h_3$ $h_1+h_2+2h_3$	$(3,1,1,1)$ $(1,3,1,1)$ $(1,1,3,1)$ $(1,1,1,3)$	$e_1+e_6+e_7$ $e_1+e_7-e_{12}$ $e_1+e_6-e_{12}$ $e_6+e_7-e_{12}$	3	4
$[3^2,1^2]$	$(0,2,0,0)$	$2(h_1+h_3)$	$(4,0,0,0)$ $(0,4,0,0)$ $(0,0,4,0)$ $(0,0,0,4)$	$e_1+e_6+e_7+e_{12}$ $e_1-e_6+e_7-e_{12}$ $e_1+e_6-e_7-e_{12}$ $e_1-e_6-e_7+e_{12}$	3	4
		$2(h_1-h_3)$	$(2,2,2,2)$	$\sqrt{2}(e_1+e_4)$		

Table 3.1: List of the smaller nilpotent orbits of $\mathfrak{so}(4,4)$ classified by α,β-labels. We have also listed representative neutral and nilpositive elements that together form a standard triple $\{h,e,f\}$ in the corresponding orbit. Nilp. and Rank(X) denote the nilpotency degree (smallest n such that $X^n=0$) and the matrix rank of the orbit in the 8×8 vector representation.

4

Hair on non-extremal D1-D5 bound states

Law of falling bodies: per second per second.

Calypso

4.1 Introduction

Certain earlier studies in black hole physics attempted to find hair on black holes, hoping that if black holes admit large number of hair parameters then they would be analogous to excited atoms. This analogy, if viable, could in turn provide some handle on understanding microscopic origin of black hole entropy. In such studies one looks for smooth and normalisable solutions of perturbations over a black hole background. Those attempts, however, could not find black hole hair, and the results led to the so-called no-hair hypothesis. A version of it states that regardless of the matter model, the end point of gravitational collapse is characterised by conserved charges only. Evidence in favour of the hypothesis is presented in the form of no-hair theorems; evidence against the hypothesis is presented by explicit construction of hairy black holes. Typically the counter-examples violate some energy conditions, or have non-minimal couplings, or have non-canonical kinetic terms. See, e.g., references [59–61] for reviews on these developments. The absence of such hair modes suggested that the analogy between black holes and atoms is not a viable one.[1]

String theory has had numerous successes in black hole physics including some key results on the statistical mechanical interpretation of the Bekenstein-Hawking entropy. In string theory at weak couplings it has been shown in great detail that certain intersecting D-brane systems with the same charge and mass as the black hole have precisely the requisite number of states [5, 62]. These calculations have been successfully extended in numerous ways, though several issues still remain unanswered. Notably, gravity (or bulk) description of these microstates is not yet fully understood. The fuzzball proposal [6,63,64] addresses this question. It argues that the black hole event horizon and its interior are replaced with quantum bound states with size of the order of the event horizon. In this program large classes of smooth supergravity solutions have been constructed, and their weak coupling description understood. The evidence from the construction of such black hole microstates suggests that the true quantum bound state indeed has a size of order

[1] These statements are under the assumption that the test fields inherit all spacetime symmetries. Dropping this assumption, recent studies [60, 61] have shown that stationary black holes do admit hair where one can draw a parallel with states of the hydrogen atom.

the event horizon. This proposal completely changes the traditional picture of the black hole horizon and its interior.

In the early days of the fuzzball proposal, perturbative hair modes[2] were used to exhibit the first examples of microstates for the three-charge system. Mathur, Saxena, and Srivastava (MSS) [17] pioneered these investigations. They constructed a BPS perturbation over certain smooth BPS D1-D5 geometries. The perturbation was found to be smooth everywhere and normalisable. This situation needs to be contrasted with black holes. As discussed above black holes seem not to admit hair, but black hole microstates in the sense of the fuzzball proposal do admit such hair. In fact such hair modes lead to further microstates, as the hair modes smoothly deform the geometry in a controlled manner to another geometry. In some cases non-linear completion of the hair modes can also be worked out, where it has been shown that the linearisation of the non-linear solution leads to the hair mode. Over the years, this circle of ideas has been a recurrent theme in the fuzzball literature [65–71] and together with other developments has culminated in the construction and understanding of the BPS superstratum [72–76] — supergravity solutions parameterised by arbitrary functions of two variables.

The key aim of the present chapter is to demonstrate that certain non-supersymmetric fuzzballs also admit hair modes. We show this by adapting MSS study to a non-supersymmetric setting. Let us recall that on the CFT side MSS started with a particularly simple 2-charge state: the single unit spectral flow (both left and right) of the NS-NS vacuum $|0\rangle_{\rm NS}$. To add 'hair' to this state, they considered the action of a chiral primary on $|0\rangle_{\rm NS}$ to get $|\psi\rangle_{\rm NS}$. Then they considered a descendant of this state in the chiral primary multiplet obtained by the action of the left lowering operator of angular momentum

$$J_0^-{}_L|\psi\rangle_{\rm NS}. \tag{4.1.1}$$

Under one unit of spectral flow on both the left and the right sectors on the state (4.1.1) we get an RR state that carries one unit of linear momentum. This final state is thought of as hair on the 2-charge state in the gravity description.

On the supergravity side, the geometry of the starting 2-charge state has an asymptotically flat region connected to spectral flowed $AdS_3 \times S^3$ core via the throat region [77,78]. MSS constructed a supergravity perturbation on top of this geometry in a matched asymptotic expansion in the following steps:

1. The perturbation solution in the inner region was obtained by applying spectral flows on the appropriate solution in the chiral primary multiplet on top of global $AdS_3 \times S^3$.

2. In the outer region the perturbation solution was obtained by explicitly solving the equations of motion and choosing the normalisable solution.

3. As the last step they matched the inner and the outer region solutions. It is very non-trivial that such a matching can be done.

In this chapter we retrace the above steps without much additional technical complications for the non-extremal 2-charge D1-D5 geometries of Jejjala, Madden, Ross and Titchener (JMaRT) [18].

[2]The term "hair" has different meanings in the black hole microstate literature. Depending on the context sometimes it has been used to refer to 'neck' degrees of freedom and sometimes to refer to 'cap' degrees of freedom. In this chapter, the hair mode we construct has its support in the neck region and it also adds momentum charge to the background geometry.

Unlike the motivation of MSS, our aim in this work is not to show that the non-extremal D1-D5-P geometries exist perturbatively; classes of such non-linear solutions are already known [40–42]. Our aim in this work is to emphasise that perturbative techniques used for finding supersymmetric fuzzballs can be taken over to non-supersymmetric set-ups as well. We adapt the MSS scheme to leading order only (because of technical complications) in the matched asymptotic expansion for the JMaRT set-up. Extending the computation to higher orders is significantly more difficult and is not attempted in this chapter. We leave that for future work, though certain ground work for this is set up in appendix 4.5. In the BPS case, it is now understood that MSS perturbation is the linearisation of a non-linear solution of IIB supergravity [79]. Perhaps it may be feasible to find the non-linear version of the perturbative solution constructed in this chapter.

The rest of the chapter is organised as follows. We start with a brief review of the 2-charge non-extremal D1-D5 bound states of Jejjala, Madden, Ross and Titchener [18] in section 4.2. In section 4.3 linearised perturbation equations are solved to leading order. We end with a brief discussion in section 4.4. In order to carry out our analysis numerous properties of harmonics on S^3 are required. Relevant properties are collected in appendix 4.5 together with various conventions and notation we follow in the main text.

4.2 Two charge non-extremal D1-D5 bound states

In this section we briefly review the 2-charge non-extremal D1-D5 bound states of Jejjala, Madden, Ross and Titchener (JMaRT) [18]. We first present the supergravity solutions, illustrate how to take limits to the inner and outer regions, and then briefly mention their CFT interpretation. The JMaRT solutions have received renewed attention in the last couple of years [35, 39, 80–82].

The self-dual two-charge JMaRT solution is obtained by setting $\delta_1 = \delta_5$ in the 2-charge solutions of [18]. In order to connect to the notation of [17] we also replace

$$a_1 \to -a, \qquad \theta \to \frac{\pi}{2} - \theta, \qquad \phi \leftrightarrow \psi. \tag{4.2.1}$$

The six-dimensional metric then simplifies to

$$\begin{aligned} ds^2 \;=\; & \frac{1}{H}\big[-(f-M)(dt+(f-M)^{-1}Mc^2 a\sin^2\theta d\phi)^2 + f(dy - f^{-1}Ms^2 a\cos^2\theta d\psi)^2\big] \\ & + H\left(\frac{dr^2}{r^2+a^2-M} + d\theta^2 + \frac{r^2}{f}\cos^2\theta d\psi^2 + \frac{r^2+a^2-M}{f-M}\sin^2\theta d\phi^2\right), \end{aligned} \tag{4.2.2}$$

where $s = \sinh\delta, c = \cosh\delta, f = r^2 + a^2\cos^2\theta$, and $H = f + Ms^2$.

The RR two-form supporting this metric takes the form

$$\begin{aligned} C \;=\; & -\frac{Masc}{H}\sin^2\theta\; dy\wedge d\phi - \frac{Masc}{H}\cos^2\theta\; dt\wedge d\psi \\ & -\frac{Msc}{H}dt\wedge dy - \frac{Msc}{H}(r^2+Ms^2)\sin^2\theta d\phi\wedge d\psi. \end{aligned} \tag{4.2.3}$$

The resulting field strength $F = dC$ can be easily checked to be self-dual $F = \star F$. Moreover, $F\wedge\star F = 0$, i.e.,

$$F_{ABC}F^{ABC} = 0. \tag{4.2.4}$$

Due to the self-duality property of F it immediately follows that $d\star F = 0$. It can also be easily checked that the six-dimensional (simplified) Einstein equations

$$R_{AB} - \frac{1}{4}F_{ACD}F_B{}^{CD} = 0, \tag{4.2.5}$$

are satisfied. The gauge charges in five-dimensions upon reduction along y are simply

$$Q_1 = Q_5 = Q = Msc, \qquad Q_p = 0. \tag{4.2.6}$$

The determinant of the (y, θ, ϕ, ψ) part of the metric (4.2.2) vanishes at $r = 0$. This signals that a circle direction shrinks to zero size there. The Killing vector with closed orbit that has zero norm at $r = 0$ is

$$\xi = \partial_y + \frac{a}{Ms^2}\partial_\psi. \tag{4.2.7}$$

That is, the direction that goes to zero size at $r = 0$ is y at fixed $(\tilde{\psi}, \phi)$ where

$$\tilde{\psi} = \psi - \frac{a}{Ms^2}y. \tag{4.2.8}$$

In order to make $y \to y + 2\pi R$ a closed orbit at fixed $(\tilde{\psi}, \phi)$ we require

$$\frac{aR}{Ms^2} = m \in \mathbb{Z}. \tag{4.2.9}$$

To have smooth degeneration of the y circle near $r = 0$ we choose the radius R as

$$R = \frac{Ms^2}{\sqrt{a^2 - M}}. \tag{4.2.10}$$

Inserting R from (4.2.10) into the integer quantisation condition (4.2.9) fixes M to be

$$M = a^2\left(1 - \frac{1}{m^2}\right). \tag{4.2.11}$$

Upon taking $m = 1$ we recover the supersymmetric solutions of [77, 78] as follows. Setting $m = 1$ in (4.2.11) we see that $M = 0$. In order to keep charges $Q_1 = Q_5 = Q = Msc$ finite we must take $\delta \to \infty$. In this limit metric (4.2.2) further simplifies to

$$\begin{aligned} ds^2 &= \frac{1}{H}\Big[- f\left(dt + \frac{aQ}{f}\sin^2\theta d\phi\right)^2 + f\left(dy - \frac{aQ}{f}\cos^2\theta d\psi\right)^2\Big] \\ &\quad + H\left(\frac{dr^2}{r^2 + a^2} + d\theta^2 + \frac{r^2}{f}\cos^2\theta d\psi^2 + \frac{r^2 + a^2}{f}\sin^2\theta d\phi^2\right), \end{aligned} \tag{4.2.12}$$

with $H = f + Q$. This metric can be rewritten in the following more recognisable form

$$\begin{aligned} ds^2 = &- \frac{1}{h}(dt^2 - dy^2) + hf\left(d\theta^2 + \frac{dr^2}{r^2 + a^2}\right) - \frac{2aQ}{hf}\left(\cos^2\theta dy d\psi + \sin^2\theta dt d\phi\right) \\ &+ h\left[\left(r^2 + \frac{a^2Q^2\cos^2\theta}{h^2f^2}\right)\cos^2\theta d\psi^2 + \left(r^2 + a^2 - \frac{a^2Q^2\sin^2\theta}{h^2f^2}\right)\sin^2\theta d\phi^2\right], \end{aligned} \tag{4.2.13}$$

where

$$h = \frac{H}{f} = 1 + \frac{Q}{f}. \tag{4.2.14}$$

This form of the 2-charge metric was the starting point in [17]. Upon setting $m = 1$ the RR 2-form field (4.2.3) simplifies to

$$\begin{aligned} C = &- \frac{Qa\sin^2\theta}{Q + f}dy \wedge d\phi - \frac{Qa\cos^2\theta}{Q + f}dt \wedge d\psi \\ &- \frac{Q}{Q + f}dt \wedge dy - \frac{Q}{Q + f}(r^2 + Q)\sin^2\theta d\phi \wedge d\psi, \end{aligned} \tag{4.2.15}$$

which also matches with the corresponding expression in [17] upon making a simple gauge transformation $C \to C + d\Lambda$ with $\Lambda = Q\phi d\psi$.

Inner and outer regions

In the next section we solve certain perturbation equations in a matched asymptotic expansion. In order to do this we split the JMaRT geometry in two overlapping regions: the inner and outer regions. We solve the perturbations equations in two regions separately and match the solutions in the overlap region.

The 'Inner' Region

To describe the above two-charge configuration from the AdS/CFT perspective we must take a near-decoupling limit where a large inner region involving $AdS_3\times S^3$ develops. This inner region is coupled to flat space via a neck region. The decoupling limit is achieved by taking the large R limit, i.e., by taking

$$\epsilon = \frac{\sqrt{Q}}{R} \ll 1, \tag{4.2.16}$$

while keeping the charge Q and other parameters of the geometry fixed. In this limit the region $r \ll \sqrt{Q}$ is identified as the inner region. This amounts to taking $H \approx Q$ in (4.2.2) and taking $Msc \approx Q$ in the cross terms in the metric. From (4.2.2) and integer quantisation (4.2.9) we get an asymptotically $AdS_3\times S^3$ metric,

$$\begin{aligned} ds^2 \;=\; & \frac{1}{Q}\big[-(f-M)(dt+(f-M)^{-1}aQ\sin^2\theta d\phi)^2 + f(dy - f^{-1}aQ\cos^2\theta d\psi)^2\big] \\ & + Q\left(\frac{dr^2}{r^2+a^2-M} + d\theta^2 + \frac{r^2}{f}\cos^2\theta d\psi^2 + \frac{r^2+a^2-M}{f-M}\sin^2\theta d\phi^2\right), \end{aligned} \tag{4.2.17}$$

supported by the C-field

$$C_{ty} = \frac{r^2}{Q}, \qquad C_{\psi\phi} = Q\sin^2\theta \tag{4.2.18}$$

$$C_{y\phi} = -a\sin^2\theta, \qquad C_{\psi t} = a\cos^2\theta. \tag{4.2.19}$$

The parameter M in equation (4.2.2) can be replaced in favour of the integer m and rotation parameter a through equation (4.2.9).

Under the change of coordinates

$$\psi_{\rm NS} = \psi - \frac{m}{R}y, \quad \phi_{\rm NS} = \phi - \frac{m}{R}t, \tag{4.2.20}$$

metric (4.2.17) becomes

$$\begin{aligned} ds^2 = \; & -\frac{1}{Q}\left(r^2+\frac{a^2}{m^2}\right)dt^2 + \frac{r^2}{Q}dy^2 + Q\left(r^2+\frac{a^2}{m^2}\right)^{-1}dr^2 \\ & + \; Q(d\theta^2 + \cos^2\theta d\psi_{\rm NS}^2 + \sin^2\theta d\phi_{\rm NS}^2). \end{aligned} \tag{4.2.21}$$

Setting $m=1$ the above metric can be recognised as exactly the $AdS_3\times S^3$ metric used by MSS in the NS-NS sector. The coordinate transformation (4.2.20) is the gravity dual of the D1-D5 CFT spectral flow transformation. Defining

$$a' = \frac{a}{m} \tag{4.2.22}$$

metric (4.2.21) can be written in a more convenient form

$$ds^2 = -\frac{(r^2+a'^2)}{Q}dt^2 + \frac{r^2}{Q}dy^2 + \frac{Q}{(r^2+a'^2)}dr^2 + Q(d\theta^2 + \cos^2\theta d\psi_{\rm NS}^2 + \sin^2\theta d\phi_{\rm NS}^2). \tag{4.2.23}$$

The F-field supporting the inner region metric (4.2.23) is simply

$$F_{tyr} = \frac{2r}{Q}, \tag{4.2.24}$$

$$F_{\theta\psi\phi} = 2Q\sin\theta\cos\theta. \tag{4.2.25}$$

From equations (4.2.9) and (4.2.16) we also have the relation

$$\epsilon = \frac{a}{m\sqrt{Q}}. \tag{4.2.26}$$

As a result, the inner region limit $r \ll \sqrt{Q}$ together with $\epsilon \ll 1$ can operationally be thought of as an expansion in powers of $\frac{r}{\sqrt{Q}}$, $\frac{a}{m\sqrt{Q}}$. In the NS-NS coordinates via an explicit calculation we see that the metric expansion is in powers of ϵ^2. Since in this chapter we are only interested in perturbation to $\mathcal{O}(\epsilon^0)$ we will not be concerned with the corrections to the inner region metric.

The 'Outer' Region

The outer region $\epsilon\sqrt{Q} \ll r < \infty$ has the metric

$$ds^2 = -\frac{r^2}{Q+r^2}(dt^2 - dy^2) + \frac{(Q+r^2)}{r^2}dr^2 + (Q+r^2)(d\theta^2 + \cos^2\theta d\psi^2 + \sin^2\theta d\phi^2), \tag{4.2.27}$$

to the leading order. The 2-form C-field supporting the outer region metric is simply

$$C_{ty} = -\frac{Q}{Q+r^2} \quad \Longrightarrow \quad F_{tyr} = \frac{2Qr}{(Q+r^2)^2}, \tag{4.2.28}$$

$$C_{\psi\phi} = Q\sin^2\theta \quad \Longrightarrow \quad F_{\theta\psi\phi} = 2Q\sin\theta\cos\theta. \tag{4.2.29}$$

The overlap of the inner and outer regions is in the region

$$\epsilon\sqrt{Q} \ll r \ll \sqrt{Q}. \tag{4.2.30}$$

The outer region limit can be operationally thought of as a power series expansion in $\frac{a}{mr}, \frac{a}{m\sqrt{Q}}$.

The outer region metric (4.2.27) does not have any non-extremal features. In particular, it does not look like non-extremal D1-D5 black hole. This is because in the JMaRT construction the fuzzball and the black hole parameter spaces are mutually exclusive.

CFT description

The 2-charge JMaRT solution corresponds to $m = 2s+1$ units of left and $m = 2s+1$ units of right spectral flows on the NS-NS vacuum. Since equal amount of left and right spectral flows are involved

$$h = \bar{h}, \tag{4.2.31}$$

and the state has no net linear momentum. When $m = 1$, i.e., $s = 0$, we get a supersymmetric configuration, a Ramond-Ramond ground state. For other values of s, supersymmetry is broken as both the left and right sectors carry (equal amount of) excitations. CFT description of JMaRT solution has been explored in great detail in the literature [18, 82], we refer the reader to these references for further details.

4.3 Perturbation

In this section we construct the RR axion and NS-NS 2-form field perturbation to leading order in both the inner and the outer regions and show their matching. The linearised perturbation equations are,

$$H_{ABC} + \frac{1}{3!}\epsilon_{ABCDEF}H^{DEF} + wF_{ABC} = 0, \tag{4.3.1}$$

$$\Box w - \frac{1}{3}F^{ABC}H_{ABC} = 0, \tag{4.3.2}$$

where F is simply dC,

$$F_{ABC} = 3\partial_{[A}C_{BC]} = \partial_A C_{BC} + \partial_B C_{CA} + \partial_C C_{AB}. \tag{4.3.3}$$

These equations are precisely the equations studied by Mathur, Saxena, and Srivastava [17]. The main difference[3] is that in [17], the background considered is supersymmetric, whereas in our study it is not.

4.3.1 CFT description

Before getting in to the supergravity analysis, it is useful to understand the CFT state to which the perturbation we construct below corresponds to. In the NS-NS sector we act with a chiral primary operator with $h = l, \bar{h} = l$ on the NS-NS vacuum. Let us denote the resulting state by $|\psi\rangle_{\rm NS}$. On this state we act with angular momentum lowering generators both on the left and on the right k and $\bar{k}$ times respectively:

$$(J_0^-{}_L)^k (J_0^-{}_R)^{\bar{k}} |\psi\rangle_{\rm NS}. \tag{4.3.4}$$

Next, on the resulting state we act with $m = 2s+1$ (odd) units of spectral flows both on the left and on the right. As a result we get an excited state in the R-R sector

$$\left[(J_0^-{}_L)^k (J_0^-{}_R)^{\bar{k}} |\psi\rangle\right]_{\rm R}^{(2s+1)}. \tag{4.3.5}$$

For general values of the $l, k, \bar{k}, m = 2s+1$ the state thus obtained carries both left and right moving excitations. As we explain momentarily, we tune $\bar{k}$ such that 'for the perturbation' $\bar{h}$ is zero, but $h \neq 0$. Such a perturbation does not carry any 'extra energy' and is tractable to leading order in our supergravity analysis.

4.3.2 Perturbation at leading order

We first construct the inner region perturbation and then the outer region.

4.3.2.1 Inner region

In the inner region (4.2.23)–(4.2.25) the perturbation equation (4.3.1) gives,

$$H_{tyr} + \frac{r}{Q^2}\left(2wQ + \frac{H_{\theta\psi\phi}}{\sin\theta\cos\theta}\right) = 0, \tag{4.3.6}$$

when all three indices are taken either on AdS_3 or on S^3. When one index is on AdS_3 and the others on S^3 we get the same equations as when one index is on S^3 and the others on AdS_3. We get

$$H_{\mu\nu a} + \frac{1}{6}\epsilon_{\mu\nu a\rho bc}g^{\rho\rho'}g^{bb'}g^{cc'}H_{\rho' b' c'} = 0, \tag{4.3.7}$$

[3] Our F and H notation conforms to more standard string theory notation, but it is interchanged compared to reference [17].

where the Greek indices refer to AdS coordinates and the lower case Latin indices to S^3 coordinates. We now expand the various fields in harmonics on S^3 as (see appendix 4.5)

$$B_{\mu\nu} = b^{I_1}_{\mu\nu} Y^{I_1}, \tag{4.3.8}$$

$$B_{ab} = b^{I_1} \tilde{\epsilon}_{ab}{}^{c} \partial_c Y^{I_1}, \tag{4.3.9}$$

$$B_{\mu a} = b^{I_3}_{\mu} Y^{I_3}_{a}, \tag{4.3.10}$$

$$w = w^{I_1} Y^{I_1}, \tag{4.3.11}$$

where $\tilde{\epsilon}_{abc}$ is the epsilon-tensor on the unit 3-sphere. We use the convention $\tilde{\epsilon}_{\theta\psi\phi} = +\sin\theta\cos\theta$. To avoid notational clutter we do not write explicit summation signs with spherical harmonics; sum over appropriate indices is understood. We can use various properties of these harmonics. Spherical harmonics on S^3 are appropriate representations of $\mathfrak{so}(4) \simeq \mathfrak{su}(2) \times \mathfrak{su}(2)$. For scalar harmonics $Y^{(l,l)}_{(m,m')}$ the upper labels tell the representations of $\mathfrak{su}(2)$'s and the corresponding lower index tells the state in the representation. Vector harmonics come in two variety: one class with $\mathfrak{su}(2)\times\mathfrak{su}(2)$ representations $(l, l+1)$ and the other $(l+1, l)$. We use the following properties of these harmonics

$$\nabla^2_{S^3} Y^{I_1} = -C(I_1) Y^{I_1}, \qquad \partial_a Y^{I_3}_{b} - \partial_b Y^{I_3}_{a} = \eta(I_3) \tilde{\epsilon}^{c}{}_{ab} Y^{I_3}_{c}, \tag{4.3.12}$$

where $C(I_1) = 4l(l+1)$ for (l,l) representation and $\eta(I_3) = -2(l+1)$ for $I_3 = (l+1, l)$ and $\eta(I_3) = +2(l+1)$ for $I_3 = (l, l+1)$.

Upon substituting the expansions (4.3.8)–(4.3.11) in (4.3.6)– (4.3.7) and using properties of spherical harmonics we find the following simplified equation

$$\nabla^2_{\text{AdS}} b^{I_1} + \left(2w^{I_1} - \frac{C(I_1)}{Q} b^{I_1} \right) = 0, \tag{4.3.13}$$

where ∇^2_{AdS} refers to the scalar Laplacian with respect to the three-dimensional 'global' AdS metric

$$ds^2_{\text{AdS}} = -\frac{(r^2 + a'^2)}{Q} dt^2 + \frac{r^2}{Q} dy^2 + \frac{Q}{(r^2 + a'^2)} dr^2. \tag{4.3.14}$$

In arriving at (4.3.13) we also use the convention $\epsilon_{tyr} = +\sqrt{-g_{\text{AdS}}}$.

Similar manipulations on equation (4.3.2) gives,

$$Q\nabla^2_{\text{AdS}} w^{I_1} - C(I_1) w^{I_1} - 8 \left(w^{I_1} - \frac{C(I_1)}{Q} b^{I_1} \right) = 0. \tag{4.3.15}$$

We now have a system of differential equations

$$\nabla^2 \begin{pmatrix} b^{I_1} \\ w^{I_1} \end{pmatrix} = \begin{pmatrix} C(I_1)/Q & -2 \\ -8C(I_1)/Q^2 & (C(I_1)+8)/Q^2 \end{pmatrix} \begin{pmatrix} b^{I_1} \\ w^{I_1} \end{pmatrix}. \tag{4.3.16}$$

We can diagonalize the system. The problem then becomes that of solving the equation

$$\nabla^2_{\text{AdS}} f - m^2 f = 0. \tag{4.3.17}$$

Since t and y are Killing directions of (4.3.14), we can take the solution to be of the form

$$f(t, y, r) = e^{-i\omega t + i k_y y} h(r), \tag{4.3.18}$$

and solve for $h(r)$. The solution corresponding to a chiral primary in the inner region is [17, 83]

$$w = \frac{e^{-2ilt(a'/Q)}}{Q(r^2+a'^2)^l}\hat{Y}^{(l)}_{\rm NS}, \tag{4.3.19}$$

$$B_{ab} = B\tilde{\epsilon}_{abc}\partial^c\hat{Y}^{(l)}_{\rm NS}, \tag{4.3.20}$$

$$B_{\mu\nu} = \frac{1}{\sqrt{Q}}\epsilon_{\mu\nu\lambda}\partial^\lambda B\hat{Y}^{(l)}_{\rm NS}, \tag{4.3.21}$$

where

$$B = \frac{e^{-2ilt(a'/Q)}}{4l(r^2+a'^2)^l}, \tag{4.3.22}$$

$$\hat{Y}^{(l)}_{\rm NS} = (Y^{(l,l)}_{(l,l)})_{\rm NS} = \sqrt{\frac{2l+1}{2}}\frac{e^{-2il\phi_{\rm NS}}}{\pi}\sin^{2l}\theta. \tag{4.3.23}$$

In these formulae all the quantities related to the sphere are with respect to unit sphere. Quantities with Greek indices refer to metric (4.3.14). This perturbation has quantum numbers

$$h^{\rm NS} = l, \qquad m^{\rm NS} = l, \qquad \bar{h}^{\rm NS} = l, \qquad \bar{m}^{\rm NS} = l. \tag{4.3.24}$$

As mentioned in the beginning of this section, we consider lowering this state with $J^-_{0\,L}$ and $J^-_{0\,R}$ k and $\bar{k}$ times respectively, i.e.,

$$(J^-_{0\,L})^k(J^-_{0\,R})^{\bar{k}}|\psi\rangle_{\rm NS}. \tag{4.3.25}$$

Such states have quantum numbers

$$h^{\rm NS} = l, \qquad m^{\rm NS} = l-k, \qquad \bar{h}^{\rm NS} = l, \qquad \bar{m}^{\rm NS} = l-\bar{k}. \tag{4.3.26}$$

In the NS-NS sector we can immediately write down the supergravity fields for the state (4.3.25):

$$w = \left(\frac{e^{-2ilt(a'/Q)}}{Q(r^2+a'^2)^l}\right)\mathcal{Y}_{\rm NS}, \tag{4.3.27}$$

$$B_{ab} = B\tilde{\epsilon}_{abc}\partial^c\mathcal{Y}_{\rm NS}, \tag{4.3.28}$$

$$B_{\mu\nu} = \left(\frac{1}{\sqrt{Q}}\epsilon_{\mu\nu\lambda}\partial^\lambda B\right)\mathcal{Y}_{\rm NS}, \tag{4.3.29}$$

where

$$B = \frac{e^{-2ilt(a'/Q)}}{4l(r^2+a'^2)^l}, \tag{4.3.30}$$

$$\mathcal{Y}_{\rm NS} = Y^{(l,l)}_{(l-k,l-\bar{k})} = \underbrace{\left\{\pounds_{\xi^-_L}\pounds_{\xi^-_L}\cdots\pounds_{\xi^-_L}\right\}}_{k-\text{times}}\underbrace{\left\{\pounds_{\xi^-_R}\pounds_{\xi^-_R}\cdots\pounds_{\xi^-_R}\right\}}_{\bar{k}-\text{times}}\hat{Y}^{(l)}_{\rm NS}(\theta,\phi_{\rm NS},\psi_{\rm NS}). \tag{4.3.31}$$

Under a spectral flow on the left-moving sector with parameter α the quantum numbers change as:

$$h' = h - \alpha m + \alpha^2\frac{c}{24}, \tag{4.3.32}$$

$$m' = m - \alpha\frac{c}{12}. \tag{4.3.33}$$

Spectral flow of the background (NS-NS vacuum) gives

$$h'_{\rm BG} = \alpha^2 \frac{c}{24}, \tag{4.3.34}$$

$$m'_{\rm BG} = -\alpha \frac{c}{12}. \tag{4.3.35}$$

Therefore for the perturbation alone, we identify

$$h'_{\rm P} = h - \alpha m, \tag{4.3.36}$$

$$m'_{\rm P} = m, \tag{4.3.37}$$

so that the full $h' = h'_{\rm BG} + h'_{\rm P}$.

Applying m (odd) units of spectral flow on the left and right sectors on the perturbation (4.3.26), we get a perturbation in the Ramond-Ramond sector with quantum numbers

$$h^{\rm R}_{\rm P} = l - m(l-k), \qquad m^{\rm R}_{\rm P} = l-k, \qquad \bar{h}^{\rm R}_{\rm P} = l - m(l-\bar{k}), \qquad \bar{m}^{\rm R}_{\rm P} = l - \bar{k}. \tag{4.3.38}$$

From these expressions we see that in general $\omega = h + \bar{h}$ is not equal to $|k_y|$ where $k_y = h - \bar{h}$. In such a situation, not all the energy of the perturbation is tied to the S^1 momentum. The residual energy goes in the 'radial motion'. For technical convenience we work with perturbations where all energy is tied to the S^1 momentum, i.e., we demand

$$\bar{h}^{\rm R}_{\rm P} = 0. \tag{4.3.39}$$

This fixes $\bar{k}$ in terms of the integers l and m,

$$\bar{k} = \frac{l}{m}(m-1). \tag{4.3.40}$$

The requirement that $\bar{k}$ must be an integer between 1 and $2l$ constrains the values of l and m.

The perturbation in the R-R coordinates then looks like

$$w = \frac{1}{Q}\frac{\mathcal{E}}{(r^2+a'^2)^l}\mathcal{Y}_{\rm R}, \tag{4.3.41}$$

$$B_{\theta\psi} = \frac{1}{4l}\frac{\mathcal{E}}{(r^2+a'^2)^l}\cot\theta\ \partial_\phi \mathcal{Y}_{\rm R}, \tag{4.3.42}$$

$$B_{\theta\phi} = -\frac{1}{4l}\frac{\mathcal{E}}{(r^2+a'^2)^l}\tan\theta\ \partial_\psi \mathcal{Y}_{\rm R}, \tag{4.3.43}$$

$$B_{\psi\phi} = \frac{1}{4l}\frac{\mathcal{E}}{(r^2+a'^2)^l}\sin\theta\cos\theta\ \partial_\theta \mathcal{Y}_{\rm R}, \tag{4.3.44}$$

$$B_{ty} = -\frac{1}{2Q^2}\frac{r^2\mathcal{E}}{(r^2+a'^2)^l}\mathcal{Y}_{\rm R}, \tag{4.3.45}$$

$$B_{yr} = \frac{ia'}{2Q}\frac{r\mathcal{E}}{(r^2+a'^2)^{l+1}}\mathcal{Y}_{\rm R}, \tag{4.3.46}$$

together with the following terms generated via the spectral flow (4.2.20),

$$B_{t\theta} = -\frac{ma'}{Q}B_{\phi\theta} = -\frac{ma'}{Q}\frac{1}{4l}\frac{\mathcal{E}}{(r^2+a'^2)^l}\tan\theta\ \partial_\psi \mathcal{Y}_{\rm R}, \tag{4.3.47}$$

$$B_{t\psi} = -\frac{ma'}{Q}B_{\phi\psi} = \frac{ma'}{Q}\frac{1}{4l}\frac{\mathcal{E}}{(r^2+a'^2)^l}\sin\theta\cos\theta\ \partial_\theta \mathcal{Y}_{\rm R}, \tag{4.3.48}$$

$$B_{y\theta} = -\frac{ma'}{Q}B_{\phi\theta} = \frac{ma'}{Q}\frac{1}{4l}\frac{\mathcal{E}}{(r^2+a'^2)^l}\cot\theta\ \partial_\phi \mathcal{Y}_{\rm R}, \tag{4.3.49}$$

$$B_{y\phi} = -\frac{ma'}{Q}B_{\psi\phi} = -\frac{ma'}{Q}\frac{1}{4l}\frac{\mathcal{E}}{(r^2+a'^2)^l}\sin\theta\cos\theta\ \partial_\theta \mathcal{Y}_{\rm R}, \tag{4.3.50}$$

where

$$\mathcal{E} = \exp\left[-\frac{i}{R}\left(l - m(l-k)\right)u\right]. \tag{4.3.51}$$

In writing these expressions we have defined $u = t+y$, and we have used the spectral flow transformations (4.2.20) to write angular dependence in the R-R coordinates (ϕ, ψ).

Two comments are in order here:

1. From these equations we see that the perturbation carries $l - m(l-k)$ units of linear momentum. Since k is an integer taking values between 0 and $2l$, we have in fact constructed $2l+1$ hair modes. All these hair modes belong to the same chiral primary multiplet.

2. One might be concerned that the left conformal weight $h_{\rm P}^{\rm R}$ in (4.3.38) is negative when $m > 1$. This is not a problem, as we note that the total h values are never negative. One can think that the perturbation draws energy from the filled Fermi sea, which makes the $h_{\rm P}^{\rm R}$ value negative.

4.3.2.2 Outer region

We now want to solve the equations (4.3.1), (4.3.2) in the outer region (4.2.27) – (4.2.29). We are interested in a solution that falls off at inifinity in a normalisable manner and matches smoothly with the inner region solution. We proceed in exactly the same manner as in the inner region. Substituting spherical harmonic expansion (4.3.8)–(4.3.11) in equation (4.3.1) we get

$$\frac{1}{r}\left(-\partial_t^2+\partial_y^2\right)b_1^I + \partial_r\left(\frac{r^3}{(Q+r^2)^2}\partial_r b^{I_1}\right) + \frac{r}{(Q+r^2)^2}\left[2Qw^{I_1} - C(I_1)b^{I_1}\right] = 0. \tag{4.3.52}$$

Similar manipulations on equation (4.3.2) gives,

$$\frac{Q+r^2}{r^2}\left(-\partial_t^2+\partial_y^2\right)w^{I_1} + \frac{1}{r(Q+r^2)}\partial_r\left(r^3\partial_r w^{I_1}\right) \tag{4.3.53}$$

$$-\frac{C(I_1)}{Q+r^2}w^{I_1} - \frac{8Q}{(Q+r^2)^3}\left[Qw^{I_1} - C(I_1)b^{I_1}\right] = 0, \tag{4.3.54}$$

For the perturbation with the (t, y) dependence of the form of

$$\mathcal{E} = \exp\left[-\frac{i}{R}\left(l - m(l-k)\right)u\right], \tag{4.3.55}$$

the $\left(-\partial_t^2+\partial_y^2\right)$ combination is zero. Therefore the above equations simplify to

$$\partial_r\left(\frac{r^3}{(Q+r^2)^2}\partial_r b^{I_1}\right)+\frac{r}{(Q+r^2)^2}\left[2Qw^{I_1}-C(I_1)b^{I_1}\right]=0, \tag{4.3.56}$$

$$\frac{1}{r(Q+r^2)}\partial_r\left(r^3\partial_r w^{I_1}\right)-\frac{C(I_1)}{Q+r^2}w^{I_1}-\frac{8Q}{(Q+r^2)^3}\left[Qw^{I_1}-C(I_1)b^{I_1}\right]=0. \tag{4.3.57}$$

These equations can be integrated as follows. We write equations (4.3.56) and (4.3.57) as

$$\frac{d^2b^{I_1}}{dr^2}+P_1\frac{db^{I_1}}{dr}+Q_1b^{I_1}=R_1, \tag{4.3.58}$$

$$\frac{d^2w^{I_1}}{dr^2}+P_2\frac{dw^{I_1}}{dr}+Q_2w^{I_1}=R_2, \tag{4.3.59}$$

where

$$P_1=\frac{3Q-r^2}{r(Q+r^2)},\qquad P_2=\frac{3}{r},\qquad Q_1=\frac{-C(I_1)}{r^2}, \tag{4.3.60}$$

$$Q_2=\frac{-C(I_1)}{r^2}-\frac{8Q^2}{r^2(Q+r^2)^2},\qquad R_1=\frac{-2Qw^{I_1}}{r^2},\qquad R_2=\frac{-8QC(I_1)b^{I_1}}{r^2(Q+r^2)^2}. \tag{4.3.61}$$

We now eliminate first derivative terms from equations (4.3.58) and (4.3.59). We write $b^{I_1}=u_1v_1$ and $w^{I_1}=u_2v_2$ and choose u_1,u_2 such that first derivative terms cancel out. We get

$$u_1=\frac{Q+r^2}{r^{\frac{3}{2}}}\quad,\quad u_2=\frac{1}{r^{\frac{3}{2}}} \tag{4.3.62}$$

and equations for v_1,v_2 become

$$\frac{d^2v_1}{dr^2}+A_1v_1=-2A_3v_2\quad,\quad\frac{d^2v_2}{dr^2}+A_2v_2=-8C(I_1)A_3v_1 \tag{4.3.63}$$

where

$$A_1=\frac{8Q}{(Q+r^2)^2}-\frac{3+4C(I_1)}{4r^2},\ A_2=-\frac{8Q^2}{r^2(Q+r^2)^2}-\frac{3+4C(I_1)}{4r^2},\ A_3=\frac{Q}{r^2(Q+r^2)}. \tag{4.3.64}$$

Writing this in the matrix form we have

$$\frac{d^2}{dr^2}\begin{pmatrix}v_1\\v_2\end{pmatrix}+\begin{pmatrix}A_1 & 2A_3\\ 8C(I_1)A_3 & A_2\end{pmatrix}\begin{pmatrix}v_1\\v_2\end{pmatrix}=0. \tag{4.3.65}$$

Diagonalising this matrix and solving the second order uncoupled ordinary differential equations for normalisable solutions, we get

$$b^{I_1}=\frac{1}{4l}\frac{1}{r^{2l}}, \tag{4.3.66}$$

$$w^{I_1}=\frac{1}{r^{2l}(r^2+Q)}. \tag{4.3.67}$$

The perturbation solution decaying at infinity therefore takes the form

$$w=\frac{\mathcal{E}}{(Q+r^2)r^{2l}}\mathcal{Y}_{\rm R}, \tag{4.3.68}$$

$$B_{ab}=B\tilde{\epsilon}_{abc}\partial^c\mathcal{Y}_{\rm R}, \tag{4.3.69}$$

$$B_{\mu\nu}=\frac{1}{\sqrt{Q+r^2}}\epsilon_{\mu\nu\rho}\partial^\rho B\ \mathcal{Y}_{\rm R}, \tag{4.3.70}$$

$$B=\frac{1}{4l}\frac{\mathcal{E}}{r^{2l}}. \tag{4.3.71}$$

Here all quantities related to the sphere are with respect to the unit sphere. Writing out all the components explicitly, the solution looks as follows:

$$w = \frac{\mathcal{E}}{(Q+r^2)r^{2l}}\mathcal{Y}_{\rm R}, \tag{4.3.72}$$

$$B_{\theta\psi} = \frac{1}{4l}\frac{\mathcal{E}}{r^{2l}}\cot\theta\ \partial_\phi\mathcal{Y}_{\rm R}, \tag{4.3.73}$$

$$B_{\theta\phi} = -\frac{1}{4l}\frac{\mathcal{E}}{r^{2l}}\tan\theta\ \partial_\psi\mathcal{Y}_{\rm R}, \tag{4.3.74}$$

$$B_{\psi\phi} = \frac{1}{4l}\frac{\mathcal{E}}{r^{2l}}\sin\theta\cos\theta\ \partial_\theta\mathcal{Y}_{\rm R}, \tag{4.3.75}$$

$$B_{ty} = -\frac{1}{2(Q+r^2)^2}\frac{\mathcal{E}}{r^{2l-2}}\mathcal{Y}_{\rm R}, \tag{4.3.76}$$

$$B_{tr} = -\frac{1}{4l}\frac{1}{r^{2l+1}}(\partial_y\mathcal{E})\mathcal{Y}_{\rm R}, \tag{4.3.77}$$

$$B_{yr} = -\frac{1}{4l}\frac{1}{r^{2l+1}}(\partial_t\mathcal{E})\mathcal{Y}_{\rm R}. \tag{4.3.78}$$

4.3.2.3 Matching

We now want to see that the solutions that we have found for the inner and outer regions join onto each other smoothly in the overlap of the two regions,

$$\epsilon\sqrt{Q} \ll r \ll \sqrt{Q}. \tag{4.3.79}$$

We can choose to do the matching at any value of r in the above range. We choose the matching radial coordinate to be the geometric mean of the two ends

$$r \sim \sqrt{\epsilon}\sqrt{Q}. \tag{4.3.80}$$

In this region, the scalar w in both the inner (4.3.41) and the outer (4.3.72) regions has the same leading order behaviour,

$$w \simeq \frac{\mathcal{E}\mathcal{Y}_{\rm R}}{Qr^{2l}}. \tag{4.3.81}$$

We see that the scalar does indeed match. To compare the NS-NS 2-form, we can construct the field strength $H = dB$ and compare the behaviour in the two regions in a given orthonormal frame. More simply we notice that from the inner region point of view

$$\frac{1}{(r^2+a'^2)} \approx \frac{1}{r^2}, \tag{4.3.82}$$

and from the the outer region point of view

$$\frac{1}{(Q+r^2)} \approx \frac{1}{Q}, \tag{4.3.83}$$

near the matching surface. We find that components $B_{\theta\psi}, B_{\theta\phi}, B_{\psi\phi}, B_{ty}$ match readily. The components that do not match B_{tr}, B_{yr} and all components generated by spectral flow in the inner region, namely $B_{t\theta}, B_{t\psi}, B_{y\theta}, B_{t\phi}$ are seen to be higher order terms. These terms will agree once inner region and outer region calculations are corrected by higher order terms.

4.4 Discussion

In this chapter we have constructed 'hair' on non-extremal two-charge bound states of Jejjala et al [18]. Our perturbation is 'extremal' as it is of the form e^{icu}. To the best of our knowledge this is the first example of a hair mode on a non-extremal smooth geometry, and also the first example beyond JMaRT of a non-extremal fuzzball with identified CFT interpretation. We have constructed the perturbation by a matching procedure. In the inner region our background is simply m units of both left and right spectral flows on the NS-NS vacuum. To construct our perturbation we have taken an appropriate state in the chiral primary multiplet on top of the NS-NS vacuum (global $AdS_3\times S^3$) and have applied left and right spectral flows to get a perturbation over the R-R state of interest. Such a perturbation in our linearised analysis can be matched on to a normalisable solution in the outer region. We have carried out the matching procedure to the leading order. We find it quite remarkable that we are able to add such a hair on the non-extremal D1-D5 bound states.

By altering the above construction slightly one can construct another class of hair modes as follows. Instead of lowering $|\psi\rangle_{\rm NS}$ with $J^-_{L,R}$ one can first apply even units (say, $2p$) of spectral flows on $|\psi\rangle_{\rm NS}$ to get an excited state in the NS-NS sector $|\psi\rangle^{(2p)}_{\rm NS}$. Then one can apply $J^-_{L,R}$ as above, and finally apply $2(m-p)+1$ units of spectral flows to get the background state corresponding to the 2-charge JMaRT. By such a procedure one will get different values for $h^{\rm R}_{\rm P}$ and $\bar{h}^{\rm R}_{\rm P}$. By demanding $\bar{h}^{\rm R}_{\rm P}=0$ one can construct a different class of hair, which can also be matched to a decaying solution in the outer region. Other variations on this procedure are also possible. It can be interesting to work out these solutions explicitly.

The JMaRT solutions are well known to suffer from ergoregion instability [84]. The reader may wonder how have we managed to add hair on an unstable geometry. The answer lies in the fact that we work in a sector completely different from the sector in which the instability of the geometry is analysed in [84]. We added extremal perturbation in the Ramond-Ramond axion and NS-NS two-form sector. The full haired solution is most likely unstable to scalar perturbations. In fact one can easily convince oneself that it is not possible to add hair modes on the JMaRT solution in the minimally coupled scalar sector [17]. It is not clear to us if one can add non-extremal perturbation to the JMaRT solutions in the (w,B) sector, i.e., perturbations with both $h^{\rm R}_{\rm P}$ and $\bar{h}^{\rm R}_{\rm P}$ non-zero.

There are several ways in which our study can be extended. It will be interesting to perform the analysis at higher order in ϵ like it was done in [17]. This is likely to be technically intricate. There are two main sources of complications: (i) the spherical harmonic expansions are significantly more involved compared to the MSS study, and (ii) features related to non-extremality of the background will appear in the perturbation analysis at higher orders. We hope to report on these calculations at some point in the future. As mentioned in the introduction, in the BPS case, it is now understood that the MSS perturbation is the linearisation of a non-linear solution of IIB supergravity [79]. Perhaps it may be feasible to find the non-linear version of the perturbative solution constructed in this chapter.

4.5 Appendix: Spherical harmonics on S^3

In this appendix we list relevant expressions and properties of spherical harmonics we needed. For explicit expressions we follow the conventions of [17], but there are typos in

their expressions that we fix below. The metric on the unit 3-sphere is

$$ds^2 = d\theta^2 + \sin^2\theta d\phi^2 + \cos^2\theta d\psi^2. \tag{4.5.1}$$

The scalar and vector harmonics satisfy the orthonormality conditions

$$\int d\Omega (Y^{I_1})^* (Y^{I_1'}) = \delta^{I_1, I_1'}, \tag{4.5.2}$$

$$\int d\Omega (Y_a^{I_2})^* Y^{I_2' a} = \delta^{I_2, I_2'}. \tag{4.5.3}$$

We use the following notation from [17]

$$\hat{Y}^{(l)} \equiv Y^{(l,l)}_{(l,l)}, \tag{4.5.4}$$

$$Y^{(l)} \equiv Y^{(l,l)}_{(l-1,l)}, \tag{4.5.5}$$

$$Y^{(l+1)} \equiv Y^{(l+1,l+1)}_{(l-1,l)}, \tag{4.5.6}$$

$$Y_a^{(l+1,l)} \equiv Y^{(l+1,l)}_{a(l-1,l)}, \tag{4.5.7}$$

$$Y_a^{(l,l+1)} \equiv Y^{(l,l+1)}_{a(l-1,l)}, \tag{4.5.8}$$

$$Y_a^{(l-1,l)} \equiv Y^{(l-1,l)}_{a(l-1,l)}, \tag{4.5.9}$$

$$Y_a^{(l+2,l+1)} \equiv Y^{(l+2,l+1)}_{a(l-1,l)}. \tag{4.5.10}$$

The above harmonics are,

$$\hat{Y}^{(l)} \equiv Y^{(l,l)}_{(l,l)} = \frac{\sqrt{2l+1}}{\sqrt{2}} \frac{e^{-2il\phi}}{\pi} \sin^{2l}\theta \tag{4.5.11}$$

$$Y^{(l)} = -\frac{\sqrt{l(2l+1)}}{\pi} e^{-i(2l-1)\phi + i\psi} \sin^{2l-1}\theta \cos\theta \tag{4.5.12}$$

$$Y^{(l+1)} = \frac{\sqrt{(2l+1)(2l+3)}}{2\pi} e^{-i(2l-1)\phi + i\psi} ((l-1) + (l+1)\cos 2\theta) \sin^{2l-1}\theta \cos\theta \tag{4.5.13}$$

$$Y_\theta^{(l+1,l)} = -\frac{e^{-i(2l-1)\phi + i\psi}}{4\pi} \frac{\sin^{2l-2}\theta}{\sqrt{l+1}} ((2l^2 - l + 1) + (l-1)(2l+1)\cos 2\theta) \tag{4.5.14}$$

$$Y_\phi^{(l+1,l)} = i\frac{e^{-i(2l-1)\phi + i\psi}}{4\pi} \frac{\sin^{2l-1}\theta \cos\theta}{\sqrt{l+1}} ((2l^2 - 5l - 1) + (2l^2 + 3l + 1)\cos 2\theta) \tag{4.5.15}$$

$$Y_\psi^{(l+1,l)} = -i\frac{e^{-i(2l-1)\phi + i\psi}}{4\pi} \frac{\sin^{2l-1}\theta \cos\theta}{\sqrt{l+1}} ((2l^2 + 3l - 1) + (l+1)(2l+1)\cos 2\theta) \tag{4.5.16}$$

$$Y_\theta^{(l,l+1)} = -\frac{e^{-i(2l-1)\phi + i\psi}}{4\pi} \sqrt{\frac{4l(2l+1)}{l+1}} \sin^{2l-2}\theta ((l-1) + l\cos 2\theta) \tag{4.5.17}$$

$$Y_\phi^{(l,l+1)} = i\frac{e^{-i(2l-1)\phi + i\psi}}{4\pi} \sqrt{\frac{4l(2l+1)}{l+1}} \sin^{2l-1}\theta \cos\theta ((l-2) + (l+1)\cos 2\theta) \tag{4.5.18}$$

$$Y_\psi^{(l,l+1)} = i\frac{e^{-i(2l-1)\phi + i\psi}}{4\pi} \sqrt{\frac{4l(2l+1)}{l+1}} \sin^{2l-1}\theta \cos\theta (l + (l+1)\cos 2\theta) \tag{4.5.19}$$

$$Y_\theta^{(l-1,l)} = \frac{e^{-i(2l-1)\phi+i\psi}}{2\pi}\sqrt{2l-1}\sin^{2l-2}\theta \tag{4.5.20}$$

$$Y_\phi^{(l-1,l)} = -i\frac{e^{-i(2l-1)\phi+i\psi}}{2\pi}\sqrt{2l-1}\sin^{2l-1}\theta\cos\theta \tag{4.5.21}$$

$$Y_\psi^{(l-1,l)} = -i\frac{e^{-i(2l-1)\phi+i\psi}}{2\pi}\sqrt{2l-1}\sin^{2l-1}\theta\cos\theta \tag{4.5.22}$$

$$\begin{aligned} Y_\theta^{(l+2,l+1)} = & -\frac{e^{-i(2l-1)\phi+i\psi}}{8\pi}\sqrt{\frac{3}{l+2}}\sin^{2l-2}\theta\left[(l-1)(2l^2+l+1)\right. \\ & \left.+\frac{2(4l^3-l+3)\cos 2\theta}{3}+\frac{(l-1)(l+1)(2l+3)\cos 4\theta}{3}\right] \end{aligned} \tag{4.5.23}$$

$$\begin{aligned} Y_\phi^{(l+2,l+1)} = & \, i\frac{e^{-i(2l-1)\phi+i\psi}}{4\pi}\sqrt{\frac{3}{l+2}}\sin^{2l-1}\theta\cos\theta\left[\frac{2l^3-3l^2+3l+4}{2}\right. \\ & \left.\frac{1}{3}(4l^3-13l-9)\cos 2\theta+\frac{(l+1)(l+2)(2l+3)}{6}\cos 4\theta\right] \end{aligned} \tag{4.5.24}$$

$$\begin{aligned} Y_\psi^{(l+2,l+1)} = & -i\frac{e^{-i(2l-1)\phi+i\psi}}{4\pi}\sqrt{\frac{3}{l+2}}\sin^{2l-1}\theta\cos\theta\left[\frac{l(2l^2+5l-1)}{2}\right. \\ & \left.+\frac{1}{3}(l+1)(4l^2+8l-3)\cos 2\theta+\frac{(l+1)(l+2)(2l+3)}{6}\cos 4\theta\right]. \end{aligned} \tag{4.5.25}$$

Raising and lowering the harmonics

The Killing forms for the metric (4.5.1) can be written as, see e.g., appendix A of [85]

$$\xi_{1L} = \cos(\psi+\phi)d\theta+\sin\theta\cos\theta\sin(\psi+\phi)d(\psi-\phi), \tag{4.5.26}$$

$$\xi_{2L} = -\sin(\psi+\phi)d\theta+\sin\theta\cos\theta\cos(\psi+\phi)d(\psi-\phi), \tag{4.5.27}$$

$$\xi_{3L} = \cos^2\theta d\psi+\sin^2\theta d\phi, \tag{4.5.28}$$

$$\xi_{1R} = -\sin(\psi-\phi)d\theta+\sin\theta\cos\theta\cos(\psi-\phi)d(\psi+\phi), \tag{4.5.29}$$

$$\xi_{2R} = \cos(\psi-\phi)d\theta+\sin\theta\cos\theta\sin(\psi-\phi)d(\psi+\phi), \tag{4.5.30}$$

$$\xi_{3R} = -\cos^2\theta d\psi+\sin^2\theta d\phi. \tag{4.5.31}$$

From these expressions, we can readily obtain the six Killing vectors on S^3 (using the order θ,ϕ,ψ),

$$\xi_{1L}^\mu = (\cos(\phi+\psi),-\cot\theta\sin(\phi+\psi),\tan\theta\sin(\phi+\psi)), \tag{4.5.32}$$

$$\xi_{2L}^\mu = (-\sin(\phi+\psi),-\cot\theta\cos(\phi+\psi),\tan\theta\cos(\phi+\psi)), \tag{4.5.33}$$

$$\xi_{3L}^\mu = (0,1,1), \tag{4.5.34}$$

$$\xi_{1R}^\mu = (\sin(\phi-\psi),\cot\theta\cos(\phi-\psi),\tan\theta\cos(\phi-\psi)), \tag{4.5.35}$$

$$\xi_{2R}^\mu = (\cos(\phi-\psi),-\cot\theta\sin(\phi-\psi),-\tan\theta\sin(\phi-\psi)), \tag{4.5.36}$$

$$\xi_{3R}^\mu = (0,1,-1). \tag{4.5.37}$$

These vectors generate the $SU(2)\times SU(2)$ algebra as

$$[\xi_{aL},\xi_{bL}] = 2\epsilon^{abc}\xi_{cL}, \qquad [\xi_{aR},\xi_{bR}] = 2\epsilon^{abc}\xi_{cR}, \qquad [\xi_{aL},\xi_{bR}] = 0, \tag{4.5.38}$$

where $a,b,c=1,2,3$, and ϵ is the completely antisymmetric symbol with $\epsilon^{123}=1$. We can now use these Killing vectors to define the raising and lowering operators on the

harmonics. Defining

$$\xi^+_L = \xi_{1L} + i\xi_{2L}, \qquad \xi^-_L = \xi_{1L} - i\xi_{2L}, \tag{4.5.39}$$

$$\xi^+_R = \xi_{2R} - i\xi_{1R}, \qquad \xi^-_R = \xi_{2R} + i\xi_{1R}, \tag{4.5.40}$$

one can check that the harmonics satisfy the following relations (here $\pounds_\xi$ denotes the Lie derivative along the vector ξ),

$$\frac{i}{2}\pounds_{\xi_{3L}}\hat{Y}^{(l)} = +l\hat{Y}^{(l)}, \tag{4.5.41}$$

$$\frac{i}{2}\pounds_{\xi_{3R}}\hat{Y}^{(l)} = +l\hat{Y}^{(l)}, \tag{4.5.42}$$

$$\pounds_{\xi^+_L}\hat{Y}^{(l)} = 0, \tag{4.5.43}$$

$$\pounds_{\xi^+_R}\hat{Y}^{(l)} = 0, \tag{4.5.44}$$

confirming that $\hat{Y}^{(l)}$'s indeed correspond to highest weight states. Moreover, one can check that

$$\pounds_{\xi^-_L}\hat{Y}^{(l)} = -2\sqrt{2l}Y^{(l)}, \tag{4.5.45}$$

$$\pounds_{\xi^+_L}Y^{(l)} = 2\sqrt{2l}\hat{Y}^{(l)}, \tag{4.5.46}$$

$$\pounds_{\xi^-_L}(\pounds_{\xi^-_R}Y^{(l+1,l+1)}_{(l,l+1)}) = -8\sqrt{(l+1)(2l+1)}Y^{(l+1)}, \tag{4.5.47}$$

$$\pounds_{\xi^-_R}(\pounds_{\xi^-_L}Y^{(l,l+1)}_{a(l,l+1)}) = -8\sqrt{l(l+1)}Y^{(l,l+1)}_a, \tag{4.5.48}$$

$$\pounds_{\xi^+_R}(\pounds_{\xi^+_L}Y^{(l+2,l+1)}_a) = 8\sqrt{3}(l+1)Y^{(l+2,l+1)}_{a(l,l+1)}. \tag{4.5.49}$$

The pre-factors in these equations are convention dependent, e.g., they depend on the normalisation in definition (4.5.40). Using these properties we were able to fix typos in expressions of vectors harmonics in [17].

Other properties of spherical harmonics we need are

$$\nabla^2 Y^{I_1} = -4l(l+1)Y^{I_1}, \tag{4.5.50}$$

$$\nabla_{[a}\nabla_{b]}Y^{I_1} = 0, \tag{4.5.51}$$

$$\nabla^a Y^{I_1}_a = 0. \tag{4.5.52}$$

The vector harmonics fall into two classes of $SU(2)\times SU(2)$ representations: $(l, l+1)$ or $(l+1, l)$. We have

$$\nabla_a Y^{I_1}_b - \nabla_b Y^{I_1}_a = \zeta(I_1)\epsilon_{abc}Y^{I_1 c}, \tag{4.5.53}$$

where $\zeta(I_1) = +2(l+1)$ for the $(l, l+1)$ representations and $\zeta(I_1) = -2(l+1)$ for the $(l+1, l)$ representations. We use the convention $\epsilon_{\theta\psi\phi} = +\sin\theta\cos\theta$ [17].

Decomposition

For completeness let us recall (see e.g., [86, 87]) that a vector field on S^3 can be uniquely decomposed into its longitudinal and transverse parts,

$$V_a = \nabla_a S + S_a, \tag{4.5.54}$$

where S is a scalar and S_a is a vector transverse on S^3, $\nabla^a S_a = 0$. The scalar field S and the transverse vector S_a can be Fourier decomposed on the sphere in terms of spherical harmonics.

Since a two-form is dual to a vector on S^3, it also admits a decomposition in terms of scalar and vector spherical harmonics. Let the 2-form be B_{ab}

$$B_{ab} = \epsilon_{abc} V^c. \tag{4.5.55}$$

Now note that on the one hand,

$$\epsilon_{abc} \nabla^b (\epsilon_{mn}{}^c B^{mn}) = -2 \nabla^b B_{ba}, \tag{4.5.56}$$

and on the other hand from (4.5.55),

$$\epsilon_{abc} \nabla^b (\epsilon_{mn}{}^c B^{mn}) = \epsilon_{abc} \nabla^b V^c = \epsilon_{abc} \nabla^b S^c. \tag{4.5.57}$$

For non-trivial vector harmonics the quantity $\epsilon_{abc} \nabla^b S^c$ is non-zero, cf. (4.5.53). Therefore, in de-Donder gauge when

$$\nabla^b B_{ba} = 0, \tag{4.5.58}$$

the decomposition of an arbitrary 2-form B_{ab} is solely in terms of derivatives of scalar harmonics [17, 83, 88],

$$B_{ab} = \sum_{I_1} b^{I_1} \epsilon_{ab}{}^c \partial_c Y^{I_1}. \tag{4.5.59}$$

5

Oscillating Shells and Oscillating Balls in AdS

> Mind you, I'm not saying that it's all a pure invention.
>
> Eumaeus

5.1 Introduction and summary

In recent times the study of thermalisation in closed quantum systems has received a surge of activity, see e.g. [89] for a review with more references. In general, a quantum system perturbed out of equilibrium decoheres and proceeds towards ergodicity. On a large enough time-scale, the system thermalises and is described by a mixed density matrix. However, contrary to this expectation, there can be situations where a quantum system dynamically reconstructs the initial state and keeps repeating this evolution, with or without damping. This phenomenon is termed quantum revival. In the context of AdS/CFT correspondence, such possible revival configurations presumably correspond to periodic or quasi-periodic dynamics resulting from gravity in an asymptotically AdS space.

In this chapter, we discuss two configurations in AdS space, namely, thin shells and solid balls, especially when they oscillate. Such configurations probe both questions of stability of AdS, and of quantum revival. Oscillatory motion in gravitational dynamics is not new. In global AdS space, a transient oscillatory motion of a thick shell has been reported in [90, 91]. The thick shell leads to a collapse situation, forming a black hole at late times. Non-transient or exactly periodic oscillatory configurations in AdS space have been explored in [92–97]. A connection with quantum revivals has also been proposed. Similar periodic configurations are also known to arise in other closely related set-ups [98–102].

It becomes clear from these studies that we need two ingredients for oscillatory dynamics in AdS. Firstly, we need to work in global AdS, and secondly, we need a non-vanishing pressure (or another repulsive force) to sustain oscillations. The necessity of a non-vanishing pressure is intuitive. To have an oscillation, one needs an interaction that competes with the attraction of gravity. In earlier works, e.g. in [96, 103], oscillatory shells have been explored, where the shell matter is described by a perfect fluid with a linear equation of state. In the current chapter, we also consider a polytropic equation of state for the shell dynamics, and a non-vanishing pressure for the ball dynamics. In both cases, we conclude that for a range of allowed parameter space, one obtains oscillatory motion.

Furthermore, reasonable energy conditions, such as the weak and null energy conditions are obeyed by these configurations.

While *a priori* there is no reason to rule out such dynamics, it remains unclear to us what the precise dual field theory descriptions are. One such possibility is certainly the *quantum revivals* that have already been pointed out in the literature [97]. We only list a few features here, and not attempt to elaborate on the identification. First, it is clear that one point functions are all thermal as seen from the AdS boundary. Non-local observables, however, do penetrate and capture the dynamical aspects of the geometry. Towards this we explicitly calculate a two-point function in the geodesic approximation in oscillatory shell backgrounds and demonstrate that the shell oscillation simply gets mapped to oscillations of the correlation function, provided the two points are sufficiently separated at the boundary.

We expect a similar behaviour to appear in the oscillating ball dynamics, though, this calculation is technically more involved. The technical complication for the ball dynamics arises from a non-vanishing pressure. The ball itself is described by a simple FRW geometry, and due to pressure matter leaks outside. The outside is therefore a Tolman-Oppenheimer-Volkoff (TOV) type solution in AdS. This TOV geometry needs to be matched onto an AdS Schwarzschild geometry. Thus, a two-point function in the dual field theory has essentially three characteristic length-scales. The short-distance behaviour of the correlator is purely thermal. The intermediate-distance behaviour of the correlator is determined by a geodesic penetrating into the TOV region of the spacetime. Finally, the long-distance behaviour of the correlator is dynamical since the corresponding geodesic probes the oscillating FRW region. Thus, the UV modes of the field theory have a thermal behaviour, which crosses over to a dynamical behaviour towards the IR. This qualitative picture is in accordance with the *top-down* thermalisation picture of [104–107] in the context of AdS/CFT correspondence.

Another intriguing feature of the oscillatory configurations is that the dynamics is confined between two radial scales. One does not immediately arrive at such a configuration with a natural choice of boundary and initial conditions at the boundary of AdS. Thus, while the presence of oscillations is rather ubiquitous, our analysis does not shed light on how one prepares this state from the perspective of the boundary theory. However, given the results of [97, 108], where a more direct numerical study exhibits similar periodic or quasi-periodic dynamics arising from a set of initial and boundary conditions, we view the above shortcoming as a limitation of our approach.

Given the existence of the oscillatory dynamics, there are various avenues to explore further, for example, how additional parameters affect the oscillatory configurations? In particular, introducing a charge is potentially interesting since it can compete with gravitational attraction. Perhaps with a non-vanishing charge, one can obtain oscillating solutions in low pressure situations. We leave this for future investigations.

The rest of the chapter is organised as follows. In section 5.2 we discuss the basic framework of junction conditions and the details of the shell dynamics, including the study of two point function in the geodesics approximation in oscillating shell backgrounds. In section 5.3 we discuss oscillating FRW balls. Section 5.4 is devoted to a discussion of the various energy conditions for the oscillating shell and oscillating ball configurations. Finally, certain details on matching the FRW ball to a TOV-type solution are discussed in the last section, 5.5, which is intended as an appendix to this chapter.

5.2 The oscillating shells

In this section we discuss oscillating shell configurations. In section 5.2.1 we start with a brief review of the analysis of [96] and make some further observations. In section 5.2.2 we compute the equal time two-point function in the geodesic approximation in oscillating shell backgrounds.

5.2.1 Shell dynamics

We begin with the formalism to discuss the motion of the shell. The same formalism will be useful later in studying the dynamics of a ball in the spirit of the Oppenheimer-Snyder model.

Consider a spherically symmetric thin shell, evolving in a $(d+1)$-dimensional background spacetime $\mathcal{M}$. The shell divides the entire spacetime in two regions: an interior (empty AdS) denoted by $\mathcal{M}_-$ and an exterior (AdS Schwarzschild) denoted by $\mathcal{M}_+$. The line elements in the two regions are given by

$$ds_\pm^2 = -f_\pm(r)dt_\pm^2 + f_\pm^{-1}(r)dr^2 + r^2 d\Omega_{d-1}^2, \tag{5.2.1}$$

where $f_-(r) = 1 + r^2$ and $f_+(r) = 1 + r^2 - \frac{m}{r^{d-2}}$. Here, we have set the AdS length to unity and m is the mass parameter (proportional to the ADM mass) of the system.

The radial coordinate r is continuous across the shell, ensuring that the area of the $(d-1)$-spheres agree on the two sides of the shell. In brief, we choose the following coordinate patches: $\mathcal{U}_+ \equiv \{t_+, r, \theta_1, \dots \theta_{d-1}\} \equiv \{x_+^\mu\}$ on $\mathcal{M}_+$, and $\mathcal{U}_- \equiv \{t_-, r, \theta_1, \dots \theta_{d-1}\} \equiv \{x_-^\mu\}$ on $\mathcal{M}_-$. Here μ ranges over all space-time directions. Clearly, Einstein equations (via the junction conditions) impose non-trivial boundary conditions on $\mathcal{U}_+ \cap \mathcal{U}_-$, thereby determining the entire manifold covered by $\mathcal{U}_+ \cup \mathcal{U}_-$.

We can choose an independent set of coordinates on the shell worldvolume

$$\mathcal{U}_{\text{shell}} \equiv \{\tau, \theta_1, ..., \theta_{d-1}\} \equiv \{y^a\}.$$

In writing this equation, we have chosen a trivial embedding along the angular directions by making use of the spherical symmetry of the problem. The coordinate τ is chosen to be the proper time of a co-moving observer on the shell. The basis vectors on the tangent space of the shell at any point can be pushed forward to spacetime vectors: $e_{\text{space-time}} \equiv \varphi_* (e_{\text{shell}})$. In explicit coordinates, this map takes the form $\partial_a = \frac{\partial x^\mu}{\partial y^a}\partial_\mu$.

Let the position of the shell be specified by

$$r = r_{\text{s}}(\tau)\ , \qquad t_\pm = t_{\pm,\text{s}}(\tau). \tag{5.2.2}$$

Then we get

$$\partial_\tau = \quad u^\mu \partial_\mu = \dot{t}_{\pm,\text{s}}\ \partial_{t_\pm} + \dot{r_{\text{s}}}\partial_r, \tag{5.2.3}$$

$$\partial_{\theta_i} = \quad \delta^\mu_{\theta_i}\partial_\mu, \quad i = 1, \dots, (d-1). \tag{5.2.4}$$

Here, the overhead dot denotes derivative w.r.t. τ, and u^μ is the four velocity of the shell. The four velocity is canonically normalised, $u^\mu u_\mu = -1$, which yields,

$$\dot{t}_{\pm,\text{s}} = \frac{\sqrt{f_\pm(r_{\text{s}}) + \dot{r_{\text{s}}}^2}}{f_\pm(r_{\text{s}})} =: \frac{\beta_\pm}{f_\pm(r_{\text{s}})}. \tag{5.2.5}$$

Since the derivatives $\dot{t}_\pm$ do not match at the location of the shell, t_+ is not continuously related to t_-. This will be carefully taken into account when we discuss spacelike geodesics crossing the shell in the next subsection.

The induced metric on the shell is:

$$ds^2_{\text{shell}} = h_{ab}dy^a dy^b = -d\tau^2 + r_{\text{s}}^2 d\Omega^2_{d-1}. \tag{5.2.6}$$

The unit normalised vector normal to the shell in $\pm$ coordinates is

$$n_{\mu,\pm} = \left(-\dot{r}_{\text{s}}, \dot{t}_{\pm,\text{s}}, 0, 0\right) \quad \Longrightarrow \quad n^{\mu}_{\pm} = \left(f_{\pm}^{-1}(r_{\text{s}})\dot{r}_{\text{s}}, f_{\pm}(r_{\text{s}})\dot{t}_{\pm,\text{s}}, 0, 0\right). \tag{5.2.7}$$

It satisfies $u^{\mu}n_{\mu,\pm} = 0$ and $n^{\mu}_{\pm}n_{\mu,\pm} = 1$. An overall (positive) sign choice has been made in writing the above normal vector, so it points from $\mathcal{M}_-$ to $\mathcal{M}_+$.

Einstein equations become a set of matching conditions on $\mathcal{U}_+ \cap \mathcal{U}_-$. These are known as the Israel junction conditions [109]. For writing down these conditions, we need to evaluate the extrinsic curvature and also assign a stress-tensor to the thin-shell matter field. The extrinsic curvature, defined as $K_{ab} = e^{\mu}{}_a e^{\nu}{}_b \nabla_{\mu} n_{\nu}$, has the following non-zero components,

$$K_{\tau\tau,\pm} = -\frac{\dot{\beta}_{\pm}}{\dot{r}_{\text{s}}}, \quad K_{\theta_1\theta_1,\pm} = \beta_{\pm} r_{\text{s}}, \tag{5.2.8}$$

$$K_{\theta_i\theta_i,\pm} = (K_{\theta_1\theta_1,\pm})\frac{h_{\theta_i\theta_i}}{r_{\text{s}}^2}, \quad i \neq 1. \tag{5.2.9}$$

Equivalently,

$$K^{\tau}{}_{\tau,\pm} = \frac{\dot{\beta}_{\pm}}{\dot{r}_{\text{s}}}, \quad K^{\theta_i}{}_{\theta_i,\pm} = \frac{\beta_{\pm}}{r_{\text{s}}}. \tag{5.2.10}$$

For simplicity, we can take the stress-tensor of the thin-shell to be of the perfect fluid form,

$$S^a{}_b = \text{diag}(-\sigma, \underbrace{p, p, \dots}_{(d-1)\,\text{terms}}), \tag{5.2.11}$$

where σ and p are the energy density and the pressure of the corresponding matter on the shell, related via a suitable equation of state.

The two Israel junction conditions are (i) continuity of metric across the shell, and (ii) jump in the extrinsic curvature is related to the stress-tensor of the thin-shell,

$$[K_{ab}] - h_{ab}[K] = -\kappa S_{ab}, \quad \text{or} \quad [K^a{}_b] = -\kappa\left(S^a{}_b - \frac{\delta^a{}_b S}{d-1}\right), \tag{5.2.12}$$

where $\kappa = 8\pi G_d$, $K \equiv h^{ab}K_{ab}$ and $S \equiv h^{ab}S_{ab}$ are the traces of the corresponding tensors. The bracket, denoted by [] represents the jump from $\mathcal{M}_-$ to $\mathcal{M}_+$

$$[\mathcal{O}] \equiv \mathcal{O}_+ - \mathcal{O}_- \tag{5.2.13}$$

for some field $\mathcal{O}$. This definition is tied to our convention of choosing the direction of the normal vector in (5.2.7).

Together with (5.2.10) and (5.2.11), the junction conditions (5.2.12) become

$$\frac{[\beta]}{r_{\text{s}}} = -\frac{\kappa\sigma}{d-1}, \tag{5.2.14}$$

$$\frac{[\dot{\beta}]}{\dot{r}_{\text{s}}} = \kappa\left(p + \sigma\frac{d-2}{d-1}\right). \tag{5.2.15}$$

Since, $f_+ \leq f_-$, we have $\beta_+ \leq \beta_-$, and by virtue of (5.2.14), we conclude $\sigma \geq 0$. The inequality here is saturated for the trivial junction where the extrinsic curvature has no jump, and the shell does not exist.

To make further progress, one needs to input an equation of state. A sufficiently general choice is the polytropic equation of state: $p = \frac{\alpha}{d-1}\sigma^{\gamma}$, where γ is the polytropic exponent. The overall constant α fixes the normalization of *e.g.* the trace of the shell energy-momentum tensor. With a polytropic equation of state, equation (5.2.15) takes the form,

$$\frac{[\dot{\beta}]}{\dot{r}_{\rm s}} = -\frac{[\beta]}{r_{\rm s}}\left(\alpha\sigma^{\gamma-1} + d - 2\right), \tag{5.2.16}$$

which can be integrated using (5.2.14) to yield,

$$-[\beta] = \left[-\frac{(d-1)^{\gamma-2}}{\kappa^{\gamma-1}}\ \alpha\ r_{\rm s}^{1-\gamma} + M r_{\rm s}^{(d-2)(\gamma-1)}\right]^{\frac{1}{1-\gamma}}, \quad \gamma \in \mathbb{Z}\setminus\{1\}\ , \tag{5.2.17}$$

where M is a constant of motion.

It is also possible to obtain analytical solutions for equation (5.2.16) with non-integer values[1] of γ, however, those seem valid case-by-case and we were not able to obtain one compact expression for all possible values of γ. The special case of $\gamma = 1$ can be worked out separately, yielding,

$$[\beta] = -M r_{\rm s}^{2-d-\alpha}, \tag{5.2.18}$$

where M is an integration constant[2]. In this case we have a linear equation of state $p = \frac{\alpha}{d-1}\sigma$. There are two cases of special interest, $\alpha = 0$ and $\alpha = 1$. $\alpha = 0$ corresponds to pressure-less dust, and $\alpha = 1$ corresponds to conformal matter for which the trace of the energy-momentum tensor vanishes.

The total energy of the shell can be defined by

$$E = \sigma\Omega_{d-1} r_{\rm s}^{d-1}. \tag{5.2.19}$$

In general, the energy so defined is clearly not conserved as r_s and σ change as the shell moves. However, in the pressure-less case, using (5.2.14) one sees that E is a constant of motion related to M by a proportionality factor.

We can recast the equations of motion of the shell as the motion of a particle in an effective potential. This is achieved by substituting the definition $\beta_{\pm} = \sqrt{f_{\pm}(r_{\rm s}) + \dot{r}_{\rm s}^{\,2}}$ in equation (5.2.14). After some simplification we get,

$$\dot{r}_{\rm s}^2 + V_{\rm eff}\qquad\qquad (r_{\rm s}) = 0, \tag{5.2.20}$$

$$V_{\rm eff}\,(r_{\rm s}) = \quad f_-\,(r_{\rm s}) - \frac{(d-1)^2}{4\sigma^2 r_{\rm s}^2}\left[f_-\,(r_{\rm s}) - f_+\,(r_{\rm s}) + \frac{\sigma^2 r_{\rm s}^2}{(d-1)^2}\right]^2. \tag{5.2.21}$$

In practice, one uses (5.2.14) to write σ as,

$$\sigma = -\frac{[\beta]\,(d-1)}{\kappa r_{\rm s}}, \tag{5.2.22}$$

and in turn uses (5.2.17) to substitute for $[\beta]$ to obtain σ in terms of other parameters. Substituting such an expression in (5.2.21), gives an equation for the dynamics of the shell in terms of the paramters $\{d, \alpha, \gamma, \kappa, m, M\}$. Of these, κ can be set to unity by an appropriate choice a units. Therefore, the physics depends on parameters $\{d, \alpha, \gamma, m, M\}$.

[1] This is certainly of physical importance, see *e.g.*, [110].

[2] For σ to be positive, the constant M in equation (5.2.18) needs to be positive, cf. (5.2.14). For the polytropic equation of state, the relation between the integration constant M and σ is not direct. Since a physical interpretation of M is not transparent, one can consider both positive and negative values of M for the polytropic equation of state. In this chapter we only consider $M > 0$.

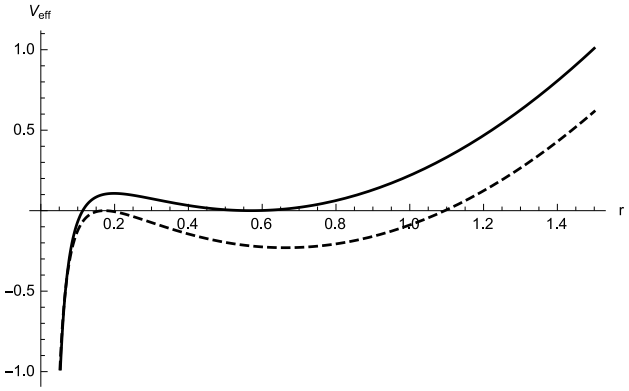

Figure 5.1: The two limiting cases within which oscillatory shell motion exists. We have chosen $\alpha = 0.3$, $d = 3$, $m = 0.1$, $M_{\text{up}}/m = 0.38$ (the top solid curve) and $M_{\text{low}}/m = 0.35$ (the bottom dashed curve).

Note that for $\gamma \neq 1$, the two terms in (5.2.17) compete with each other, and define a natural scale for the dynamics,

$$\mathcal{O}\left(\frac{(d-1)^{\gamma-2}}{\kappa^{\gamma-1}}\ \alpha\ r_{\text{cross}}^{1-\gamma}\right) = \mathcal{O}\left(M r_{\text{cross}}^{(d-2)(\gamma-1)}\right), \tag{5.2.23}$$

where r_{cross} denotes the crossover scale which connects two different dynamical regimes, described respectively by an $r_{\text{s}}^{1-\gamma}$ potential and the inverse of it. In general, with various possibilities, the full dynamics is likely to be very rich and worth exploring. We focus only on certain sub-classes in this chapter.

Let us start by briefly reviewing the oscillatory solutions that are already discussed in [96]. This corresponds to setting $\gamma = 1$. The effective potential can be rewritten as,

$$V_{\text{eff}} = 1 + r_{\text{s}}^2 - \frac{m^2}{4M^2} r_{\text{s}}^{2\alpha} - \frac{m}{2} r_{\text{s}}^{2-d} - \frac{M^2}{4} r_{\text{s}}^{-2(\alpha+d-2)}, \tag{5.2.24}$$

where M is now the constant appearing in the first integral of motion in (5.2.18). To find oscillatory shell dynamics, one can proceed as follows.

We impose $V_{\text{eff}} = 0$ and $\partial_{r_{\text{s}}} V_{\text{eff}} = 0$, to find algebraic solutions characterized by

$$\left\{m\left(d, \alpha, r_{\text{s}}\right), M\left(d, \alpha, r_{\text{s}}\right)\right\}. \tag{5.2.25}$$

These values can be viewed as special cases, when two roots of the effective potential coalesce. See figure 5.1. Evidently, if this is a local minimum, and the effective potential can be lowered by tuning other parameters in the system, oscillatory shell dynamics will ensue. Explicit expressions for $m\left(d, \alpha, r_{\text{s}}\right)$ and $M\left(d, \alpha, r_{\text{s}}\right)$ are given in reference [96]. For a fixed value of mass m_* less than a maximum value,

$$m_* \leq m_{\text{max}}(d, \alpha), \tag{5.2.26}$$

the equation

$$m_* = m\left(d, \alpha, r_{\text{s}}\right), \tag{5.2.27}$$

yields two roots of r_{s}, denoted by r_{up} and r_{low}. The function $M\left(d, \alpha, r_{\text{s}}\right)$ evaluated at these two roots yield two values of M, denoted by M_{up} and M_{low}. Choosing a value of M such that

$$M_{\text{low}} \leq M \leq M_{\text{up}}, \tag{5.2.28}$$

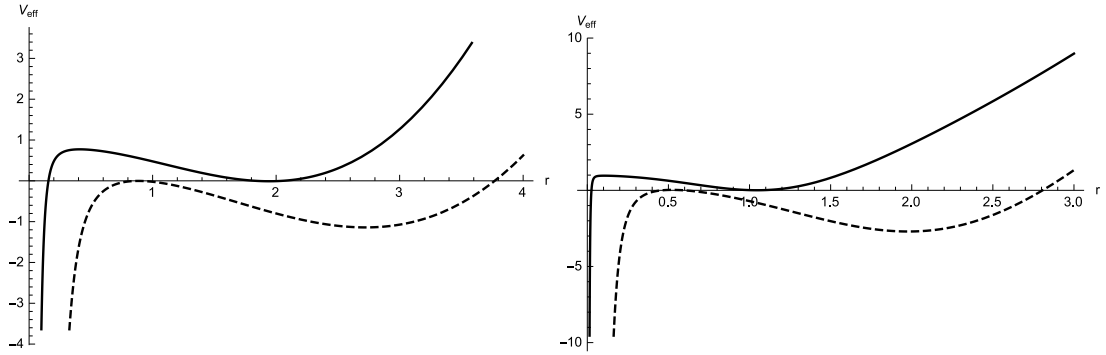

Figure 5.2: The limiting cases within which oscillatory shell motion exists. The plot on the left corresponds to $\gamma = 2$, $\alpha = -0.4$, $m = 0.94$, $M = 0.006$ (dashed) and $m = 0.1$, $M = 0.012$ (solid). The plot on the right corresponds to $\gamma = 3$, $\alpha = -0.05$, $m = 0.5$, $M = 0.002$ (dashed) and $m = 0.004$, $M = 0.026$ (solid). The two plots indicate that increasing γ brings the two limiting cases closer to each other.

for a suitably fixed value of m, the shell undergoes oscillatory motion. The function $m_{\text{max}}(d, \alpha)$ is such that for fixed m the oscillatory solutions exist only beyond a critical non-zero value $\alpha = \alpha_{\text{crit}}$. For $d = 4$ we have explicitly checked that once we choose an $\alpha > \alpha_{\text{crit}}$, the range $(M_{\text{up}} - M_{\text{low}})$ increases with increasing α. For $\alpha < \alpha_{\text{crit}}$ only collapsing solutions exist.

Let us comment on the typicality of such oscillatory configurations with a non-trivial polytropic exponent. In principle, the above analysis can be carried out for any value of γ. However, we only discuss explicitly the cases with $\gamma = 2$ and $\gamma = 3$, which is perhaps sufficient for the generic story. The algebraic expressions associated with this analysis are fairly involved and we refrain from presenting them explicitly. Instead, we summarise the generic finding in figure 5.2 in terms of the features of the effective potential. The main features are as follows.

In producing figure 5.2, we have chosen a negative value of α for both $\gamma = 2$ and $\gamma = 3$. Interestingly, $\gamma = 1$ is an exception to this generic observation, for which potential wells appear on the $\alpha > 0$ branch. Furthermore, it can be easily seen that as far as satisfying a reasonable energy condition is concerned, negative values for α are allowed. For example, ensuring weak energy condition requires $\sigma \geq 0$ and $\sigma + p \geq 0$. For positive σ and for $\gamma = 1$, the weak energy condition only requires $\alpha \geq -(d-1)$. As another example, for $\gamma = 3$ weak energy condition only requires $\alpha \geq -\frac{d-1}{\sigma^2}$, which leaves a window for choosing a negative value of α.

Finally, for general integer values of γ, the oscillatory regime can be characterized by a 3-tuple: (α, M, m). For a fixed value of α, both M and m need to be tuned to obtain the potential well. In figure 5.2, we have shown the corresponding extremal cases, by tuning both M and m to the respective values quoted in the figure caption. It is noteworthy that we have not found an oscillatory configuration along the $\gamma < 0$ branch, assuming that both $m > 0$ and $M > 0$.

To add further support to the existence of oscillatory configurations, we have also explored a few non-integer values of γ. In particular, we here comment on the results that one obtains for $d = 3$ and $\gamma = \frac{1}{2}$ or $\gamma = \frac{3}{2}$. First of all, the analogue of relation

(5.2.17) in these cases yields,

$$-[\beta] = \frac{1}{16 r_{\rm s}} \left(\sqrt{2} r_{\rm s} \alpha - M\right)^2, \quad \gamma = \tfrac{1}{2}, \tag{5.2.29}$$

$$-[\beta] = \frac{4 M^2 r_{\rm s}}{\left(r_{\rm s} \pm \sqrt{2} M \alpha\right)^2}, \quad \gamma = \tfrac{3}{2}. \tag{5.2.30}$$

Using these relations, one can obtain the corresponding effective potentials. We find that for $\gamma = \frac{1}{2}$, oscillatory configurations exist in the $\alpha < 0$ branch; while, for $\gamma = \frac{3}{2}$, they exist on both $\alpha > 0$ and $\alpha < 0$ branches, depending on the choice of the sign in the denominator of (5.2.30).

Let us now briefly comment on the holographic interpretation. Collapsing shells correspond to states in the dual field theory that thermalise. However, it is important to note that the very concept of thermalisation is often observable dependent, see *e.g.* the discussions in [104, 105]. In systems that do thermalise, correlations over arbitrarily long distances eventually settle to the corresponding thermal values. Thus, the dynamics *terminates* at a particular *thermalisation time*, depending on the energy-scale at which one is probing.

The oscillatory configurations, in comparison, are quite unique. Let us say that for the given set of parameters the dynamics of the shell is confined in the radial range $r = r_{\rm s}^-$ to $r = r_{\rm s}^+$. Then, local observables, such as the expectation value of energy-momentum tensor, do not exhibit any imprint of the oscillatory dynamics, and hence are indistinguishable from usual thermal states. For any non-local boundary operator that probes bulk region $r > r_{\rm s}^+$, the system is always static and thermal. For any non-local boundary operator that probes beyond this bulk region, the system never thermalizes. We numerically study spacelike geodesics in the next subsection and demonstrate this explicitly. Thus, we have a dynamical state, for which the thermalization time is either $t_{\rm therm} = 0$ or $t_{\rm therm} = \infty$. Presently, we do not have a good understanding of the nature of this state in the dual field theory.

5.2.2 Geodesics in oscillating shells

To probe the oscillatory dynamics from the perspective of the boundary theory, we compute the equal time two-point function of an operator of large conformal dimension in the geodesic approximation. Such a two-point function via a saddle point approximation [111, 112] is:

$$\langle \mathcal{O}(\vec{x}) \mathcal{O}(\vec{x}') \rangle \sim e^{-2\Delta \Sigma(\vec{x}, \vec{x}')}. \tag{5.2.31}$$

Here $\mathcal{O}$ and Δ are the operator and its conformal dimension, respectively. The length of the bulk spacelike geodesic connecting the points $(t, \vec{x})$ and $(t, \vec{x}')$ is denoted by $\Sigma(\vec{x}, \vec{x}')$. Our goal here is to capture the imprint of the oscillatory dynamics on this correlation function.

We study geodesic lengths of spacelike geodesics anchored at a fixed value of boundary angular separation, $\Delta\varphi$. Since the shell expands and contracts periodically, the geodesics experience varying conditions near the shell. This is expected to lead to an oscillatory evolution of the correlation function, which we verify by an explicit calculation. To calculate the geodesics we follow [103]. A geodesic anchored at two points at the same time on the boundary must have a turning point in the bulk. The turning point is characterized by vanishing of the radial and temporal derivatives with respect to the proper length of the geodesic.

We impose these boundary conditions in the bulk at the turning point $(\bar{t}, \bar{r})$. Then we integrate the geodesic equations towards the AdS boundary. The data at the turning

point map to the data at the boundary. The data we need to extract from such geodesics include the angular separation, time at the boundary, and the geodesic length, denoted $\Delta\varphi_{\rm b}, t_{\rm b}, \Sigma$. By varying $(\bar{t}, \bar{r})$ in the bulk and solving the geodesic equations, we generate a boundary dataset $(\Delta\varphi_{\rm b}, t_{\rm b}, \Sigma)$.

The affinely parameterised spacelike geodesic equations can be easily integrated both in the inside and outside regions to give the following first order equations:

$$f_{\pm} t' = E_{\pm}, \tag{5.2.32}$$

$$r^2 \phi' = L_{\pm} , \tag{5.2.33}$$

$$(r')^2 = f_{\pm}\left(1 - \frac{L_{\pm}^2}{r^2}\right) + E_{\pm}^2. \tag{5.2.34}$$

In these equations prime denotes derivatives with respect to the proper distance σ along the spacelike geodesic. Here $E_{\pm}$ and $L_{\pm}$ are the constants of motion. To ensure that the geodesic smoothly crosses the shell, we need to match the constants of motion appropriately on the two sides of the shell. To this end, we follow the treatment of [103, 113].

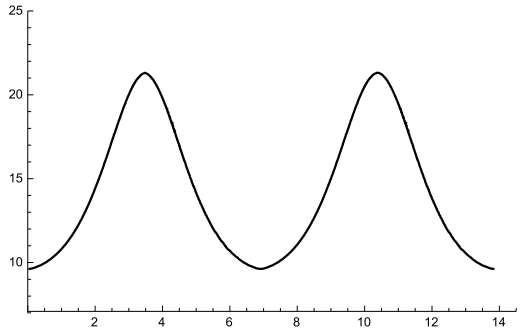

Figure 5.3: A typical behaviour of renormalised geodesic length for fixed $\Delta\phi = 0.15$ as a function of time t_+ when the shell undergoes oscillatory motion. The coordinate t_+ is taken to be zero at the beginning of an oscillation cycle, when the shell is at its lower turning point. Various parameters are: $\ell = 1, d = 4, \alpha = 0.992, m = 24.45$, and the lower turning of the shell is taken to be at $r_{\rm s}^- = 6.90$. The rest of the parameters are fixed by these values. In our conventions the y axis is 10^{20} times e^{-L} where L is the proper length of the geodesics.

The idea is to construct a coordinate system that is sufficiently smooth in a neighbourhood across the shell, and use it to transform quantities from the inside of the shell to the outside. The time coordinate for this coordinate system is chosen to be the proper time of the shell τ. The spatial coordinate is naturally chosen to be the proper distance λ away from the shell along spacelike geodesics normal to the shell. In terms of our inside and outside regions, the coordinate transformations,

$$(t_{\pm}, r, \theta_i) \to (\tau, \lambda, \theta_i). \tag{5.2.35}$$

do the work. Using these coordinates one arrives at the equations relating t'_- to t'_+ and

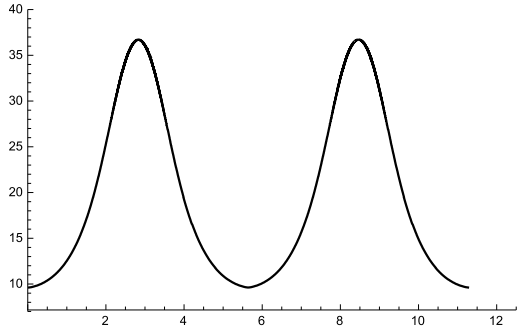

Figure 5.4: Renormalised geodesic length for fixed $\Delta\phi = 0.15$ as a function time t_+ with different pressure on the shell. Parameter values are same as in Figure 5.3 except $\alpha = 0.995$. For different values of α, while keeping the other parameters same, the location of the upper turning point $r_{\rm s}^+$ of the shell changes. As a result the oscillation period is different. Geodesic lengths are also different.

relating r' from the inside to the outside region [113][3]

$$\left.\frac{dt_-}{d\sigma}\right|_{r=r_{\rm s}} = \left.\frac{dt_+}{d\sigma}\right|_{r=r_{\rm s}} \frac{\beta_{\rm s-}\beta_{\rm s+} - \dot{r}_{\rm s}^2}{f_-} + \left.\frac{dr_+}{d\sigma}\right|_{r=r_{\rm s}} \frac{\dot{r}_{\rm s}}{f_- f_+}(\beta_{\rm s+} - \beta_{\rm s-}), \tag{5.2.36}$$

$$\left.\frac{dr_-}{d\sigma}\right|_{r=r_{\rm s}} = \left.\frac{dt_+}{d\sigma}\right|_{r=r_{\rm s}} \dot{r}_{\rm s}(\beta_{\rm s+} - \beta_{\rm s-}) + \left.\frac{dr_+}{d\sigma}\right|_{r=r_{\rm s}} \frac{\beta_{\rm s-}\beta_{\rm s+} - \dot{r}_{\rm s}^2}{f_+}, \tag{5.2.37}$$

where $\beta_{\rm s\pm} = \sqrt{f_{\rm s\pm} + \dot{r}_{\rm s}^2}$. The inside and the outside derivatives of the continuous radial coordinate r at the location of the shell are denoted as $\frac{dr_+}{d\sigma}\big|_{r=r_{\rm s}}$ and $\frac{dr_-}{d\sigma}\big|_{r=r_{\rm s}}$. Note that we only need to know the first derivatives of the $\pm$ coordinates with respect to the paramter σ to match the geodesic across the shell. These conditions together with equations (5.2.32)–(5.2.34) allow us to relate E_+ to E_-.

We solve equations (5.2.32)–(5.2.34) separately for the inside and the outside and match them across the shell according to (5.2.36) and (5.2.37). We begin by integrating a geodesic from its turning point $(\bar{t}, \bar{r})$ in the inside region. At the turning point,

$$t' = 0, \tag{5.2.38}$$

$$r' = 0, \tag{5.2.39}$$

which fixes the constants of motion to be,

$$E_- = 0, \tag{5.2.40}$$

$$L_- = \bar{r}. \tag{5.2.41}$$

We integrate geodesic equations (5.2.32)–(5.2.34) up to the location of the shell $r_{\rm s}$ with $f = f_-$. At this point, we switch to using the function f_+. We also need to use the constants of motion for the exterior. These are given by

$$E_+ = \sqrt{1 - \frac{\bar{r}^2}{r_{\rm s}^2}}\frac{\dot{r}_{\rm s}}{\sqrt{f_-}}(\sqrt{f_+ + \dot{r}_{\rm s}^2} - \sqrt{f_- + \dot{r}_{\rm s}^2}), \tag{5.2.42}$$

$$L_+ = \bar{r}, \tag{5.2.43}$$

[3] See section 2.2 and appendix B of [113] for details.

where E_+ is deduced using (5.2.36) or (5.2.37) and the geodesic equations. Since the ϕ and the r coordinates are continuous the conserved angular momentum does not change $L_+ = L_-$.

In figures 5.3 and 5.4 we have plotted the geodesic lengths for a fixed value of boundary angular separation $\Delta\varphi$ as a function of the boundary time t_+. The coordinate t_+ is taken to be zero at the beginning of an oscillation cycle where $r_s = r_s^-$. We can clearly see that the geodesic length oscillates with a fixed period. The period precisely corresponds to the period of the oscillation of the shell. Thus, the two-point function under study in the oscillating shell background captures features of the oscillations.

We have chosen to plot geodesic lengths as a function of the time t_+. One can straightforwardly relate t_+ to the proper time of the shell τ or to t_-. We did not find any qualitative difference between the above graphs and the ones where the x-axis is taken to be proper time τ on the shell. We want to emphasise that our aim is to illustrate the qualitative behaviour of spacelike geodesics in oscillating shell backgrounds, as opposed to a detailed numerical analysis of these equations. At the turning points $\dot{r}_s$ vanishes, and naively there are $1/0$ type expressions encountered while doing numerical integrations. We regulate such nuisances with a simple minded approach. For example, in the specific example of $1/\dot{r}_s$, instead of taking the integration from $r = r_s^-$ we take it from $r = r_s^- + \epsilon$ with sufficiently small epsilon (and check that our results to do not depend on epsilon).

5.3 The oscillating balls

In this section we consider the motion of a ball of matter of uniform density and pressure under its own gravity. The case of pressure-less dust was studied by Oppenheimer and Snyder [114]. In the context of the AdS/CFT correspondence, references [103,115] studied similar dynamical situation in AdS background. We consider non-vanishing pressure. We are specifically interested in exploring the possibility of oscillatory motion of the ball.

5.3.1 Oscillating FRW solutions

The interior of a d-dimensional solid ball can be described by a Friedmann-Robertson-Walker (FRW) metric with $k = +1$, *i.e.* positively curved $t =$ constant slices,

$$ds_-^2 = -dt^2 + R^2(t)\left(d\chi^2 + \sin^2\chi\, d\Omega_{d-1}^2\right), \tag{5.3.1}$$

sourced by by perfect fluid stress-tensor

$$T_{\mu\nu} = (\sigma + p)u_\mu u_\nu + p g_{\mu\nu}, \quad u^\mu = (1, 0, \ldots, 0), \tag{5.3.2}$$

with an equation of state $p = w\sigma$. The radial and the time coordinates are denoted by χ and t, respectively. The function $R(t)$ is the scale factor.

Einstein equations give the Friedmann equation for the scale factor

$$1 + R^2 + \dot{R}^2 = \frac{2\kappa\sigma}{d(d-1)} R^2, \tag{5.3.3}$$

where we have used the value of the cosmological constant $\Lambda = -\frac{d(d-1)}{2\ell^2}$ and have set the AdS length ℓ to unity. The conservation of the energy-momentum tensor gives

$$\sigma R^{(w+1)d} = \text{constant}. \tag{5.3.4}$$

Eliminating σ from the Friedmann equation (5.3.3) using the conservation equation (5.3.4) we get,

$$1 + R^2 + \dot{R}^2 = \frac{2\kappa\sigma_0 R_0^{(w+1)d}}{d(d-1)R^{(w+1)d-2}}, \tag{5.3.5}$$

where σ_0 is the initial density of the collapsing matter and R_0 is the initial scale factor.

We are interested in knowing if oscillatory solutions are possible to equation (5.3.5). In order to explore this, we rewrite that equation as

$$\dot{R}^2 + V_{\text{eff}}(R) = 0, \tag{5.3.6}$$

with the effective potential

$$V_{\text{eff}}(R) = 1 + R^2 - \frac{c}{R^\beta}, \tag{5.3.7}$$

where

$$c = \frac{2\kappa\sigma_0}{d(d-1)} R_0^{(w+1)d}, \qquad \beta = (w+1)d - 2. \tag{5.3.8}$$

For oscillatory dynamics, the effective potential (5.3.7) must develop a minimum in between two roots of equation $V_{\text{eff}}(R) = 0$. Let the roots be at $R = R_1$ and $R = R_2$ and the minimum be at $R = R_*$ with $R_1 < R_* < R_2$. Then,

$$V_{\text{eff}}(R_*) < 0, \qquad V'_{\text{eff}}(R_*) = 0 \qquad \text{and} \qquad V''_{\text{eff}}(R_*) > 0. \tag{5.3.9}$$

It is straightforward to see that

$$V'_{\text{eff}}(R_*) = 0 \quad \Longrightarrow \quad \beta = -\frac{2}{c} R_*^{2+\beta}. \tag{5.3.10}$$

For physically reasonable initial parameters $\sigma_0 > 0$ and $R_0 > 0$, thus the parameter c is positive. Equation (5.3.10) then implies that $\beta < 0$, i.e.,

$$w < -\left(\frac{d-2}{d}\right). \tag{5.3.11}$$

The second derivative of the potential (5.3.7) at $R = R_*$ is

$$V''_{\text{eff}}(R_*) = 2\,(\beta + 2)\,. \tag{5.3.12}$$

Requiring $V''_{\text{eff}}(R_*) > 0$ gives $\beta > -2$ or equivalently $w > -1$. Thus, within the range

$$0 > \beta > -2, \qquad -1 < w < -\left(\frac{d-2}{d}\right), \tag{5.3.13}$$

oscillatory ball dynamics is possible. Curiously the pressure $p = w\sigma$ must always be negative. We analyse the issue of energy conditions in section 5.4. Next we comment on whether such an oscillatory FRW solution can be matched to an appropriate exterior solution.

5.3.2 Matching to an exterior star

In the Oppenheimer-Snyder (OS) model the FRW metric that describes the interior of a collapsing star is matched to an empty Schwarzschild solution that describes the exterior of the collapsing star. The FRW metric is supported only by uniform pressure-less dust. The fact that such a smooth matching can be done is a remarkable fact about the OS

model. The pressure-less nature of the interior solution is an important ingredient. The OS model has been generalised to AdS space, see *e.g.* [115].

Here we are interested in a generalisation of the OS model in AdS with non-zero pressure. In particular, we are interested in knowing if an oscillatory solution of the previous subsection can be taken to be the interior of an oscillating configuration in AdS. This turns out to be a difficult problem to analyse. In section 5.5 we report some progress on this problem. We construct a matched metric when the equation of state $p = p(\sigma)$ is arbitrary, and can be chosen independently for the interior and the exterior of the model. The distinction between the interior and the exterior is as the two sides of a "shock wave" across which the metric is continuous. We find that the pressure and energy density suffer a discontinuity across the shock surface. Such shock waves are the counterparts of fluid dynamical shock waves on curved backgrounds. A detailed study of such systems was done by Smoller and Temple [116], who also constructed a flat space generalisation of the OS model with non-zero pressure. Our analysis in section 5.5 closely follows their construction.

When we demand that the extrinsic curvature also remains continuous (as in the OS model, and in contrast to the thin-shell model), the set-up becomes over-constrained. One way to achieve extrinsic curvature continuity is by *not* demanding an equation of state for the interior or for the exterior solution. We can treat pressure and density as independent dynamical variables, say for the interior solution. By doing so, one can fix the pressure and density for the interior solution from the exterior solution. This strategy has its shortcomings, but this is one way in which interior and exterior solutions can be matched [116]. We illustrate how such a matching is to be done, from a given outside solution to an appropriate inside solution. For our problem, however, the matching needs to done the other way, *i.e.*, given an FRW solution of the previous subsection, can we find an appropriate exterior solution? Unfortunately, we do not know a full answer to this question. Given the analysis of section 5.5, it seems feasible that some exterior star solution can be matched to a given interior solution, however, the precise details of such an analysis are likely to be complicated and are left for future investigations.

5.4 Energy conditions

In this section we analyse various energy conditions for the above discussed oscillating solutions.

5.4.1 Oscillating shells

In the case of oscillating shells one can consider two independent notions of energy conditions. One is associated with the shell stress-energy tensor (5.2.11) and the other is associated with the Einstein tensor constructed from the induced metric (5.2.6). Interestingly, these two turn out to have independent characters, as we discuss below.

Energy conditions with S_{ab}

Since the surface stress tensor (5.2.11) is of the perfect fluid form with σ and p given by (5.2.14), null energy condition is equivalent to the statement that $\sigma + p \geq 0$ and the weak energy condition is equivalent to the statement that $\sigma \geq 0$, $\sigma + p \geq 0$.

At the turning points of the oscillating shell where $\dot{r}_{\rm s} = 0$, we have from equations (5.2.14),

$$\sigma = \frac{d-1}{\kappa r_{\rm s}}\left(\sqrt{1+r_{\rm s}^2} - \sqrt{1+r_{\rm s}^2 - \frac{m}{r_{\rm s}^{d-2}}}\right), \tag{5.4.1}$$

$$\sigma + p = \frac{r_{\rm s} + \frac{(d-2)}{2}\frac{m}{r_{\rm s}^{d-1}} - \frac{V'_{\rm eff}(r_{\rm s})}{2}}{\kappa\sqrt{1+r_{\rm s}^2 - \frac{m}{r_{\rm s}^{d-2}}}} - \frac{r_{\rm s} - \frac{V'_{\rm eff}(r_{\rm s})}{2}}{\kappa\sqrt{1+r_{\rm s}^2}} + \frac{1}{\kappa r_{\rm s}}\left(\sqrt{1+r_{\rm s}^2} - \sqrt{1+r_{\rm s}^2 - \frac{m}{r_{\rm s}^{d-2}}}\right). \tag{5.4.2}$$

From these expressions it is clear that σ is positive definite, provided $m > 0$. The right hand side of expression (5.4.2) is positive definite provided $2r_{\rm s} > V'_{\rm eff}(r_{\rm s})$. For a given configuration (*i.e.*, a given set of parameters), a straightforward numerical check can confirm if this is indeed the case or not. For the cases we have checked, we found that both weak and null energy conditions are satisfied at the turning points. We also found that for all the cases that we have checked, $\sigma + p$ is positive for the entire motion of the oscillatory shells. Thus, the null and weak energy conditions seem to be satisfied for the surface stress tensor all along the oscillation of the shell.

Energy conditions with G_{ab}

From the induced metric (5.2.6) we can define an effective stress tensor $\kappa T_{ab} := G_{ab} = R_{ab} - \frac{1}{2}g_{ab}R$. This stress tensor turns out to be of the perfect fluid form, which allows us to define an effective energy density and pressure. We find

$$\sigma_{\rm eff} = \frac{(d-1)(d-2)}{2\kappa r_{\rm s}^2}(1+\dot{r}_{\rm s}^2), \qquad p_{\rm eff} = -\frac{(d-2)}{\kappa}\left(\frac{\ddot{r}_{\rm s}}{r_{\rm s}} + \frac{(d-3)(1+\dot{r}_{\rm s}^2)}{2r_{\rm s}^2}\right), \tag{5.4.3}$$

as a result

$$\sigma_{\rm eff} + p_{\rm eff} = \frac{(d-2)}{\kappa r_{\rm s}^2}(1 + \dot{r}_{\rm s}^2 - r_{\rm s}\ddot{r}_{\rm s}). \tag{5.4.4}$$

At the bounce $\dot{r}_{\rm s}^2 = 0$, therefore

$$\sigma_{\rm eff} + p_{eff} = \frac{(d-2)}{\kappa r_{\rm s}^2}(1 - r_{\rm s}\ddot{r}_{\rm s}). \tag{5.4.5}$$

We note that $\sigma_{\rm eff} + p_{\rm eff} > 0$ at the bounce provided $\ddot{r}_{\rm s} < r_{\rm s}^{-1}$, *i.e.*, if the bounce is sufficiently 'gentle'. A very similar set of conditions were discussed in [117] in a different context. From the definition of effective potential (5.2.20), we have $\ddot{r}_{\rm s} = -\frac{1}{2}V'_{\rm eff}(r_{\rm s})$. Therefore,

$$\sigma_{\rm eff} = \frac{(d-1)(d-2)}{2\kappa r_{\rm s}^2}(1 - V_{\rm eff}(r_{\rm s})), \qquad \sigma_{\rm eff} + p_{\rm eff} = \frac{(d-2)}{\kappa r_{\rm s}^2}\left(1 - V_{\rm eff}(r_{\rm s}) + \frac{1}{2}r_{\rm s}V'_{\rm eff}(r_{\rm s})\right). \tag{5.4.6}$$

The energy density $\sigma_{\rm eff}$ so defined is always positive. For a given set of parameters, one can easily check numerically whether $\sigma_{\rm eff} + p_{\rm eff}$ is positive or not. We find that for all the cases that we have checked $\sigma_{\rm eff} + p_{\rm eff} > 0$ for oscillatory shells. Therefore, null and weak energy conditions so defined also seem to be satisfied all along the motion of the shell.

5.4.2 Oscillating balls

Now we discuss the energy conditions for the oscillating FRW metrics of section 5.3. The energy density and pressure can be read off from the Einstein's equations. We get

$$\sigma = \frac{d(d-1)}{2\kappa R^2}\left(1 + R^2 + \dot{R}^2\right), \qquad \sigma + p = \frac{(d-1)}{\kappa R^2}(1 + \dot{R}^2 - R\ddot{R}). \tag{5.4.7}$$

Using the effective potential we once again get expressions very similar to (5.4.6),

$$\sigma = \frac{d(d-1)}{2\kappa R^2}(1 + R^2 - V_{\text{eff}}(R)), \qquad \sigma + p = \frac{(d-1)}{\kappa R^2}\left(1 - V_{\text{eff}}(R) + \frac{1}{2}RV'_{\text{eff}}(R)\right). \tag{5.4.8}$$

These expressions for the potential (5.3.7) become,

$$\sigma = \frac{d(d-1)c}{2\kappa R^{\beta+2}}, \qquad \sigma + p = \frac{(d-1)(\beta+2)c}{\kappa R^{\beta+2}}. \tag{5.4.9}$$

A requirement for oscillations is precisely $\beta + 2 > 0$, cf. (5.3.13). Therefore, we note that both null and weak energy conditions are satisfied all along the motion of the ball. It is intriguing (and perhaps counterintuitive) that negative pressure is needed to sustain these oscillations. We note that with zero cosmological constant, accelerated expansion also requires negative pressure precisely in the range (5.3.13).[4]

5.5 Oppenheimer-Snyder model with non-zero pressure in AdS

The OS model requires that the pressure of the collapsing star be identically zero. In this section we construct a generalisation of the Oppenheimer-Snyder (OS) model in AdS with non-zero pressure. We first construct a matched metric when the equation of state $p = p(\sigma)$ is arbitrary, and can be chosen independently for the interior and the exterior of the model. The distinction between the interior and the exterior is as the two sides of a "shock wave" across which the metric is continuous. When we demand that the extrinsic curvature also remains continuous, the set-up becomes over-constrained. One way to achieve extrinsic curvature continuity is by *not* demanding an equation of state for the interior Friedmann-Robertson-Walker (FRW) solution. That is, to treat pressure and density as independent dynamical variables. Doing this has its shortcoming, but this is one way in which exterior solution can be matched to an interior solution with pressure.[5]

We find that the pressure and energy density suffer a discontinuity across the shock surface. Such "shock waves" are the counterparts of fluid dynamical shock waves on curved backgrounds. A detailed study of such systems was done by Smoller and Temple [116], who also constructed a flat space generalisation (*i.e.*, with $\Lambda = 0$) of the OS model with non-zero pressure. Our analysis below closely follows their construction. We work in four spacetime dimensions. This appendix is a preliminary study; it serves to illustrate how such a matching is to be done, from a given outside solution to an appropriate inside solution. We do not address several physics issues *e.g.* energy conditions for the inside solution, or if the matching can be done the other way – given an inside solution can it be matched to an appropriate outside solution?

Interior solution: FRW in AdS

As in the OS model, the inside metric is taken to be the Friedmann-Robertson-Walker (FRW) solution

$$ds^2 = -dt^2 + R^2(t)\left(\frac{1}{1-kr^2}dr^2 + r^2 d\Omega^2\right), \tag{5.5.1}$$

[4] We thank Jorge Rocha and Vitor Cardoso for this observation.

[5] Another approach could be to introduce a surface stress-tensor at the interface, as in the thin-shell model. We do not pursue this idea here.

with the perfect fluid stress tensor source where p and σ only depend on time t. Einstein's equations give

$$\dot{\sigma} = -3\frac{\dot{R}}{R}(p+\sigma), \tag{5.5.2}$$

$$\dot{R}^2 + k = \frac{8\pi}{3}\sigma R^2 - \frac{R^2}{\ell^2}, \tag{5.5.3}$$

$$\frac{\ddot{R}}{R} = -\frac{4\pi}{3}(\sigma + 3p) - \frac{1}{\ell^2}. \tag{5.5.4}$$

Equation (5.5.2) is equivalent to

$$\frac{d}{dR}(\sigma R^3) = -3pR^2. \tag{5.5.5}$$

When pressure is zero this equation tells that the "mass" $M = \frac{4\pi}{3}\sigma R^3$ contained inside the star remains constant as the star evolves in time. With non-zero pressure we see that this is not the case. There is exchange of matter between the interior and the exterior, which needs to be carefully taken into account while matching the two solutions.

Exterior solution: TOV equations in AdS

The non-zero pressure for the interior solution also requires non-zero pressure for the exterior solution. This is so, because in the presence of pressure, matter can flow across the shock surface. Thus the exterior geometry is a spherically symmetric "star" with non-zero pressure and energy density, as opposed to the vacuum Schwarzschild solution in the OS model. Such configurations are described by the Tolman-Oppenheimer-Volkoff (TOV) equations. Therefore, our next aim is to get the TOV equations in AdS space. Let us start with the metric (see also [118])

$$d\bar{s}^2 = -B(\bar{r})d\bar{t}^2 + A(\bar{r})^{-1}d\bar{r}^2 + \bar{r}^2 d\Omega^2. \tag{5.5.6}$$

Typically this set-up is used for describing the "interior of a star" but in our case it describes the "exterior of the ball". It is supported by the perfect fluid stress tensor

$$\bar{T}_{\mu\nu} = \bar{p}g_{\mu\nu} + (\bar{p} + \bar{\sigma})\bar{u}_\mu \bar{u}_\nu, \tag{5.5.7}$$

with some equation of state

$$\bar{p} = \bar{p}(\bar{\sigma}), \tag{5.5.8}$$

and where fluid is taken to be not moving, *i.e.*,

$$\bar{u}_\mu = (\sqrt{B(\bar{r})}, 0, 0, 0). \tag{5.5.9}$$

The above equations are all written in barred notation so that they can be distinguished from the interior unbarred notation when we do the matching. We take the function $A(\bar{r})$ to be of the form

$$A(\bar{r}) = \left(1 - \frac{2M(\bar{r})}{\bar{r}} + \frac{\bar{r}^2}{\ell^2}\right), \tag{5.5.10}$$

where we have set Newton's constant and the speed of light to unity, but the AdS length is kept explicitly for clarity. The function $M(\bar{r})$ is so far undetermined. It is akin to the ADM mass. Einstein's equations in four-dimensions,

$$R_{\mu\nu} - \frac{1}{2}Rg_{\mu\nu} - \frac{3}{\ell^2}g_{\mu\nu} = 8\pi\bar{T}_{\mu\nu}, \tag{5.5.11}$$

give the following ordinary differential equations,

$$\frac{dM(\bar{r})}{d\bar{r}} = 4\pi\bar{r}^2\bar{\sigma}, \tag{5.5.12}$$

$$\frac{B'(\bar{r})}{B(\bar{r})} = -\frac{2\bar{p}'(\bar{r})}{\bar{p}+\bar{\sigma}}, \tag{5.5.13}$$

$$-\bar{r}^2\frac{d}{d\bar{r}}\bar{p} = M(\bar{r})\bar{\sigma}\left(1+\frac{\bar{p}}{\bar{\sigma}}\right)\left(1+\frac{\bar{r}^3}{M(\bar{r})}\left(4\pi\bar{p}+\frac{1}{\ell^2}\right)\right)\left(1-\frac{2M}{r}+\frac{r^2}{\ell^2}\right)^{-1}. \tag{5.5.14}$$

These equations are the generalisation of text book TOV equations with non-zero cosmological constant. In the limit $\ell \to \infty$ they reduce to the standard TOV equations, see *e.g.* [119].

A slightly better presentation is possible if we work with the following variables [118]

$$B(\bar{r}) = A(\bar{r})e^{2\chi(\bar{r})}. \tag{5.5.15}$$

Then the above equations simplify to

$$\frac{dM(\bar{r})}{d\bar{r}} = 4\pi\bar{r}^2\bar{\sigma}, \tag{5.5.16}$$

$$p'(\bar{r}) = -\frac{1}{2}\frac{B'(\bar{r})}{B(\bar{r})}(\bar{p}+\bar{\sigma}), \tag{5.5.17}$$

$$\chi'(\bar{r}) = 4\pi\bar{r}(\bar{p}+\bar{\sigma})A(\bar{r})^{-1}. \tag{5.5.18}$$

Matching

We now do the matching and also find the matching surface. In order to do so, we construct $(\bar{t},\bar{r})$ coordinate system for the FRW metric. To make sure that the areas of 2-spheres agree in the two coordinate systems at the matching surface, we must demand

$$\bar{r} = R(t)r. \tag{5.5.19}$$

We first write FRW metric in $(t,\bar{r})$ coordinates. From (5.5.19) we have

$$d\bar{r} = Rdr + \dot{R}rdt. \tag{5.5.20}$$

Using this, the FRW metric (5.5.1) can be written in the $(t,\bar{r})$ coordinates as

$$ds^2 = -\left\{1-\frac{\dot{R}^2\bar{r}^2}{R^2-k\bar{r}^2}\right\}dt^2 + \frac{R^2}{R^2-k\bar{r}^2}d\bar{r}^2 - \frac{2R\dot{R}\bar{r}}{R^2-k\bar{r}^2}dtd\bar{r} + \bar{r}^2d\Omega^2, \tag{5.5.21}$$

which upon inserting (5.5.3) becomes

$$ds^2 = \frac{1}{R^2-k\bar{r}^2}\left\{-R^2\left(1-\frac{8\pi}{3}\sigma R^2r^2+\frac{r^2R^2}{\ell^2}\right)dt^2 + R^2d\bar{r}^2 - 2R\dot{R}\bar{r}d\bar{r}dt\right\} + \bar{r}^2d\Omega^2. \tag{5.5.22}$$

Our aim is to match the interior metric in $(\bar{t},\bar{r})$ coordinates to the TOV metric (5.5.6). TOV metric does not have any cross-term, therefore, we next define a mapping $t = t(\bar{t},\bar{r})$ to eliminate the cross term $d\bar{r}dt$ in metric (5.5.22).

It is notationally more convenient to consider the general metric of the form

$$d\tilde{s}^2 = -C(t,\bar{r})dt^2 + D(t,\bar{r})d\bar{r}^2 + 2E(t,\bar{r})dtd\bar{r}. \tag{5.5.23}$$

Consider a function $\psi(t,\bar{r})$ that satisfies

$$\partial_{\bar{r}}(\psi C) + \partial_t(\psi E) = 0. \tag{5.5.24}$$

The coordinate $\bar{t}$ defined via

$$d\bar{t} = \psi(Cdt - Ed\bar{r}) \tag{5.5.25}$$

is an exact differential and also eliminates the cross term in (5.5.23) to give

$$d\tilde{s}^2 = -(\psi^{-2}C^{-1})d\bar{t}^2 + \left(D + \frac{E^2}{C}\right)d\bar{r}^2. \tag{5.5.26}$$

Applying this recipe to metric (5.5.22) and comparing $d\bar{r}^2$ term with TOV metric (5.5.6), we obtain the equation of the *shock surface*

$$M(\bar{r}) = \frac{4\pi}{3}\sigma(t)\bar{r}^3. \tag{5.5.27}$$

This is an equation in the (t,r) coordinates, since $\bar{r} = R(t)r$.

The function ψ needs to be determined such that $d\bar{t}^2$ terms from the two sides also match on the shock surface (5.5.27). This leads to the requirement

$$\frac{1}{\psi^2 R^2}\frac{1}{(R^2 - k\bar{r}^2)}\left(1 - \frac{8\pi}{3}\sigma\bar{r}^2 + \frac{\bar{r}^2}{\ell^2}\right)^{-1} = B(\bar{r}) \tag{5.5.28}$$

on the shock surface.

The picture is as follows: the function $\psi(t,\bar{r})$ is determined by the solution of the first order linear partial differential equation (5.5.24) where

$$C = \left(1 - \frac{8\pi}{3}\sigma\bar{r}^2 + \frac{\bar{r}^2}{\ell^2}\right)R^2, \tag{5.5.29}$$

$$E = -R\dot{R}\bar{r}, \tag{5.5.30}$$

subject to the initial data (5.5.28) on the surface (5.5.27). If this problem can be solved, the two metrics can be matched continuously.

Jump in density

From equation (5.5.12), we have that the mass function $M(\bar{r})$ for the TOV metric is given by

$$M(\bar{r}_0) = \int_0^{\bar{r}_0} 4\pi\bar{\sigma}(\bar{r})\bar{r}^2 d\bar{r}. \tag{5.5.31}$$

In writing this equation we are imagining that the TOV metric is continued to $\bar{r}$ values less than that of the shock surface. The quantity $M(\bar{r})$ represents the total mass that is generating the TOV solution outside the shock wave. For a physically reasonable model of a star $\frac{d\sigma}{d\bar{r}} < 0$, therefore,

$$M(\bar{r}_0) > \frac{4\pi}{3}\bar{\sigma}(\bar{r}_0)\bar{r}_0^3. \tag{5.5.32}$$

Compare this equation with (5.5.27). This allows us to conclude that at the shock surface

$$\sigma > \bar{\sigma}, \qquad [\sigma] \equiv \bar{\sigma} - \sigma < 0, \tag{5.5.33}$$

i.e., density inside is greater than the density outside.

Shock speed

Differentiating (5.5.27) with respect to t, we find the shock speed

$$\dot{\bar{r}} = \frac{\dot{\sigma}\bar{r}}{3[\sigma]}. \tag{5.5.34}$$

Since $[\sigma] < 0$, the shock speed is negative if $\dot{\sigma} > 0$. We also note that $\dot{\sigma}$ is indeed positive for a collapsing situation as $\dot{R} < 0$, cf. (5.5.2).

Continuity of extrinsic curvature

Smoller and Temple [116] also show that in the present set-up, the continuity of the extrinsic curvature is equivalent to the statement that the normal-normal component of the external stress-tensor has no jump,

$$[T]^{\mu\nu} n_\mu n_\nu = 0. \tag{5.5.35}$$

Explicitly, we have for the inside

$$T^{\mu\nu} n_\mu n_\nu = p(n \cdot n) + (p + \sigma)(u \cdot n)^2, \tag{5.5.36}$$

$$= p(n \cdot n) + (p + \sigma) n_0^2, \tag{5.5.37}$$

where we have used the fact that $u^\mu = (1, 0, 0, 0)$ for the FRW set-up. Similarly, we have for the outside

$$\bar{T}^{\mu\nu} \bar{n}_\mu \bar{n}_\nu = \bar{p}(\bar{n} \cdot \bar{n}) + (\bar{p} + \bar{\sigma})(\bar{u} \cdot \bar{n})^2, \tag{5.5.38}$$

$$= \bar{p}(\bar{n} \cdot \bar{n}) + \frac{1}{B(\bar{r})}(\bar{p} + \bar{\sigma})\bar{n}_0^2. \tag{5.5.39}$$

Therefore the jump condition (5.5.35) becomes

$$\bar{p}(\bar{n} \cdot \bar{n}) - p(n \cdot n) + \frac{1}{B(\bar{r})}(\bar{\sigma} + \bar{p})\bar{n}_0^2 - (\sigma + p) n_0^2 = 0. \tag{5.5.40}$$

We note that n_μ and $\bar{n}_\mu$ are components of the same vector n_μ. More explicitly, we write the shock surface as

$$\varphi(t, r) = r - r(t) = 0. \tag{5.5.41}$$

with the normal $d\varphi = n_\mu dx^\mu$. This gives $n_0 = -\dot{r}$. To obtain components in the barred coordinates, we rewrite the shock surface as

$$\varphi(\bar{t}, \bar{r}) = \frac{\bar{r}}{R(t(\bar{t}, \bar{r}))} - r(t(\bar{t}, \bar{r})) = 0, \tag{5.5.42}$$

which gives $\bar{n}_0 = -\frac{\dot{\bar{r}}}{R}\frac{\partial t}{\partial \bar{t}}$, where we have used the fact that $\bar{r} = rR(t)$. Equation (5.5.25) then yields,

$$\bar{n}_0 = -\frac{\dot{\bar{r}}}{\psi C R}. \tag{5.5.43}$$

Inserting equation (5.5.28) into expression (5.5.43) gives

$$\bar{n}_0^2 = \frac{B}{AR^2}(1 - kr^2)\dot{\bar{r}}^2. \tag{5.5.44}$$

Using these various elements, the jump condition (5.5.40) becomes,

$$(\sigma + \bar{p})\dot{r}^2 - (\bar{\sigma} + \bar{p})\frac{1 - kr^2}{AR^2}\dot{\bar{r}}^2 + (p - \bar{p})\frac{1 - kr^2}{R^2} = 0. \tag{5.5.45}$$

This equation is an additional constraint that must be satisfied on the shock surface. It is a complicated relation between $p, \bar{p}, \sigma, \bar{\sigma}, R$ on the shock surface $r = r(t)$. In the OS limit, where $\bar{\sigma} = \bar{p} = 0$ it reduces to

$$\sigma \dot{r}^2 + p \frac{1 - kr^2}{R^2} = 0. \tag{5.5.46}$$

Under the assumption that g_{rr} of the FRW metric is positive, *i.e.*, $\frac{1-kr^2}{R^2} > 0$ and $\sigma > 0$, we conclude that the only way this constraint can be satisfied is when

$$p = 0, \qquad \dot{r} = 0. \tag{5.5.47}$$

This means that the FRW interior must be pressure free and the shock surface is $r =$ `constant`, which are both features of the OS model.

Inside solution, given the outside

Now it seems that we have an over-constrained situation. Given an equation of state $\bar{p} = \bar{p}(\bar{\sigma})$, we can in principle integrate TOV equations to find the exterior solution on and outside the shock surface. For this solution to be matched to an interior FRW solution, we need to know $R(t), \sigma(t)$, and $p(t)$. Given an equation of state for the interior solution, we need to know only two functions, say, $R(t), \sigma(t)$. These two functions can be determined by the two Friedmann equations (5.5.2)–(5.5.3). Then, how to ensure that the constraint (5.5.45) is satisfied? It seems that we have three equations for two variables.

The picture that Smoller and Temple proposed for this problem is to view pressure in the FRW metric as an independent dynamical variable, rather than fixed by an equation of state. The idea then is to determine p from equation (5.5.2). Substituting this p in (5.5.45) to get an equation only involving $\sigma(t)$ and $R(t)$. Solution of that equation together with (5.5.3) completely specifies the FRW metric inside.

More explicitly, it proceeds as follows. Rewriting (5.5.2), we have

$$p = -\sigma - \frac{\dot{\sigma} R}{3\dot{R}}. \tag{5.5.48}$$

Using (5.5.34) into this equation we get

$$p = -\bar{\sigma} - [\sigma] \frac{R\dot{r}}{r\dot{R}}, \tag{5.5.49}$$

which gives the variable $p(t)$ in terms of the unknowns $R(t)$ and $\sigma(t)$ on the shock surface $r(t)$. Substituting (5.5.49) in (5.5.45) gives the constraint equation (5.5.35) in its most useful form,

$$\alpha \dot{r}^2 + \beta \dot{r} + \gamma = 0, \tag{5.5.50}$$

with

$$\alpha = \frac{\sigma + \bar{p}}{1 - kr^2} - \frac{\bar{\sigma} + \bar{p}}{A}, \tag{5.5.51}$$

$$\beta = -\frac{2\dot{R}r}{AR}(\bar{\sigma} + \bar{p}) + \frac{1}{\bar{r}\dot{R}}(\sigma - \bar{\sigma}), \tag{5.5.52}$$

$$\gamma = -\left(1 + \frac{\dot{R}^2 r^2}{A}\right)\left(\frac{\bar{\sigma} + \bar{p}}{R^2}\right). \tag{5.5.53}$$

All functions appearing in (5.5.50) and (5.5.3) are expressed in terms of unknowns $r(t)$[6] and $R(t)$. The solution to these equations determines the shock surface and FRW scale factor, and from these two quantities we know $\sigma(t)$ via (5.5.27) and $p(t)$ via (5.5.49). Hence the full interior FRW metric is determined. The matched FRW solution is such that the metric and the extrinsic curvature are continuous across the shock.

Shortcomings

As mentioned in the beginning of this discussion, *a priori* the above analysis does not ensure any physical condition for the interior solution. Since $p(t)$ and $\sigma(t)$ are explicitly known at the end of the procedure, one can always check if it is physically reasonable or not, *i.e.*, whether some energy condition is satisfied or not. Moreover, the way this construction is set-up, it allows us to match a given exterior TOV solution to an appropriate interior FRW solution. It is not at all obvious if the logic can be implemented the other way round, namely, given an FRW solution (possible oscillating), can one find an appropriate TOV solution where the metric and extrinsic curvature are matched continuously? We leave this investigation for future studies.

[6]Equivalently, $\sigma(t)$, cf. (5.5.27).

Bibliography

[1] S. W. Hawking and W. Israel, General Relativity. Univ. Pr., Cambridge, UK, 1979. http://www.cambridge.org/us/knowledge/isbn/item1131443/?site_locale=en_US.

[2] J. D. Bekenstein, "Black holes and entropy," Phys. Rev. **D7** (1973) 2333–2346.

[3] S. W. Hawking, "Particle Creation by Black Holes," Commun. Math. Phys. **43** (1975) 199–220. [,167(1975)].

[4] A. Sen, "Extremal black holes and elementary string states," Mod. Phys. Lett. **A10** (1995) 2081–2094, arXiv:hep-th/9504147 [hep-th].

[5] A. Strominger and C. Vafa, "Microscopic origin of the Bekenstein-Hawking entropy," Phys. Lett. **B379** (1996) 99–104, arXiv:hep-th/9601029 [hep-th].

[6] S. D. Mathur, "The Fuzzball proposal for black holes: An Elementary review," Fortsch. Phys. **53** (2005) 793–827, arXiv:hep-th/0502050 [hep-th].

[7] G. W. Gibbons and N. P. Warner, "Global structure of five-dimensional fuzzballs," Class. Quant. Grav. **31** (2014) 025016, arXiv:1305.0957 [hep-th].

[8] K. Skenderis and M. Taylor, "The fuzzball proposal for black holes," Phys. Rept. **467** (2008) 117–171, arXiv:0804.0552 [hep-th].

[9] I. Bena and N. P. Warner, "Black holes, black rings and their microstates," Lect. Notes Phys. **755** (2008) 1–92, arXiv:hep-th/0701216 [hep-th].

[10] V. Balasubramanian, J. de Boer, S. El-Showk, and I. Messamah, "Black Holes as Effective Geometries," Class. Quant. Grav. **25** (2008) 214004, arXiv:0811.0263 [hep-th].

[11] B. D. Chowdhury and A. Virmani, "Modave Lectures on Fuzzballs and Emission from the D1-D5 System," in 5th Modave Summer School in Mathematical Physics Modave, Belgium, August 17-21, 2009. 2010. arXiv:1001.1444 [hep-th].

[12] P. Breitenlohner, D. Maison, and G. W. Gibbons, "Four-Dimensional Black Holes from Kaluza-Klein Theories," Commun. Math. Phys. **120** (1988) 295.

[13] G. Bossard, H. Nicolai, and K. S. Stelle, "Universal BPS structure of stationary supergravity solutions," JHEP **07** (2009) 003, arXiv:0902.4438 [hep-th].

[14] G. Bossard, Y. Michel, and B. Pioline, "Extremal black holes, nilpotent orbits and the true fake superpotential," JHEP **01** (2010) 038, arXiv:0908.1742 [hep-th].

[15] G. Bossard and C. Ruef, "Interacting non-BPS black holes," Gen. Rel. Grav. **44** (2012) 21–66, arXiv:1106.5806 [hep-th].

[16] D. Katsimpouri, A. Kleinschmidt, and A. Virmani, "An inverse scattering formalism for STU supergravity," JHEP **03** (2014) 101, arXiv:1311.7018 [hep-th].

[17] S. D. Mathur, A. Saxena, and Y. K. Srivastava, "Constructing 'hair' for the three charge hole," Nucl. Phys. **B680** (2004) 415–449, arXiv:hep-th/0311092 [hep-th].

[18] V. Jejjala, O. Madden, S. F. Ross, and G. Titchener, "Non-supersymmetric smooth geometries and D1-D5-P bound states," Phys. Rev. **D71** (2005) 124030, arXiv:hep-th/0504181 [hep-th].

[19] I. Bena and N. P. Warner, "Bubbling supertubes and foaming black holes," Phys. Rev. **D74** (2006) 066001, arXiv:hep-th/0505166 [hep-th].

[20] E. Cremmer and B. Julia, "The SO(8) Supergravity," Nucl. Phys. **B159** (1979) 141–212.

[21] R. Gilmore, Lie Groups, Lie algebras, and Some of Their Applications. Dover Publications. Inc., Mineola, New York, 2005.

[22] M. Henneaux, D. Persson, and P. Spindel, "Spacelike Singularities and Hidden Symmetries of Gravity," Living Rev. Rel. **11** (2008) 1, arXiv:0710.1818 [hep-th].

[23] R. Gilmore, Lie groups, physics, and geometry: An introduction for physicists, engineers and chemists. Cambridge, UK: Univ. Pr. (2008) 319 p, 2008. http://www.cambridge.org/catalogue/catalogue.asp?isbn=9780521884006.

[24] S. Helgason, Differential Geometry, Lie Groups, and Symmetric Spaces. ISSN. Elsevier Science, 1979.

[25] A. Knapp, Lie Groups Beyond an Introduction. Progress in Mathematics. Birkhäuser Boston, 2002.

[26] P. Breitenlohner and D. Maison, "On the Geroch Group," Ann. Inst. H. Poincare Phys. Theor. **46** (1987) 215.

[27] P. Breitenlohner and D. Maison, "Solitons in Kaluza-Klein Theories," unpublished notes, June 1986 .

[28] V. A. Belinsky and V. E. Zakharov, "Integration of the Einstein Equations by the Inverse Scattering Problem Technique and the Calculation of the Exact Soliton Solutions," Sov. Phys. JETP **48** (1978) 985–994. [Zh. Eksp. Teor. Fiz.75,1953(1978)].

[29] V. A. Belinsky and V. E. Sakharov, "Stationary Gravitational Solitons with Axial Symmetry," Sov. Phys. JETP **50** (1979) 1–9. [Zh. Eksp. Teor. Fiz.77,3(1979)].

[30] V. A. Belinsky and E. Verdaguer, Gravitational solitons,. Univ. Pr., Cambridge, UK, 2001.

[31] R. Emparan and H. S. Reall, "Black Holes in Higher Dimensions," Living Rev. Rel. **11** (2008) 6, arXiv:0801.3471 [hep-th].

[32] H. Iguchi, K. Izumi, and T. Mishima, "Systematic solution-generation of five-dimensional black holes," Prog. Theor. Phys. Suppl. **189** (2011) 93–125, arXiv:1106.0387 [gr-qc].

[33] J. V. Rocha, M. J. Rodriguez, O. Varela, and A. Virmani, "Charged black rings from inverse scattering," Gen. Rel. Grav. **45** (2013) 2099–2121, arXiv:1305.4969 [hep-th].

[34] D. Katsimpouri, A. Kleinschmidt, and A. Virmani, "Inverse Scattering and the Geroch Group," JHEP **02** (2013) 011, arXiv:1211.3044 [hep-th].

[35] D. Katsimpouri, A. Kleinschmidt, and A. Virmani, "An Inverse Scattering Construction of the JMaRT Fuzzball," JHEP **12** (2014) 070, arXiv:1409.6471 [hep-th].

[36] B. Chakrabarty and A. Virmani, "Geroch Group Description of Black Holes," JHEP **11** (2014) 068, arXiv:1408.0875 [hep-th].

[37] M. C. Camara, G. L. Cardoso, T. Mohaupt, and S. Nampuri, "A Riemann-Hilbert approach to rotating attractors," JHEP **06** (2017) 123, arXiv:1703.10366 [hep-th].

[38] G. L. Cardoso and J. C. Serra, "New gravitational solutions via a Riemann-Hilbert approach," JHEP **03** (2018) 080, arXiv:1711.01113 [hep-th].

[39] B. Chakrabarty, J. V. Rocha, and A. Virmani, "Smooth non-extremal D1-D5-P solutions as charged gravitational instantons," JHEP **08** (2016) 027, arXiv:1603.06799 [hep-th].

[40] G. Bossard and S. Katmadas, "A bubbling bolt," JHEP **07** (2014) 118, arXiv:1405.4325 [hep-th].

[41] G. Bossard and S. Katmadas, "Floating JMaRT," JHEP **04** (2015) 067, arXiv:1412.5217 [hep-th].

[42] I. Bena, G. Bossard, S. Katmadas, and D. Turton, "Non-BPS multi-bubble microstate geometries," JHEP **02** (2016) 073, arXiv:1511.03669 [hep-th].

[43] I. Bena, G. Bossard, S. Katmadas, and D. Turton, "Bolting Multicenter Solutions," JHEP **01** (2017) 127, arXiv:1611.03500 [hep-th].

[44] G. Bossard, S. Katmadas, and D. Turton, "Two Kissing Bolts," JHEP **02** (2018) 008, arXiv:1711.04784 [hep-th].

[45] P. Berglund, E. G. Gimon, and T. S. Levi, "Supergravity microstates for BPS black holes and black rings," JHEP **06** (2006) 007, arXiv:hep-th/0505167 [hep-th].

[46] I. Bena, N. Bobev, and N. P. Warner, "Spectral Flow, and the Spectrum of Multi-Center Solutions," Phys. Rev. **D77** (2008) 125025, arXiv:0803.1203 [hep-th].

[47] A. Sahay and A. Virmani, "Subtracted Geometry from Harrison Transformations: II," JHEP **07** (2013) 089, arXiv:1305.2800 [hep-th].

[48] E. O. Colgain, M. M. Sheikh-Jabbari, J. F. Vázquez-Poritz, H. Yavartanoo, and Z. Zhang, "Warped Ricci-flat reductions," Phys. Rev. **D90** no. 4, (2014) 045013, arXiv:1406.6354 [hep-th].

[49] J. P. Gauntlett, J. B. Gutowski, C. M. Hull, S. Pakis, and H. S. Reall, "All supersymmetric solutions of minimal supergravity in five- dimensions," Class. Quant. Grav. **20** (2003) 4587–4634, arXiv:hep-th/0209114 [hep-th].

[50] J. P. Gauntlett and J. B. Gutowski, "General concentric black rings," Phys. Rev. **D71** (2005) 045002, arXiv:hep-th/0408122 [hep-th].

[51] A. Virmani, "Subtracted Geometry From Harrison Transformations," JHEP **07** (2012) 086, arXiv:1203.5088 [hep-th].

[52] I. Bena, M. Guica, and W. Song, "Un-twisting the NHEK with spectral flows," JHEP **03** (2013) 028, arXiv:1203.4227 [hep-th].

[53] M. Cvetič, M. Guica, and Z. H. Saleem, "General black holes, untwisted," JHEP **09** (2013) 017, arXiv:1302.7032 [hep-th].

[54] V. Breunhölder and J. Lucietti, "Moduli space of supersymmetric solitons and black holes in five dimensions," Commun. Math. Phys. **365** no. 2, (2019) 471–513, arXiv:1712.07092 [hep-th].

[55] I. Bena and P. Kraus, "Microstates of the D1-D5-KK system," Phys. Rev. **D72** (2005) 025007, arXiv:hep-th/0503053 [hep-th].

[56] D. Collingwood and W. McGovern, Nilpotent Orbits In Semisimple Lie Algebra: An Introduction. Mathematics series. Taylor & Francis, 1993.

[57] H. Dietrich, W. A. de Graaf, D. Ruggeri, and M. Trigiante, "Nilpotent orbits in real symmetric pairs and stationary black holes," Fortsch. Phys. **65** no. 2, (2017) 1600118, arXiv:1606.02611 [math.RT].

[58] D. Ruggeri and M. Trigiante, "Stationary $D = 4$ Black Holes in Supergravity: The Issue of Real Nilpotent Orbits," Fortsch. Phys. **65** no. 5, (2017) 1700007, arXiv:1612.04743 [hep-th].

[59] J. D. Bekenstein, "Black hole hair: 25 - years after," in Physics. Proceedings, 2nd International A.D. Sakharov Conference, Moscow, Russia, May 20-24, 199 pp. 216–219. 1996. arXiv:gr-qc/9605059 [gr-qc].

[60] C. A. R. Herdeiro and E. Radu, "Asymptotically flat black holes with scalar hair: a review," Int. J. Mod. Phys. **D24** no. 09, (2015) 1542014, arXiv:1504.08209 [gr-qc].

[61] V. Cardoso and L. Gualtieri, "Testing the black hole 'no-hair' hypothesis," Class. Quant. Grav. **33** no. 17, (2016) 174001, arXiv:1607.03133 [gr-qc].

[62] I. Mandal and A. Sen, "Black Hole Microstate Counting and its Macroscopic Counterpart," Nucl. Phys. Proc. Suppl. **216** (2011) 147–168, arXiv:1008.3801 [hep-th]. [Class. Quant. Grav.27,214003(2010)].

[63] O. Lunin and S. D. Mathur, "AdS / CFT duality and the black hole information paradox," Nucl. Phys. **B623** (2002) 342–394, arXiv:hep-th/0109154 [hep-th].

[64] S. D. Mathur, "Black Holes and Beyond," Annals Phys. **327** (2012) 2760–2793, arXiv:1205.0776 [hep-th].

[65] O. Lunin, "Adding momentum to D-1 - D-5 system," JHEP **04** (2004) 054, arXiv:hep-th/0404006 [hep-th].

[66] S. D. Mathur and D. Turton, "Microstates at the boundary of AdS," JHEP **05** (2012) 014, arXiv:1112.6413 [hep-th].

[67] O. Lunin, S. D. Mathur, and D. Turton, "Adding momentum to supersymmetric geometries," Nucl. Phys. **B868** (2013) 383–415, arXiv:1208.1770 [hep-th].

[68] S. D. Mathur and D. Turton, "Momentum-carrying waves on D1-D5 microstate geometries," Nucl. Phys. **B862** (2012) 764–780, arXiv:1202.6421 [hep-th].

[69] M. Shigemori, "Perturbative 3-charge microstate geometries in six dimensions," JHEP **10** (2013) 169, arXiv:1307.3115 [hep-th].

[70] E. J. Martinec and B. E. Niehoff, "Hair-brane Ideas on the Horizon," JHEP **11** (2015) 195, arXiv:1509.00044 [hep-th].

[71] E. J. Martinec, "The Cheshire Cap," JHEP **03** (2015) 112, arXiv:1409.6017 [hep-th].

[72] I. Bena, M. Shigemori, and N. P. Warner, "Black-Hole Entropy from Supergravity Superstrata States," JHEP **10** (2014) 140, arXiv:1406.4506 [hep-th].

[73] I. Bena, S. Giusto, R. Russo, M. Shigemori, and N. P. Warner, "Habemus Superstratum! A constructive proof of the existence of superstrata," JHEP **05** (2015) 110, arXiv:1503.01463 [hep-th].

[74] S. Giusto and R. Russo, "Superdescendants of the D1D5 CFT and their dual 3-charge geometries," JHEP **03** (2014) 007, arXiv:1311.5536 [hep-th].

[75] S. Giusto, E. Moscato, and R. Russo, "AdS_3 holography for 1/4 and 1/8 BPS geometries," JHEP **11** (2015) 004, arXiv:1507.00945 [hep-th].

[76] I. Bena, E. Martinec, D. Turton, and N. P. Warner, "Momentum Fractionation on Superstrata," JHEP **05** (2016) 064, arXiv:1601.05805 [hep-th].

[77] J. M. Maldacena and L. Maoz, "Desingularization by rotation," JHEP **12** (2002) 055, arXiv:hep-th/0012025 [hep-th].

[78] V. Balasubramanian, J. de Boer, E. Keski-Vakkuri, and S. F. Ross, "Supersymmetric conical defects: Towards a string theoretic description of black hole formation," Phys. Rev. **D64** (2001) 064011, arXiv:hep-th/0011217 [hep-th].

[79] S. Giusto, L. Martucci, M. Petrini, and R. Russo, "6D microstate geometries from 10D structures," Nucl. Phys. **B876** (2013) 509–555, arXiv:1306.1745 [hep-th].

[80] E. G. Gimon, T. S. Levi, and S. F. Ross, "Geometry of non-supersymmetric three-charge bound states," JHEP **08** (2007) 055, arXiv:0705.1238 [hep-th].

[81] P. de Lange, D. R. Mayerson, and B. Vercnocke, "Structure of Six-Dimensional Microstate Geometries," JHEP **09** (2015) 075, arXiv:1504.07987 [hep-th].

[82] B. Chakrabarty, D. Turton, and A. Virmani, "Holographic description of non-supersymmetric orbifolded D1-D5-P solutions," JHEP **11** (2015) 063, arXiv:1508.01231 [hep-th].

[83] J. M. Maldacena and A. Strominger, "AdS(3) black holes and a stringy exclusion principle," JHEP **12** (1998) 005, arXiv:hep-th/9804085 [hep-th].

[84] V. Cardoso, O. J. C. Dias, J. L. Hovdebo, and R. C. Myers, "Instability of non-supersymmetric smooth geometries," Phys. Rev. **D73** (2006) 064031, arXiv:hep-th/0512277 [hep-th].

[85] I. Kanitscheider, K. Skenderis, and M. Taylor, "Holographic anatomy of fuzzballs," JHEP **04** (2007) 023, arXiv:hep-th/0611171 [hep-th].

[86] U. H. Gerlach and U. K. Sengupta, "Homogeneous Collapsing Star: Tensor and Vector Harmonics for Matter and Field Asymmetries," Phys. Rev. **D18** (1978) 1773–1784.

[87] A. Ishibashi and R. M. Wald, "Dynamics in nonglobally hyperbolic static space-times. 3. Anti-de Sitter space-time," Class. Quant. Grav. **21** (2004) 2981–3014, arXiv:hep-th/0402184 [hep-th].

[88] S. Deger, A. Kaya, E. Sezgin, and P. Sundell, "Spectrum of D = 6, N=4b supergravity on AdS in three-dimensions x S**3," Nucl. Phys. **B536** (1998) 110–140, arXiv:hep-th/9804166 [hep-th].

[89] A. Polkovnikov, K. Sengupta, A. Silva, and M. Vengalattore, "Nonequilibrium dynamics of closed interacting quantum systems," Rev. Mod. Phys. **83** (2011) 863, arXiv:1007.5331 [cond-mat.stat-mech].

[90] P. Bizon and A. Rostworowski, "On weakly turbulent instability of anti-de Sitter space," Phys. Rev. Lett. **107** (2011) 031102, arXiv:1104.3702 [gr-qc].

[91] A. Buchel, L. Lehner, and S. L. Liebling, "Scalar Collapse in AdS," Phys. Rev. **D86** (2012) 123011, arXiv:1210.0890 [gr-qc].

[92] O. J. C. Dias, G. T. Horowitz, and J. E. Santos, "Gravitational Turbulent Instability of Anti-de Sitter Space," Class. Quant. Grav. **29** (2012) 194002, arXiv:1109.1825 [hep-th].

[93] M. Maliborski and A. Rostworowski, "Time-Periodic Solutions in an Einstein AdS–Massless-Scalar-Field System," Phys. Rev. Lett. **111** (2013) 051102, arXiv:1303.3186 [gr-qc].

[94] G. T. Horowitz and J. E. Santos, "Geons and the Instability of Anti-de Sitter Spacetime," Surveys Diff. Geom. **20** (2015) 321–335, arXiv:1408.5906 [gr-qc].

[95] P. Bizoń, M. Maliborski, and A. Rostworowski, "Resonant Dynamics and the Instability of Anti–de Sitter Spacetime," Phys. Rev. Lett. **115** no. 8, (2015) 081103, arXiv:1506.03519 [gr-qc].

[96] J. Mas and A. Serantes, "Oscillating Shells in Anti-de Sitter Space," Int. J. Mod. Phys. **D24** no. 09, (2015) 1542003, arXiv:1507.01533 [gr-qc].

[97] E. da Silva, E. Lopez, J. Mas, and A. Serantes, "Holographic Quenches with a Gap," JHEP **06** (2016) 172, arXiv:1604.08765 [hep-th].

[98] S. Gao and J. P. S. Lemos, "Collapsing and static thin massive charged dust shells in a Reissner-Nordstrom black hole background in higher dimensions," Int. J. Mod. Phys. **A23** (2008) 2943–2960, arXiv:0804.0295 [hep-th].

[99] T. Delsate, J. V. Rocha, and R. Santarelli, "Collapsing thin shells with rotation," Phys. Rev. **D89** (2014) 121501, arXiv:1405.1433 [gr-qc].

[100] J. V. Rocha, "Gravitational collapse with rotating thin shells and cosmic censorship," Int. J. Mod. Phys. **D24** no. 09, (2015) 1542002, arXiv:1501.06724 [gr-qc].

[101] V. Cardoso and J. V. Rocha, "Collapsing shells, critical phenomena and black hole formation," Phys. Rev. **D93** no. 8, (2016) 084034, arXiv:1601.07552 [gr-qc].

[102] R. Brito, V. Cardoso, and J. V. Rocha, "Interacting shells in AdS spacetime and chaos," Phys. Rev. **D94** no. 2, (2016) 024003, arXiv:1602.03535 [hep-th].

[103] O. Taanila, "Holographic thermalization and Oppenheimer-Snyder collapse," arXiv:1507.00878 [hep-th].

[104] V. Balasubramanian, A. Bernamonti, J. de Boer, N. Copland, B. Craps, E. Keski-Vakkuri, B. Muller, A. Schafer, M. Shigemori, and W. Staessens, "Thermalization of Strongly Coupled Field Theories," Phys. Rev. Lett. **106** (2011) 191601, arXiv:1012.4753 [hep-th].

[105] V. Balasubramanian, A. Bernamonti, J. de Boer, N. Copland, B. Craps, E. Keski-Vakkuri, B. Muller, A. Schafer, M. Shigemori, and W. Staessens, "Holographic Thermalization," Phys. Rev. **D84** (2011) 026010, arXiv:1103.2683 [hep-th].

[106] D. Garfinkle and L. A. Pando Zayas, "Rapid Thermalization in Field Theory from Gravitational Collapse," Phys. Rev. **D84** (2011) 066006, arXiv:1106.2339 [hep-th].

[107] D. Garfinkle, L. A. Pando Zayas, and D. Reichmann, "On Field Theory Thermalization from Gravitational Collapse," JHEP **02** (2012) 119, arXiv:1110.5823 [hep-th].

[108] G. Mandal, R. Sinha, and T. Ugajin, "Finite size effect on dynamical entanglement entropy: CFT and holography," arXiv:1604.07830 [hep-th].

[109] E. Poisson, A Relativist's Toolkit: The Mathematics of Black-Hole Mechanics. Cambridge University Press, 2009.

[110] S. Chandrasekhar, An Introduction to the Study of Stellar Structure. Dover Books on Astronomy Series. Dover Publications, Incorporated, 2012. https://books.google.co.in/books?id=joWn8s2BF04C.

[111] T. Banks, M. R. Douglas, G. T. Horowitz, and E. J. Martinec, "AdS dynamics from conformal field theory," arXiv:hep-th/9808016 [hep-th].

[112] V. Balasubramanian and S. F. Ross, "Holographic particle detection," Phys. Rev. **D61** (2000) 044007, arXiv:hep-th/9906226 [hep-th].

[113] V. Keranen, H. Nishimura, S. Stricker, O. Taanila, and A. Vuorinen, "Gravitational collapse of thin shells: Time evolution of the holographic entanglement entropy," JHEP **06** (2015) 126, arXiv:1502.01277 [hep-th].

[114] J. R. Oppenheimer and H. Snyder, "On Continued gravitational contraction," Phys. Rev. **56** (1939) 455–459.

[115] S. B. Giddings and A. Nudelman, "Gravitational collapse and its boundary description in AdS," JHEP **02** (2002) 003, arXiv:hep-th/0112099 [hep-th].

[116] J. Smoller and B. Temple, "Shock-wave solutions of the einstein equations: The Oppenheimer-Snyder model of gravitational collapse extended to the case of non-zero pressure," B. Arch. Rational Mech. Anal. **128** (1994) 249.

[117] C. Molina-Paris and M. Visser, "Minimal conditions for the creation of a Friedman-Robertson-Walker universe from a 'bounce'," Phys. Lett. **B455** (1999) 90–95, arXiv:gr-qc/9810023 [gr-qc].

[118] J. de Boer, K. Papadodimas, and E. Verlinde, "Holographic Neutron Stars," JHEP **10** (2010) 020, arXiv:0907.2695 [hep-th].

[119] S. Weinberg, Gravitation and Cosmology. John Wiley and Sons, New York, 1972. http://www-spires.fnal.gov/spires/find/books/www?cl=QC6.W431.